Technische Universität München

TUM School of Engineering and Design

Investigations on the Industrial Applicability of Laser Electrode Structuring in Lithium-ion Battery Production

Lucas Christian Hille

Vollständiger Abdruck der von der TUM School of Engineering and Design der Technischen Universität München zur Erlangung eines

Doktors der Ingenieurwissenschaften (Dr.-Ing.)

genehmigten Dissertation.

Vorsitz:	Prof. Dr.-Ing. Rüdiger Daub
Prüfende der Dissertation:	1. Prof. Dr.-Ing. Michael F. Zäh
	2. Prof. Alessandro Fortunato

Die Dissertation wurde am 18.06.2024 bei der Technischen Universität München eingereicht und durch die TUM School of Engineering and Design am 28.10.2024 angenommen.

Editors' Preface

In times of global challenges, such as climate change, the transformation of mobility, and an ongoing demographic change, production engineering is crucial for the sustainable advancement of our industrial society. The impact of manufacturing companies on the environment and society is highly dependent on the equipment and resources employed, the production processes applied, and the established manufacturing organization. The company's full potential for corporate success can only be taken advantage of by optimizing the interaction between humans, operational structures, and technologies. The greatest attention must be paid to becoming as resource-saving, efficient, and resilient as possible to operate flexibly in the volatile production environment.

Remaining competitive while balancing the varying and often conflicting priorities of sustainability, complexity, cost, time, and quality requires constant thought, adaptation, and the development of new manufacturing structures. Thus, there is an essential need to reduce the complexity of products, manufacturing processes, and systems. Yet, at the same time, it is also vital to gain a better understanding and command of these aspects.

The research activities at the *Institute for Machine Tools and Industrial Management* (*iwb*) aim to continuously improve product development and manufacturing planning systems, manufacturing processes, and production facilities. A company's organizational, manufacturing, and work structures, as well as the underlying systems for order processing, are developed under strict consideration of employee-related requirements and sustainability issues. However, the use of computer-aided and artificial intelligence-based methods and the necessary increasing degree of automation must not lead to inflexible and rigid work organization structures. Thus, questions concerning the optimal integration of ecological and social aspects in all planning and development processes are of utmost importance.

The volumes published in this book series reflect and report the results from the research conducted at *iwb*. Research areas covered span from the design and development of manufacturing systems to the application of technologies in manufacturing and assembly. The management and operation of manufacturing systems, quality assurance, availability, and autonomy are overarching

topics affecting all areas of our research. In this series, the latest results and insights from our application-oriented research are published, and it is intended to improve knowledge transfer between academia and a wide industrial sector.

Rüdiger Daub Gunther Reinhart Michael Zaeh

Preface

This dissertation has been elaborated during my occupation as a research associate at the *Institute for Machine Tools and Industrial Management* at the *Technical University of Munich*.

I would like to express my sincere gratitude to Prof. Dr.-Ing. Michael F. Zaeh for giving me the opportunity of this doctorate and for his valuable supervision during the past years. Together with Prof. Dr.-Ing. Gunther Reinhart and Prof. Dr.-Ing. Ruediger Daub, you have created a prosperous environment for young scientists that enables cutting-edge research.

In addition, I would like to thank Prof. Dr. Alessandro Fortunato for acting as co-advisor to this dissertation and Prof. Dr.-Ing. Ruediger Daub for assuming the chair of my thesis defense.

I extend my deepest appreciation to my former colleagues whose collaborative efforts, mutual willingness to support each other, and shared passion made working a pleasure. The team's balance between scientific professionalism and unprofessional sense of humor significantly fueled my long-term motivation for this dissertation. A special thank goes to Johannes Kriegler, who has been a mentor and indispensable intellectual sparring partner for me during the past years. Furthermore, I want to acknowledge Jan Bernd Habedank's scientific legacy which enabled this dissertation's work in the first place. Finally, I am thankful for the careful review of this document by Johannes Kriegler, Josef Keilhofer, and Celestine Singer, who have significantly enriched its form and content.

Lastly, I owe a debt of gratitude to my family and friends whose unwavering encouragement, support, and understanding sustained me throughout this academic endeavor, providing a constant source of strength and motivation.

Lucas Hille

Contents

List of Abbreviations

AR	aspect ratio
BPP	beam parameter product
BT	bachelor's thesis
CA	cost accounting
CAL	calendered
CC	constant current
CCE	cell cycling experiment
CE	coulombic efficiency
CMC	carboxymethyl cellulose
CV	constant voltage
CW	continous wave
DLIP	direct laser interference patterning
DOD	depth of discharge
DOE	diffractive optical element
DRY	dried
EDX	energy-dispersive X-ray spectroscopy
EIS	electrochemical impedance spectroscopy
EV	electric vehicle
FWHM	full width at half maximum
HAZ	heat-affected zone
ICA	incremental capacity analysis
ICL	irreversible capacity loss
IRLS	iteratively re-weighted least squares
iwb	Institute for Machine Tools and Industrial Management
LCO	lithium cobalt oxide
LFP	lithium iron phosphate
LIB	lithium-ion battery
LIBS	laser-induced breakdown spectroscopy
$LiPF_6$	lithium hexafluorophosphate
LM	light microscopy
LMO	lithium manganese oxide

LSM	laser scanning microscopy
LTO	lithium titanium oxide
MIP	mercury intrusion porosimetry
MT	master's thesis
NCA	lithium nickel cobalt aluminum oxide
NMC	lithium nickel manganese cobalt oxide
NMP	N-methyl-2-pyrrolidone
OCV	open-circuit voltage
P	publication
P2D	pseudo-two-dimensional
PB	pulse burst
PE	polyethylene
POT	pull-off testing
PP	polypropylene
PTFE	polytetrafluoroethylene
PVDF	polyvinylidene difluoride
REF	reference
SBR	styrene butadiene rubber
SEI	solid electrolyte interphase
SEM	scanning electron microscopy
SIB	sodium-ion battery
SLM	spatial light modulator
SO	scientific objective
SOC	state of charge
SOH	state of health
SOM	self-organized microstructure
SSB	solid-state battery
ST	semester's thesis
SWCNT	single-walled carbon nanotube
TEM	transverse electromagnetic mode
TLM	transmisson-line model
TUM	Technical University of Munich
VC	Vinylene carbonate
WET	solvent-containing
WG	weighing
WLI	white light interferometry
ZIB	zinc-ion battery

List of Symbols

Latin symbols

Symbol	Unit	Description
A_e	m^2	electrode area
AR	—	aspect ratio
BPP	m rad	beam parameter product
BPP_{real}	m rad	real beam parameter product
C	$C = h^{-1}$	C-rate[1]
C_6	—	carbon
C_e	$J K^{-1} m^{-3}$	electron heat capacity
C_{ph}	$J K^{-1} m^{-3}$	phonon heat capacity
D_{hole}	m	hole diameter
DOD	%	depth of discharge
d_e	m	electrode thickness
d_{hole}	m	hole depth
$E_{1/2/3/4}$	J	energy level 1/2/3/4
$\Delta E_{1,2}$	J	transition energy between states 1 and 2
E_p	J	pulse energy
e^-	—	electron
F	$C mol^{-1}$	Faraday's constant
f_p	Hz	pulse repetition rate
h	J s	Planck's constant
I	A	current
I_l	$J cm^{-2}$	laser intensity
$I_{l,0}$	$J cm^{-2}$	maximum laser intensity
j	$mA cm^{-2}$	current density
j_0	$mA cm^{-2}$	equilibrium current density
k_B	$J K^{-1}$	Boltzmann's constant
$Li^{(+)}$	—	lithium (ion)
l	m	distance
l_{eff}	m	effective distance
m_{cell}	kg	cell mass

[1] The unit C of the C-rate should not be confused with the unit C (coulomb) for the electric charge.

m_e	kg	electrode mass
M^2	—	beam quality factor
MO_2	—	layered oxide
N	—	number of particles
$N_{1/2/3/4}$	—	number of particles at energy level 1/2/3/4
N_M	—	MacMullin number
P	W	power
P_{abs}	W	absorbed power
P_{avg}	W	average power
P_{peak}	W	peak power
P_{ref}	W	reflected power
P_{spec}	$W\,kg^{-1}$	specific power
P_{tra}	W	transmitted power
P_{vol}	$W\,L^{-1}$	power density
Q	A h	capacity
Q_0	A h	nominal capacity
Q_{charge}	A h	charge capacity
$Q_{discharge}$	A h	discharge capacity
Q_{max}	A h	maximum available capacity
q	$W\,m^{-2}$	heat flux
R	Ω	resistance
R_{beam}	m	beam curvature
R_{ion}	Ω	ionic resistance
$\overline{R}$	$J\,mol^{-1}\,K^{-1}$	universal gas constant
r	m	radius
S	W	optical energy input
SOC	%	state of charge
SOH	%	state of health
T	K	temperature
T_e	K	electron temperature
T_p	s	pulse period time
T_{PB}	s	pulse burst (PB) period time
T_{ph}	K	phonon temperature
t	s	time
t_C	h	(dis)charge time
U	V	voltage
U_0	V	open-circuit voltage
V_{cell}	m^3	cell volume
V_{pore}	m^3	pore volume
V_e	m^3	electrode volume
W	W h	energy content
W_{spec}	$W\,h\,kg^{-1}$	specific energy
W_{vol}	$W\,h\,L^{-1}$	energy density
w	m	beam waist
w_0	m	minimal beam waist
x	—	stoichiometric factor

z	m	beam propagation direction
z_R	m	Rayleigh length

Greek symbols

Symbol	Unit	Description
α_a	—	anode charge transfer coefficient
α_{abs}	—	absorption coefficient
α_{BM}	—	Bruggeman factor
α_c	—	cathode charge transfer coefficient
β	%	mass fraction
γ	$W\,m^{-3}\,K^{-1}$	electron lattice coupling
ε	%	porosity
η	V	overpotential
η_{abs}	—	absorptivity
η_{act}	V	activation overpotential
η_{CE}	%	coulombic efficiency (CE)
η_{dif}	V	diffusion overpotential
η_{ohm}	V	ohmic overpotential
η_{ref}	—	reflectance
η_{tra}	—	transmissivity
Θ	°	divergence angle
κ	$S\,cm^{-2}$	ionic conductivity
κ_e	$W\,m^{-1}\,K^{-1}$	electron thermal conductivity
κ_{eff}	$S\,cm^{-2}$	effective ionic conductivity
λ	m	wavelength
μ_a	V	anode standard potential
μ_c	V	cathode standard potential
ν	Hz	frequency
ρ	$kg\,m^{-3}$	density
τ	—	tortuosity
τ_e	s	electron cooling time
τ_{eff}	—	effective tortuosity
τ_l	s	laser pulse duration
τ_{ph}	s	lattice heating time

Chapter 1

Introduction

"They created a rechargeable world."
– THE ROYAL SWEDISH ACADEMY OF SCIENCES (2019)

1.1 Motivation

Lithium-ion batteries (LIBs) are an indispensable cornerstone of the technological landscapes in modern societies. Since their commercialization by *Sony Corporation* in 1991, they have seen widespread application in smartphones, laptops, and other portable electronic devices (BLOMGREN 2017). Over the last decade, LIBs have additionally emerged as a pivotal enabler of electromobility (MASIAS et al. 2021) and will be essential to the forthcoming transition toward renewable energy sources, enabling a balancing of their inherent fluctuations in energy supply (XU et al. 2023). The development of LIBs has been acknowledged by awarding the 2019 Nobel Prize in Chemistry to the scientists John B. Goodenough, M. Stanley Whittingham, and Akira Yoshino (THE ROYAL SWEDISH ACADEMY OF SCIENCES 2019).

LIBs exhibit several distinct advantages setting them apart from other battery technologies. Their exceptional energy density and specific energy permit the efficient storage of substantial energy quantities within compact and lightweight configurations (BUDDE-MEIWES et al. 2013). Additionally, LIBs possess a low self-discharge and nearly-zero memory effect, allowing them to retain their charge over long periods of inactivity (KIM et al. 2019).

As a result, global LIB production capacities are predicted to increase remarkably in the near future (DUFFNER et al. 2021; MAULER et al. 2021). The development is mainly driven by the global battery market for automotive applications, which is expected to continue growing in the upcoming years (INTERNATIONAL ENERGY AGENCY 2023). At the same time, battery prices are declining as deployments increase (FRITH et al. 2023).

Despite the aforementioned beneficial characteristics of LIBs, further advances of the technology are essential to meet future customer demands, especially for

automotive applications. Current electric vehicles (EVs) suffer from a restricted driving range due to the limited available capacity of commercial LIBs (ANDRE et al. 2017; CHOI and WANG 2018). The crucial components in this context are the electrodes and their capability to store lithium ions. To increase the energy density of an LIB, the mass and volume fraction of the active material in the cell can be augmented by thick and highly-compressed electrode coatings (GALLAGHER et al. 2015). However, this results in a deteriorated ion diffusion in the electrolyte through the porous electrode coatings, especially at high currents (GAO et al. 2018; ZHENG et al. 2012). The phenomenon culminates in the emergence of overpotentials, thereby limiting the fast charging and discharging capability of LIBs (BUQA et al. 2005; PARK et al. 2020) (cf. Section 2.1.4). Furthermore, lithium plating, i.e., the deposition of metallic lithium at the anode, is expedited, resulting in accelerated cell aging and safety concerns (UHLMANN et al. 2015; YANG et al. 2017).

A potential resolution to this predicament lies in the creation of microscopic channels in the electrode coatings, which is referred to as *electrode structuring* in the literature and within the frame of this thesis. By shortening the effective ion diffusion trajectories (NEMANI et al. 2015), cell-internal overpotentials can be mitigated and the LIB power density is enhanced (HABEDANK, KRAFT, et al. 2018; KRAFT et al. 2020). Ultrashort-pulsed laser radiation has been demonstrated as a suitable tool for electrode structuring by selectively ablating a small fraction of the electrode coatings (HABEDANK, ENDRES, et al. 2018). Enhanced fast charging and reduced lithium plating by laser structuring of electrodes were experimentally proven using laboratory-scale coin cells (HABEDANK, KRIEGLER, et al. 2019). Furthermore, an accelerated wetting with electrolyte during the production of LIBs was shown in numerous studies (BERHE and LEE 2021; HABEDANK, GUENTER, et al. 2019; KLEEFOOT et al. 2021; PFLEGING and PRÖLL 2014).

1.2 Objective

Up to date, laser structuring of electrodes is limited to academic research in laboratory environments because of diverse challenges. Firstly, interdependencies of the process with electrode parameters, such as the electrode type, i.e., anode versus cathode, or porosity, are convoluted and poorly understood. Furthermore, the process design requires high effort in time and material due to an unclear impact of specific processing parameters on the resulting hole geometries and a manual analysis of the latter. Additionally, ideal modalities of integrating laser structuring into the existing process chain of LIB production are ambiguous. Also, laser electrode structuring currently operates at low processing rates in laboratory settings, which do not meet industrial electrode manufacturing throughputs. Finally, the economic and technical viability of laser electrode structuring in comparison to alternative processes, especially mechanical electrode structuring, remains unknown.

This dissertation addresses the above-mentioned issues of laser electrode structuring with a variety of purposefully chosen experimental and theoretical methods. Initially, graphite anodes and lithium nickel manganese cobalt oxide (NMC) cathodes were laser-structured to evaluate the respective impact on the electrochemical performance improvements, i.e., the increase in LIB rate capability and decrease in electrode tortuosity. The understanding of interdependencies between electrode properties and laser structuring was deepened by analyzing laser-structured graphite anodes possessing diverse initial bulk porosities. Furthermore, three different options for integrating the structuring process into the production chain of electrode manufacture were realized and resulting electrode properties were examined. In order to facilitate the process design, an analytical model was developed, enabling an automated characterization of hole geometries in topography images of laser-structured electrodes. The influence of a large variety of process parameters on resulting hole geometries was investigated in a comprehensive experimental study. In addition, multibeam structuring using a diffractive optical element (DOE) for beam splitting was realized. The process scaling was assessed technically and economically based on theoretical considerations. Finally, laser structuring was evaluated in comparison to mechanical structuring of electrodes with respect to resulting product characteristics and production engineering aspects.

In conclusion, this dissertation advances the industrial applicability of laser electrode structuring by studying its material interdependencies, process design, process integration, process scaling, and economic viability.

1.3 Thesis structure

This publication-based thesis is divided into six chapters. Following the introduction given in this chapter, the theoretical foundations of LIBs and laser technology are detailed in Chapter 2. Subsequently, the research gap is defined in Chapter 3 based on the current state of literature covering laser-based electrode structuring and additional processing alternatives. Chapter 4 gives an overview of the research approach and methodology used in this dissertation. In the following, Chapter 5 presents and discusses the results obtained in this thesis based on the embedded publications. Finally, the key insights of the dissertation are summarized and an outlook on potential future areas of research is given in Chapter 6.

Chapter 2

Fundamentals

This chapter provides the theoretical foundations for this thesis. In the first Section 2.1, technical parameters, components, operating principle, and production of LIBs are explained. Subsequently, the generation, propagation, and interaction with solid matter of laser radiation are detailed in Section 2.2.

2.1 Lithium-ion batteries

2.1.1 Terminology

LIBs are galvanic systems that store energy in chemical form and allow to convert it into electrical energy on demand. The term *LIB* encompasses all types of battery cells in which lithium ions act as charge carriers and solid electrodes, such as layered oxides or graphite, provide host lattices for the ions (cf. Section 2.1.3).

A distinction is made between primary and secondary energy storage systems. Primary batteries exhibit a single electrochemical reaction that irreversibly converts chemical energy into electrical energy, rendering them incapable of being recharged. In contrast, secondary batteries, or accumulators, undergo reversible electrochemical processes, allowing them to be recharged and reused multiple times while maintaining their energy storage capabilities. A *cell* is the smallest functional galvanic element consisting of two different electrodes immersed in an electrolyte solution. (DANIEL and BESENHARD 2011, pp. 3–8)

In accordance with common conventions, this thesis employs the terms *battery* and *cell* interchangeably, while the term *accumulator* is not utilized. Unless specifically indicated otherwise, *battery* and *cell* consistently pertain to LIBs within the framework of this thesis. Furthermore, the terms *anode* and *cathode* are assigned to the electrodes as components based on their function during discharge, although this allocation is incorrect for the charging process from an electrochemical perspective.

2.1.2 Technical parameters

This section defines technical terms of LIBs, which are used in this dissertation. Please note that the explanations are limited to the context of this work and are not derived in detail. For further information, the interested reader is referred to electrochemical standard literature, such as ATKINS and PAULA (2005) or HAMANN et al. (2007).

Voltage

The open-circuit voltage (OCV) U_0 is defined as the potential difference between the electrodes of a galvanic cell that are not externally connected (KURZWEIL and DIETLMEIER 2018, p. 43). For calculation of the OCV, the difference in the standard potentials $\mu_{a/c}$ of the anode and cathode at thermodynamic equilibrium is used. Following the sign convention of a positive voltage, the theoretical OCV is determined as (KURZWEIL and DIETLMEIER 2018, pp. 170–171)

$$U_0 = \mu_c - \mu_a \, . \tag{2.1}$$

Capacity

The nominal capacity Q_0 of an LIB represents the amount of electrical charge that can be exchanged between the anode and the cathode under defined discharge conditions specified by the manufacturer (STERNER and STADLER 2014, p. 218). Thus, it mainly depends on the chemical composition and quantity of the active materials (DANIEL and BESENHARD 2011, p. 22). The actual capacity Q is the amount of charge that is accessible at a defined condition of the battery at the beginning of or during the discharge process. It is influenced by parameters such as the discharge current I, the cutoff voltage U, or the prevailing temperature T (KORTHAUER 2013, p. 16).

Coulombic efficiency

The capacity share obtained in a discharge process in relation to the capacity fed into the LIB during previous charging is called the coulombic efficiency (CE)

$$\eta_{CE} = \frac{Q_{discharge}}{Q_{charge}} \tag{2.2}$$

and quantifies the reversibility of the electrochemical energy storage capability (DANIEL and BESENHARD 2011, p. 24).

Energy content

The available energy content W of an electrochemical energy storage device is calculated as the product of the average discharge voltage U and the actual capacity Q (KORTHAUER 2013, p. 16):

$$W = U \cdot Q \,. \tag{2.3}$$

When normalizing the energy content to the mass m_{cell} or the volume V_{cell} of the cell, the specific energy W_{spec}, which is also called gravimetric energy density, and the volumetric energy density W_{vol} are obtained, respectively (KORTHAUER 2013, p. 16):

$$W_{\text{spec}} = \frac{W}{m_{\text{cell}}} \quad \text{and} \tag{2.4a}$$

$$W_{\text{vol}} = \frac{W}{V_{\text{cell}}} \,. \tag{2.4b}$$

Power

The electrical power P of an LIB describes the delivered electrical energy per unit of time and is equivalent to the product of the current I and the voltage U (KORTHAUER 2013, p. 16):

$$P = I \cdot U \,. \tag{2.5}$$

Analogously to the energy content, the power can be normalized to the cell mass and volume (cf. Equations 2.4), yielding the specific power P_{spec} and power density P_{vol}, respectively:

$$P_{\text{spec}} = \frac{P}{m_{\text{cell}}} \quad \text{and} \tag{2.6a}$$

$$P_{\text{vol}} = \frac{P}{V_{\text{cell}}} \,. \tag{2.6b}$$

C-rate

The charging or discharging current of an LIB is typically specified by the so-called C-rate C, which relates the absolute current I to the nominal capacity Q_0 of the electrochemical energy storage device (KURZWEIL and DIETLMEIER 2018, p. 233):

$$C = \frac{I}{Q_0} \,. \tag{2.7}$$

Accordingly, the reciprocal value of the C-rate yields the time t_C during which an LIB with the nominal capacity Q_0 is charged or discharged at a specific current I (KURZWEIL and DIETLMEIER 2018, p. 234):

$$t_C = \frac{1}{C} \, . \tag{2.8}$$

The C-rate allows to compare the charge and discharge currents for LIBs of different capacities. For instance, discharging with 2 C means that an LIB is discharged with a current corresponding to a discharge of the full nominal capacity Q_0 in half an hour[1]. At high discharge currents, the actual obtainable capacity Q of an accumulator may differ from the manufacturer-specified nominal capacity Q_0 (KURZWEIL and DIETLMEIER 2018, p. 234). The reasons for this include current-dependent internal resistances of the cell due to internal transport processes, reaction kinetics, the temperature T, as well as aging and recovery effects in the cell (KURZWEIL and DIETLMEIER 2018, p. 235).

State of charge and depth of discharge

The charging state of an LIB is characterized by the complementary terms state of charge (SOC) and depth of discharge (DOD):

$$SOC = \frac{Q}{Q_0} \quad \text{and} \tag{2.9a}$$

$$DOD = 1 - SOC \, . \tag{2.9b}$$

Accordingly, the SOC of an electrochemical energy storage device indicates the remaining cell capacity Q as a function of the nominal capacity Q_0. Thus, the SOC of an LIB equals 1 and 0 in fully charged and discharged state, respectively (KURZWEIL and DIETLMEIER 2018, p. 233).

State of health

The state of health (SOH) characterizes the condition of an LIB with respect to its maximum available capacity Q_{max} and its nominal capacity Q_0 at the time of manufacture (KURZWEIL and DIETLMEIER 2018, p. 245):

$$SOH = \frac{Q_{\text{max}}}{Q_0} \, . \tag{2.10}$$

Aging, i.e., the decline in SOH over time and/or repeated cycling, occurs due to a variety of physical and chemical mechanisms, which can be categorized into loss of lithium inventory, loss of active positive electrode material and loss of active negative electrode material (BIRKL et al. 2017).

[1] It should be noted that the C-rate C possesses the unit $\mathrm{C} = \mathrm{h}^{-1}$, which should not be confused with the unit C (coulomb) for the electric charge.

Performance

The term performance lacks a precise definition and is used in this thesis to encompass various electrochemical aspects of an LIB, such as the specific energy, the energy density, the power, the applicable charge current, the safety characteristics, and the lifetime (ANDRE et al. 2015).

2.1.3 Composition

The main functional components of an LIB are the two electrodes, a separator, and the electrolyte liquid (cf. Figure 2.1). Furthermore, LIBs typically feature a casing to shield the cell-internal components from the environment.

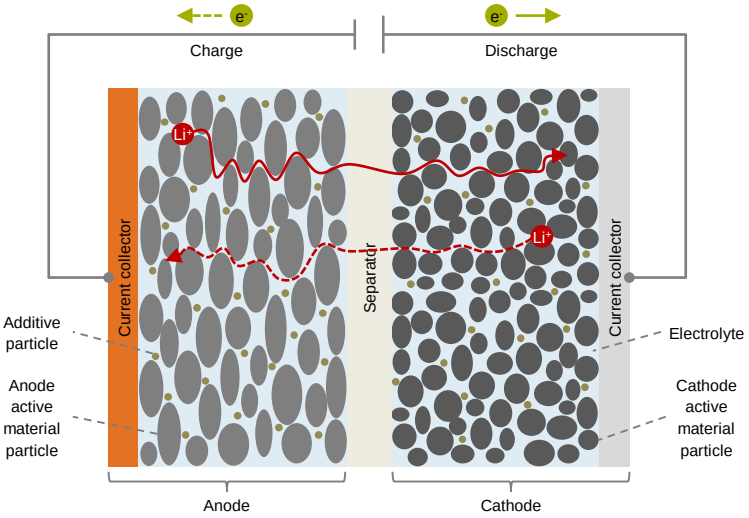

Figure 2.1: Schematic representation of the composition and operating principle of an LIB with indication of an exemplary lithium ion (Li^+) diffusion path and the electron (e^-) flow direction for both the charge (dashed lines) and the discharge process (solid lines), respectively

Electrodes

The electrodes used in LIBs are mainly composite materials that allow for the reversible insertion of lithium ions through an intercalation reaction. In this context, intercalation refers to the process of incorporating lithium ions into a solid host lattice (KURZWEIL and DIETLMEIER 2018, p. 165). While commercially available LIBs typically use graphite or other carbon compounds as active materials for the anode (ANDRE et al. 2017), a large variety of materials

such as lithium iron phosphate (LFP), lithium cobalt oxide (LCO), lithium manganese oxide (LMO), NMC, and lithium nickel cobalt aluminum oxide (NCA) is employed for the cathode (ANDRE et al. 2015). The selection of electrode materials for LIBs is based on several criteria, including the electrochemical properties of the material, its durability during operation, the availability of individual components, costs, environmental aspects, and toxicity (STERNER and STADLER 2014, p. 251). Besides the active materials, electrodes contain small fractions, i.e., a few mass percent, of additives that improve cohesion between particles and the coating's adhesion to the current collectors (KORTHAUER 2013, p. 111). Polyvinylidene difluoride (PVDF) processed with N-methyl-2-pyrrolidone (NMP) is a common polymer binder for cathodes, while water-based carboxymethyl cellulose (CMC) combined with styrene butadiene rubber (SBR) is often used for anodes (KWADE et al. 2018). In addition, anodes and cathodes are normally blended with a few percent of conductive additives, such as carbon black, to improve the electric conductivity within the electrodes (DOMINKO et al. 2003; KWADE et al. 2018).

Current collectors

In LIBs, metallic foils are typically used as current collectors. They should possess sufficient mechanical, chemical, and electrochemical stability, allow good adhesion of the active materials, have high electrical conductivity, and be available at moderate material costs (STERNER and STADLER 2014, p. 258). Normally, copper with a thickness of 6 µm to 10 µm and aluminum with a thickness of 12 µm to 20 µm are employed as current collectors for the anode and cathode, respectively (KWADE et al. 2018). Due to the formation of lithium-aluminum alloys at low anode potentials, the application of cost-effective and lightweight aluminum instead of copper is limited to the cathode side (KORTHAUER 2013, p. 23).

Electrolyte

The electrolyte enables the transport of ions between the electrodes via diffusion. Requirements for the electrolyte include high conductivity and electrochemical stability over a wide temperature and voltage range, as well as compatibility with other system components of the LIB, safety, ecological compatibility, and cost-effective production. In liquid electrolytes, lithium hexafluorophosphate ($LiPF_6$) is often used as the conducting salt, while ethers, esters, and organic carbonates are considered state-of-the-art solvents. (KORTHAUER 2013, pp. 62–63) Besides the conducting salt and the solvent, additives such as Vinylene carbonate (VC) are typical constituents of the electrolyte to improve the cell's cycle stability (KORTHAUER 2013, p. 71). In addition to liquid electrolytes, inorganic solid-state or polymer electrolytes can be used (STERNER and STADLER 2014, p. 254) but are not considered further in this thesis.

Separator

To prevent physical contact between the two electrodes and thus an electrical short circuit in the LIB, an electrolyte-filled microporous membrane, known as the separator, is placed between the anode and the cathode. While choosing particularly thin separators reduces the resistance within the cell, thicker separators provide greater safety during cell operation. Separators for LIBs should be of defined porosity, good wettability, high shape stability, as well as high chemical, mechanical, and thermal resilience (STERNER and STADLER 2014, p. 258). Membranes made of polyethylene (PE) and polypropylene (PP) are commonly used in LIBs (KORTHAUER 2013, p. 82).

Casing

The active components of LIBs are shielded from the environment by casings with high chemical, mechanical, and thermal stability. Depending on the intended use, LIBs are manufactured as cylindrical, prismatic, or pouch cells (KURZWEIL and DIETLMEIER 2018, p. 225). Depending on the chosen cell type, the casing features different types of contacts to extract the current. The housing always contains at least one metal layer since all plastics are permeable to moisture and cannot provide sufficient diffusion resistance to certain organic solvents. Thus, casings are typically manufactured from aluminum or steel depending on weight and cost requirements (KORTHAUER 2013, p. 112).

2.1.4 Operation

Functional principle

In LIBs, the storage of electrical energy is based on the reversible intercalation of lithium ions into the active material of the electrodes (STERNER and STADLER 2014, p. 250). Using an example system consisting of graphite (C_6) as anode material and LMO as cathode material, the occurring redox reactions are explained in the following. In charged state, the anode's active material is present in a chemically reduced form. When the cell is discharged, lithium ions (Li^+) are created through an oxidation reaction and de-intercalate from the host lattice (KURZWEIL and DIETLMEIER 2018, p. 166):

$$Li_x C_6 \rightarrow x Li^+ + x e^- + C_6 \ . \tag{2.11}$$

In the equation, $x \in [0;1]$ is the stoichiometric factor of lithium in the reaction. Concurrently with the reaction, an electron e^- is released into the external circuit, performing electrical work (cf. solid lines in Figure 2.1) (STERNER and STADLER 2014, p. 251). The ions de-intercalated from the anode diffuse in the electrolyte through the separator into the cathode. Here, the lithium ions are

intercalated into the host lattice, and the layered oxide is consequently reduced through the intercalation reaction (KURZWEIL and DIETLMEIER 2018, p. 166):

$$\mathrm{Li}_{1-x}\mathrm{MO}_2 + x\mathrm{Li}^+ + x\mathrm{e}^- \rightarrow \mathrm{LiMO}_2 \,. \tag{2.12}$$

One electron from the external circuit is supplied to the cathode for each intercalated lithium ion maintaining charge neutrality (STERNER and STADLER 2014, p. 251). During charge, the reactions of Equations 2.11 and 2.12 are reversed.

Overpotentials

The charge and mass transport associated with the operating principle of an LIB explained above culminate in a deviation of the cell voltage U from the OCV U_0 during operation, which is called overpotential (VETTER 1961, p. 9)

$$\eta = U - U_0. \tag{2.13}$$

The overpotential originates from different physical phenomena (NYMAN et al. 2010; STUVE 2014, p. 1451):

- Activation overpotential η_{act}: The charge transfer reaction at the interface between the solid electrode and the liquid electrolyte is restricted. This limitation is influenced by the prevailing conditions in the electrolyte and the specific properties of the electrode material, such as its chemical composition and electrochemically active surface area (DANIEL and BESENHARD 2011, p. 19). The resulting activation overpotential η_{act} is considered in the Butler–Volmer equation

  $$j = j_0 \cdot \left[\exp\left(\frac{\alpha_{\mathrm{a}} F \eta_{\mathrm{act}}}{\overline{R}T} \right) - \exp\left(-\frac{\alpha_{\mathrm{c}} F \eta_{\mathrm{act}}}{\overline{R}T} \right) \right] , \tag{2.14}$$

  which features the charge transfer coefficients α_{a} and α_{c} for anode and cathode, respectively (ERDEY-GRÚZ and VOLMER 1930). Furthermore, j is the electrode current density, j_0 the exchange current density at equilibrium, $\overline{R}$ the universal gas constant, and F Faraday's constant (DANIEL and BESENHARD 2011, p. 852).

- Ohmic overpotential η_{ohm}: The ohmic resistance of an LIB results from the electrolyte's ionic resistivity and the solid components' electronic resistivity. The limited conductivities of both components, especially the first one, give rise to a cell overpotential (NYMAN et al. 2010).

- Diffusion overpotential η_{dif}: During operation of an LIB, lithium ions simultaneously intercalate and de-intercalate at both electrodes. As a result, a concentration gradient is established in the cell, which is counteracted by lithium-ion diffusion through the electrolyte. At high current densities, however, diffusion cannot entirely compensate the concentration gradients, causing diffusion overpotentials in the cell (DANIEL and BESENHARD 2011, p. 20).

At high currents, overpotentials might shift the voltage toward the upper or lower cutoff voltage before an SOC of 1 or 0 is reached, respectively. Consequently, the actual capacity Q of an LIB is reduced compared to the nominal capacity Q_0. The operation of the LIB is stopped at the cutoff voltages to avoid aging and/or safety risks. Exceeding the upper cutoff voltage triggers an exothermic decomposition of the electrode materials and the electrolyte. (STERNER and STADLER 2014, p. 266) Furthermore, a metallic deposition of the lithium ions on the anode may occur during charging above the cutoff voltage. This phenomenon is called lithium plating and poses severe safety risks as the metallic lithium dendrites can puncture the separator, leading to a short circuit within the cell and, consequently, overheating and inflammation of the electrolyte. (KORTHAUER 2013, p. 25)

Electrode properties

The concentration gradients and diffusion overpotentials discussed above are significantly influenced by the porous microstructure of the employed electrodes. As stated in Section 2.1.3 and depicted in Figure 2.1, conventional electrodes are particle-based. Consequently, the porosity ε of an electrode is defined as the pore volume V_{pore}, which is filled with electrolyte, divided by the total electrode volume V_{e}, encompassing particles and void space:

$$\varepsilon = \frac{V_{\text{pore}}}{V_{\text{e}}} \,. \tag{2.15}$$

The porosity ε can be calculated from the thickness d_{e}, area A_{e}, and mass m_{e} of an electrode coating as well as the mass fractions β_i and the theoretical crystal density values ρ_i of the individual constituents i (GULBINSKA 2014, pp. 66–67):

$$\varepsilon = 1 - \frac{m_{\text{e}}}{d_{\text{e}} \cdot A_{\text{e}}} \cdot \sum_i \frac{\beta_i}{\rho_i} \,. \tag{2.16}$$

The diffusion of charge carriers through a porous medium is affected by the so-called tortuosity τ, which links the effective length of an ion diffusion path l_{eff} to the shortest conceivable distance l between two intercalation points (CARMAN 1997):

$$\tau = \frac{l_{\text{eff}}}{l} \,. \tag{2.17}$$

The tortuosity is related to the porosity via the Bruggeman relation (ABRAHAM 1993; BRUGGEMAN 1935)

$$\tau = \varepsilon^{-\alpha_{\text{BM}}} \tag{2.18}$$

with α_{BM} being a proportionality factor, which is often approximated as 0.5 for idealized spherical particles of identical size. Yet, this assumption is inaccurate

for many battery electrodes since it underestimates the tortuosity in cases of non-ideal electrode structures (LANDESFEIND et al. 2016; PATEL et al. 2003; THORAT et al. 2009).

The MacMullin number N_M relates the intrinsic ionic conductivity κ of the electrolyte to the effective conductivity κ_{eff} through a porous medium (PATEL et al. 2003):

$$N_M = \frac{\kappa}{\kappa_{eff}} . \tag{2.19}$$

It provides an alternative way to define the tortuosity in addition to the definition given in Equation 2.17 (ABRAHAM 1993; PATEL et al. 2003):

$$\tau_{eff} = N_M \cdot \varepsilon . \tag{2.20}$$

This is useful, as the geometric interpretation of the tortuosity from Equation 2.17 does not account for ion-flow constrictions caused by the cross-sectional area or particle surface morphology (HOLZER et al. 2013; WIEDENMANN et al. 2013). Combining Equations 2.19 and 2.20, τ_{eff} can be calculated from the ionic resistance R_{ion}, which is determinable using electrochemical impedance spectroscopy (EIS) (LANDESFEIND et al. 2016).

The diffusion properties of an electrode are not only influenced by its porosity but also by the electrode thickness. Assuming a constant porosity, a higher loading, i.e., a higher amount of material per electrode area, increases the electrode thickness. Thereby, the share of energy-storing active material compared to inactive components in the cell rises, which improves the energy density (GALLAGHER et al. 2015). Yet, the diffusion through thick electrodes is inhibited by elongated diffusion paths, impeding the applicable currents and reducing the power density (GAO et al. 2018; ZHENG et al. 2012). The design of electrodes for LIBs typically either aims at balancing the energy density and the power density or stresses one aspect depending on the intended application (WITT et al. 2021).

2.1.5 Production

To meet the growing global demand, LIBs are fabricated on large-scale industrial production lines (MAULER et al. 2021). The manufacturing process chain is characterized by a high degree of complexity and interdependencies (KWADE et al. 2018; WESTERMEIER et al. 2014). It can be clustered into the three major segments electrode production, cell assembly, and cell conditioning (cf. Figure 2.2). The individual manufacturing steps and diverse processes are discussed in the following based on the pilot production line for pouch cells at the *Institute for Machine Tools and Industrial Management (iwb)* of the *Technical University of Munich (TUM)* (REINHART et al. 2013).

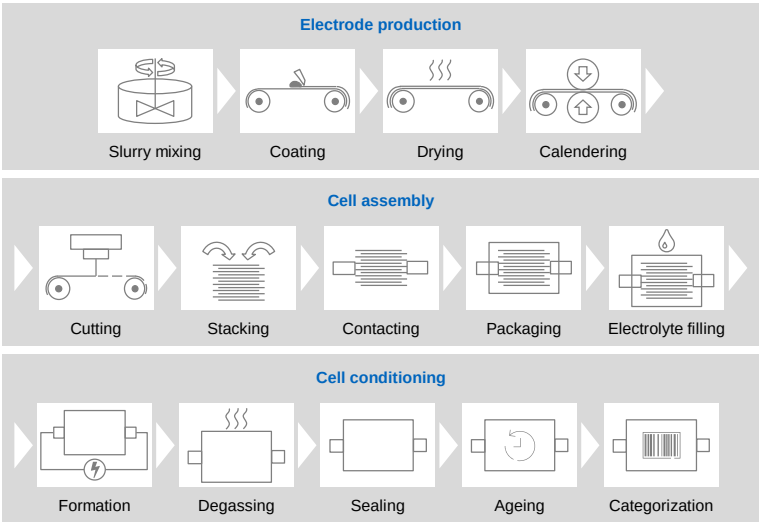

Figure 2.2: Schematic representation of the process chain for the manufacture of LIB pouch cells at the *iwb* of the *TUM* (adapted from SCHREINER et al. (2021))

Electrode production

The electrode manufacture starts with the mixing of the active material powder, binder additive, and conductive additive into a solvent to form a paste commonly referred to as slurry. Based on the chemistry of the solid components, purified water or NMP are typically used as solvents (KORTHAUER 2013, p. 23). The viscous slurry is coated onto the metallic current collector foils with doctor blades or slot dies (KURZWEIL and DIETLMEIER 2018, p. 228). For large-format[2] LIBs consisting of several layers, the current collector foils are coated from both sides. The solvent is evaporated from the laminate using convection drying, infrared radiation, or laser radiation (FINK et al. 2023; NEB et al. 2022). The porosity of the coatings is adjusted by a process known as calendering, in which rollers compress the electrodes to a desired thickness (KURZWEIL and DIETLMEIER 2018, p. 228).

Cell assembly

The production processes of the cell assembly differ depending on the chosen cell type, i.e., round, prismatic, or pouch cells, and are exemplarily explained for pouch cells in the following. After cutting the electrode coils into separate

[2] In this thesis, LIBs exceeding coin cell dimensions and featuring several layers of electrodes are considered *large format*.

sheets using mechanical punching or laser radiation (LUTEY et al. 2016, 2017), the cell batch is created by stacking of anodes, cathodes, and the separator (KORTHAUER 2013, p. 225). Besides single-sheet stacking, continuous winding of an anode-separator-cathode-separator stack into a so-called jelly roll is possible (KORTHAUER 2013, p. 226). After stack building, the electrodes are electrically contacted to metallic tabs consisting of slender aluminum sheets and nickel-plated copper sheets for the cathode and anode, respectively. The process may be realized with ultra-sonic welding (KURZWEIL and DIETLMEIER 2018, p. 229) or laser beam welding (GRABMANN et al. 2022). The tabs serve as conductors for electrical current, enabling its extraction from the cell while concurrently representing the external poles of the LIB. Subsequently, the pre-assembled cell stacks are encased in a composite enclosure consisting of a metallic layer and several polymer linings referred to as pouch foil, with only the aforementioned tabs extending beyond the confines of this enclosure (KORTHAUER 2013, p. 228). An aperture is left open at one side of this packaging, serving as the point of ingress for the subsequent injection of the electrolyte. The cell is then temporarily sealed to enable the formation (not explicitly depicted in Figure 2.2). At one or several points during cell assembly, additional drying steps might be incorporated to reduce residual moisture in the components. Furthermore, the whole cell assembly until final sealing is typically conducted in a dry room. (KWADE et al. 2018)

For research and development purposes, LIBs can be alternatively assembled into small-scale coin cells in laboratory environments. The interested reader is referred to the existing literature by MARKS et al. (2011) and MURRAY et al. (2019) for further details.

Cell conditioning

Before starting the cell conditioning, a rest time is needed to ensure the full permeation of the entire electrode stack with electrolyte. The LIB formation process constitutes the initial charging and discharging of the assembled cell, with the actual number of cycles varying depending on the requirements of the cell chemistry (KURZWEIL and DIETLMEIER 2018, p. 230). Consequently, during the formation of an LIB, the functional interplay of the anode, cathode, separator, and electrolyte is initially evaluated, making it a quality control measure (KORTHAUER 2013, p. 230). To determine the cell's characteristics, charging with constant current (CC) followed by a constant voltage (CV) phase in combination with a CC discharge is often applied (STERNER and STADLER 2014, p. 266). In the course of formation, a passivation layer, the so-called solid electrolyte interphase (SEI), is formed on the anode particles by the decomposition of electrolyte constituents (GIALAMPOUKI et al. 2019). During this process, gases evolve within the LIB, necessitating their release in a degassing step after formation before the cell undergoes final sealing. Typically, the battery conditioning features several days of storage at elevated temperatures and a final categorization of LIBs into different quality classes (KORTHAUER 2013, p. 243).

2.2 Laser technology

2.2.1 Terminology

The term laser is an acronym for *light amplification by stimulated emission of radiation*. Although it technically just describes the physical mechanism, it is also used for technical devices and the generated radiation (RENK 2017, p. 4). Laser radiation can be categorized into the so-called *continous wave (CW)* radiation, which possesses a constant power, and pulsed laser radiation with periodic power fluctuations over time. Pulsed laser radiation for materials processing is often divided into *short-pulsed* and *ultrashort-pulsed* based on the applied pulse durations, resulting in deviating ablation behaviors, which are discussed in Section 2.2.4 (LEITZ et al. 2011).

2.2.2 Generation of laser radiation

Stimulated emission

The creation of laser radiation can be understood with Bohr's model of the atom. When electromagnetic radiation interacts with electrons of an excited particle, it may lead to light amplification through stimulated radiation emission (cf. Figure 2.3) (HÜGEL and GRAF 2009, p. 47). The fundamental prerequisite is that the transition energy $\Delta E_{1,2}$ between the discrete energy states E_1 and E_2 must correspond to the photon energy of the incident radiation, which is given by the product of Planck's constant h and the frequency ν of the radiation (HÜGEL and GRAF 2009, p. 47):

$$\Delta E_{1,2} = h\nu \,. \tag{2.21}$$

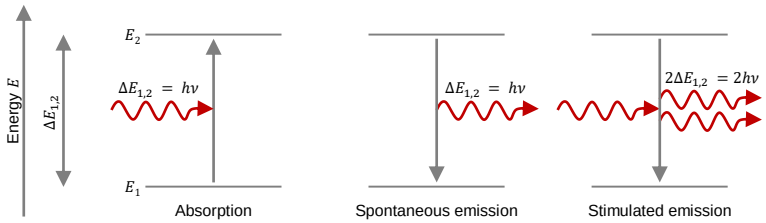

Figure 2.3: Schematic representation of the fundamental interaction processes between photons and an atom (adapted from HÜGEL and GRAF (2009, p. 45) and TRÄGER (2012, p. 643))

In order to effectively amplify a beam of the appropriate frequency as it passes through a layer of matter via induced emission, a greater number of particles N must be in the upper excited level (N_2) than in the lower level (N_1), a condition

known as population inversion (EICHLER et al. 2018, p. 34). Yet, this condition deviates from the population density at thermal equilibrium as given by the Boltzmann distribution (TRÄGER 2012, p. 645):

$$\frac{N_2}{N_1} = \exp\left(-\frac{E_2 - E_1}{k_B T}\right) . \tag{2.22}$$

Herein, T is the absolute temperature and k_B is Boltzmann's constant. From Equation 2.22, it becomes clear that a population inversion $N_2 > N_1$ requires a non-equilibrium state, which is only possible by continuously supplying energy, a process referred to as pumping (HÜGEL and GRAF 2009, p. 49).

However, when N_1 and N_2 approach each other, the pumping process will eventually happen with the same rate as the de-exciting processes of spontaneous and stimulated emission, which is called saturation (TRÄGER 2012, p. 645). Hence, in two-level systems as depicted in Figure 2.3, the medium can become transparent, but laser operation cannot be achieved. For realizing the required population inversion, at least one additional energy level to separate the pumping process from the stimulated emission transition is necessary. (HÜGEL and GRAF 2009, p. 51)

Ideally, laser operation is accomplished through a four-level system, as illustrated in Figure 2.4. From the ground level E_1, the particles are pumped to the highest-energy level E_4, from where the majority quickly relaxes to the upper laser niveau E_3 by mostly non-radiative processes. The stimulated emission occurs from E_3 to E_2, and from E_2 the particles rapidly return to the ground state E_1, typically without emission of radiation. (HÜGEL and GRAF 2009, p. 52) Thus, in a four-level system, occupation inversion is easier to produce than in a three-level system, since E_2 is essentially empty. It is of particular importance, that the relaxation from E_4 to E_3 happens significantly quicker than the laser transition $E_3 \rightarrow E_2$ to build up a population in the upper laser level E_3. (TRÄGER 2012, p. 646)

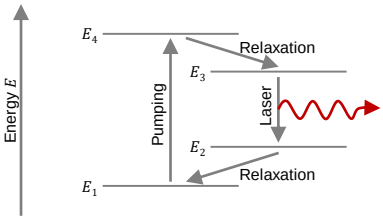

Figure 2.4: Schematic representation of a four-level system for the generation of laser radiation (adapted from HÜGEL and GRAF (2009, p. 51) and TRÄGER (2012, p. 645))

Laser resonator

In order to create a directed laser beam of high intensity, laser sources consist of three main components (cf. Figure 2.5). The laser-active medium or gain medium amplifies light by stimulated emission as explained in Section 2.2.2. A pump source, typically an electrical or optical energy source, e.g., a lamp or another laser source, provides energy to create the population inversion in the laser-active medium. Two mirrors trap the light and thereby form a resonator, in which the light is guided multiple times through the laser-active medium, which can be of solid, liquid, or gaseous state. (TRÄGER 2012, pp. 642–643) By making one of the mirrors partly transmissive, a fraction of the light escapes the resonator and forms the laser beam. While the laser-active medium determines the wavelength λ of the laser beam and can influence the temporal behavior of the laser, the geometric characteristics of the beam, which are explained in Section 2.2.3, are primarily determined by the laser resonator. (HÜGEL and GRAF 2009, p. 56)

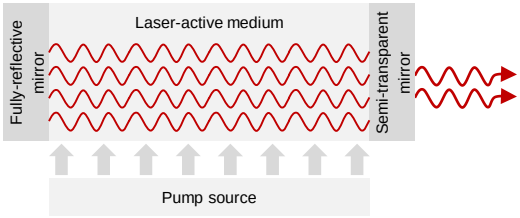

Figure 2.5: Schematic representation of a resonator for the generation of laser radiation (adapted from TRÄGER (2012, p. 643))

Pulsed operation

Pulsed laser operation can be created using various technical approaches resulting in diverse pulse durations and pulse repetition rates (EICHLER et al. 2018, p. 315). For materials processing, laser sources based on Q-switching and mode-locking are mostly utilized. Q-switching involves the suppression of the laser oscillation by high resonator losses until the maximum population inversion is reached in the active medium. Then, the Q-factor[3] is quickly increased, resulting in a rapid build-up and release of the laser power in short, intense pulses (EICHLER et al. 2018, p. 318). Q-switches can be realized actively, e.g., by acousto-optic modulators or electro-optic modulators, and passively, e.g., by saturable absorption (EICHLER et al. 2018, pp. 319, 326). For generating ultrashort laser pulses, a technique called mode locking is typically applied (TRÄGER 2012, p. 1069). By synchronizing the phases between the oscillating modes

[3]The Q-factor is the "ratio of the energy stored in the resonator and the energy loss per oscillation period" (RENK 2017, p. 45).

such that the field amplitudes constructively superposition, very short pulses with high intensity are created (EICHLER et al. 2018, p. 323).

2.2.3 Characteristics of laser radiation

Gaussian beams

In laser resonators, various transversal field distributions, so-called transverse electromagnetic modes (TEMs), can be formed (EICHLER et al. 2018, p. 209). The fundamental transverse mode TEM_{00} in resonators with spherical mirrors is characterized by a radial Gaussian intensity distribution (EICHLER et al. 2018, p. 211) (cf. Figure 2.6):

$$I_l = I_{l,0} \exp\left(\frac{-2r^2}{w^2(z)}\right) . \tag{2.23}$$

Herein, z denotes the beam's propagation direction, r the radial direction, and $I_{l,0}$ the maximum beam intensity. For most practical applications, the beam radius w is defined as the value at which the intensity has radially decreased to $1/e^2 \approx 13.5\,\%$ of its peak value $I_{l,0}$, i.e., 86.5 % of the total power is encompassed within the area with radius w (EICHLER et al. 2018, p. 211–212).

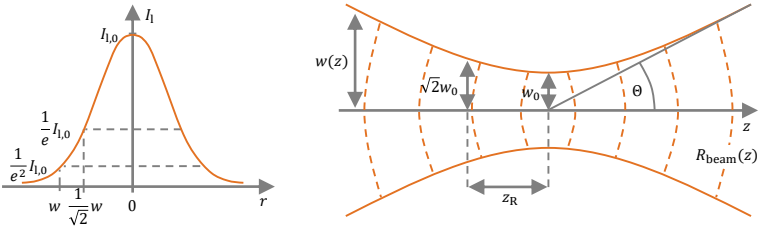

Figure 2.6: Left: Intensity distribution of a Gaussian beam perpendicular to the propagation direction featuring the peak intensity $I_{l,0}$ and the beam radius w (adapted from EICHLER et al. (2018, p. 211)); right: Propagation of a Gaussian beam along the z-axis with denotation of the lateral beam radius w, the Rayleigh length z_R, the minimal beam radius w_0, the divergence angle Θ, and a local wavefront radius R_{beam} (adapted from EICHLER et al. (2018, p. 212))

The beam radius changes in the propagation direction z according to (cf. Figure 2.6)

$$w(z) = w_0 \sqrt{1 + \left(\frac{z}{z_R}\right)^2} . \tag{2.24}$$

Herein, w_0 is the minimal beam radius at $z = 0$

$$w_0 = w(z = 0) = \sqrt{\frac{z_R \lambda}{\pi}} \tag{2.25}$$

and

$$z_R = \frac{\pi w_0^2}{\lambda} \tag{2.26}$$

is the so-called Rayleigh length, at which the intensity is one half of the peak intensity at $z = 0$ (EICHLER et al. 2018, p. 212). At large distances from the beam waist, $w(z)$ approximates a linear behaviour with z. Thus, a divergence angle

$$\Theta = \lim_{z \gg z_R} \frac{w(z)}{z} = \frac{w_0}{z_R} = \frac{\lambda}{\pi w_0} \tag{2.27}$$

of the Gaussian beam can be defined (cf. Figure 2.6). The parabolic phase planes of the Gaussian beam are characterized by the curvature

$$R_{beam}(z) = z + \frac{z_R^2}{z} \,. \tag{2.28}$$

At the beam waist, $R_{beam} \xrightarrow{z \to 0} \infty$ holds, corresponding to plane wave fronts, while the phase planes are spheres around $z = 0$ at large distances from the beam waist. (EICHLER et al. 2018, p. 213)

The quality of an ideal Gaussian beam is often characterized by its beam parameter product (BPP), which is defined as

$$BPP = \Theta \cdot w_0 = \frac{\lambda}{\pi} \,. \tag{2.29}$$

For most real laser beams, the intensity distribution diverges from the TEM_{00} profile, resulting in an increase of the beam radius and the divergence angle (EICHLER et al. 2018, p. 222). This behavior is considered in the BPP by the so-called beam quality factor M^2:

$$BPP_{real} = M^2 \frac{\lambda}{\pi} \,. \tag{2.30}$$

For ideal Gaussian beams, M^2 becomes minimal, i.e., $M^2 = 1$, while it is higher for real laser beams, i.e., $M^2 > 1$. (EICHLER et al. 2018, p. 223)

Pulsed laser radiation

The average power P_{avg} of pulsed laser radiation is the product of the pulse energy E_p and the pulse repetition rate f_p (EICHLER et al. 2018, p. 53):

$$P_{avg} = E_p \cdot f_p \,. \tag{2.31}$$

Herein, f_p is equivalent to the reciprocal of the time between successive pulse peaks T_p (cf. Figure 2.7):

$$f_p = \frac{1}{T_p} \,. \tag{2.32}$$

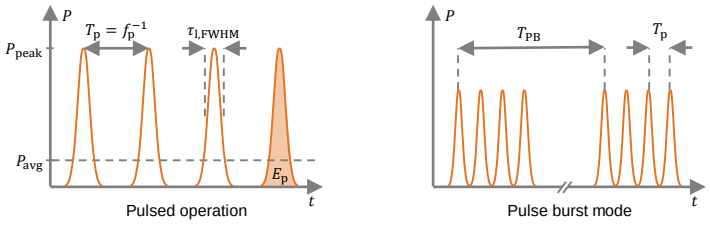

Figure 2.7: Schematic representation of pulsed laser radiation with a Gaussian pulse shape in conventional (left) and pulse burst (PB) operation (right), denoting the peak power P_{peak}, average power P_{avg}, pulse repetition rate f_p, pulse period time T_p, pulse duration $\tau_{l,FWHM}$, pulse energy E_p, and burst period time T_{PB} (adapted from BLIEDTNER et al. (2013, p. 85))

The pulse peak power P_{peak} is the maximum occurring optical power and can be calculated as

$$P_{peak} = \frac{E_p}{\tau_l} \tag{2.33}$$

for rectangular pulses of pulse duration τ_l. In the case of other pulse shapes, a constant pre-factor has to be considered. For example, the peak power of Gaussian-shaped pulses with a full width at half maximum (FWHM) $\tau_{l,FWHM}$ is given by (EICHLER et al. 2018, p. 53)

$$P_{peak} = 0.94 \cdot \frac{E_p}{\tau_{l,FWHM}} \,. \tag{2.34}$$

Besides the conventional pulsed operation, some beam sources are capable of emitting pulse trains consisting of several pulses with a high pulse repetition rate up to the gigahertz range. These so-called pulse bursts (PBs) are separated by a period time T_{PB} (cf. Figure 2.7) and allow for processing benefits, such as a high material removal rate, compared to single pulses of the same energy (LICKSCHAT et al. 2021; METZNER et al. 2021; NEUENSCHWANDER et al. 2015; NEUENSCHWANDER et al. 2019).

2.2.4 Laser materials processing

Absorption and attenuation

The usage of laser radiation for manufacturing processes is based on the conversion of electromagnetic radiation energy into heat in the workpiece (HÜGEL and GRAF 2009, p. 114). The laser power P penetrating the substrate may be partly reflected P_{ref}, absorbed P_{abs}, or transmitted P_{tra} (HÜGEL and GRAF 2009, p. 116):

$$P = P_{ref} + P_{abs} + P_{tra} \,. \tag{2.35}$$

By defining the terms reflectance η_{ref}, absorptivity η_{abs} and transmissivity η_{tra}, Equation 2.35 can be rewritten as (HÜGEL and GRAF 2009, p. 116)

$$1 = \frac{P_{\mathrm{ref}}}{P} + \frac{P_{\mathrm{abs}}}{P} + \frac{P_{\mathrm{tra}}}{P} = \eta_{\mathrm{ref}} + \eta_{\mathrm{abs}} + \eta_{\mathrm{tra}} \,. \tag{2.36}$$

In solid matter, the part of the irradiated intensity I_{l} that is not reflected is absorbed by free and quasi-free electrons in metals or non-saturated compounds of graphite, for instance (POPRAWE 2005, p. 311). The attenuation is described by the Beer-Lambert law

$$I_{\mathrm{l}}(z) = (1 - \eta_{\mathrm{ref}}) \cdot I_{\mathrm{l}} \cdot \exp\left(-\alpha_{\mathrm{abs}} \cdot z\right) \tag{2.37}$$

featuring the absorption coefficient α_{abs} and the penetration depth z (HÜGEL and GRAF 2009, p. 119). Equation 2.37 implies a logarithmic dependence of the penetration depth on the intensity (POPRAWE 2005, p. 311). Besides the linear absorption behavior assumed in Equation 2.37, the simultaneous absorption of several photons in the substrate, called multi-photon absorption, may occur at sufficient photon densities, i.e., high intensities (POPRAWE 2005, p. 312). The effect increases the absorption of ultrashort-pulsed laser radiation (cf. the following section) (LEITZ et al. 2011) and enables the processing of dielectric materials, in which the bandgap exceeds the photon energy (POPRAWE 2005, p. 312).

Light-matter interaction

Processing of solid substrates with CW laser radiation can be described using heat transfer models based on the relationships explained in the previous section (MAZUMDER and STEEN 1980). In contrast, the interaction of pulsed laser radiation with a workpiece has to be regarded on an atomic level, as elucidated in the following based on solid metallic substrates.

When a laser beam penetrates a target, the radiation energy is absorbed by the substrate's free electrons followed by a thermalization of the electron subsystem, an energy transfer to phonons[4], and energy dissipation by electron heat transport into the material. The behavior can be described by a one-dimensional, two-temperature model assuming very quick thermalization within the electron subsystem and negligible thermal conductivity in the lattice subsystem (ANISIMOV et al. 1974; CHICHKOV et al. 1996):

$$C_{\mathrm{e}} \frac{\partial T_{\mathrm{e}}}{\partial t} = -\frac{\partial q(z)}{\partial z} + S(z) - \gamma(T_{\mathrm{e}} - T_{\mathrm{ph}}) \quad \text{with} \tag{2.38a}$$

$$q(z) = -\kappa_{\mathrm{e}} \frac{\partial T_{\mathrm{e}}}{\partial z} \quad \text{and} \tag{2.38b}$$

$$C_{\mathrm{ph}} \frac{\partial T_{\mathrm{ph}}}{\partial t} = \gamma(T_{\mathrm{e}} - T_{\mathrm{ph}}) \,. \tag{2.38c}$$

[4]Phonons are quasiparticles describing the quantized vibrational energy in lattices (SIMON 2013, p. 83).

Herein, $T_{e/ph}$ are the electron and phonon temperature, respectively, $C_{e/ph}$ denote the respective volumetric heat capacities of the electron and phonon subsystems, t is the time, z is the spatial direction perpendicular to the target surface, γ characterizes the electron-lattice coupling, $q(z)$ is the heat flux, κ_e is the electron thermal conductivity, and $S(z)$ is the laser heating power (cf. Equation 2.37) (POPRAWE 2005, p. 313). The model in Equations 2.38 features three characteristic time scales, the electron cooling time $\tau_e = C_e/\gamma$, the lattice heating time $\tau_{ph} = C_{ph}/\gamma$, and the duration of the laser pulse τ_l, defining three different regimes[5] of the laser-material interaction, which are briefly discussed in the following (CHICHKOV et al. 1996):

- Femtosecond laser pulses: If $\tau_l \ll \tau_e$, the electron-lattice coupling and thermal conduction into the target can be neglected. Hence, the attainable lattice temperature is determined by the average electron cooling time, which was shown to be in the order of a few picoseconds (FANN et al. 1992; SCHOENLEIN et al. 1987; WANG et al. 1994). In this regime, the ablation depth per pulse depends logarithmically on the pulse fluence[6] (NOLTE et al. 1997). The ablation process occurs as a direct solid-vapor or solid-plasma transition, allowing a high precision in the created structures (CHICHKOV et al. 1996).

- Picosecond laser pulses: In the case of $\tau_e \ll \tau_l \ll \tau_{ph}$, the electron cooling happens due to energy exchange with the lattice. However, the condition for strong evaporation, the fluence threshold for ablation, and the ablation depth per pulse remain unchanged compared to femtosecond pulses as the same expressions for the lattice temperature are obtained. At the sample surface, solid-vapor ablation dominates, but inside the target a liquid phase develops, reducing the processing precision. (CHICHKOV et al. 1996)

- Nanosecond pulses: If $\tau_l \gg \tau_{ph}$, the electron and phonon temperatures coincide, i.e., $T_e = T_{ph}$. Hence, the laser heats the target to its melting temperature and subsequently to its vaporization temperature. In this case, the main energy loss is due to heat conduction in the material and the threshold fluence needed for evaporation is proportional to $\sqrt{\tau_l}$. As the thermal energy can propagate into the material and create a relatively large melt pool, the evaporation happens from liquid material, impairing the creation of precise structures. (CHICHKOV et al. 1996)

Based on the above-explained diverse ablation mechanisms, laser radiation can be categorized into the *short-pulsed* and *ultrashort-pulsed* regime (cf. Figure 2.8). In short-pulsed processing, i.e., using nanosecond pulses, the material vapor pushes the liquid to the hole edges where it is expelled (POPRAWE 2005, p. 292).

[5] For regimes which are not covered in the enumeration, no clear assignment can be made.
[6] The fluence is "the optical energy delivered per unit area" (PASCHOTTA 2024a).

Due to the considerable heat conduction in the sample, a pronounced heat-affected zone (HAZ) extending beyond the ablated area evolves. In ultrashort-pulsed laser materials processing, i.e., using femtosecond pulses, high pressures, densities, and temperatures result in a high acceleration of the ionized material. The continuous evaporation of material is hindered by the short interaction time, creating an overheated liquid (cf. Figure 2.8) (LEITZ et al. 2011). The rapid expansion of the resulting mixture of liquid droplets and vapor is described in the literature as phase explosion or explosive boiling (LU et al. 2002; MANNION et al. 2004; MIOTELLO and KELLY 1999). Although a precise definition of the short- and ultrashort regime is lacking, pulses with a duration of a few tens of picoseconds and less are typically denoted as ultrashort-pulsed (PASCHOTTA 2024c).

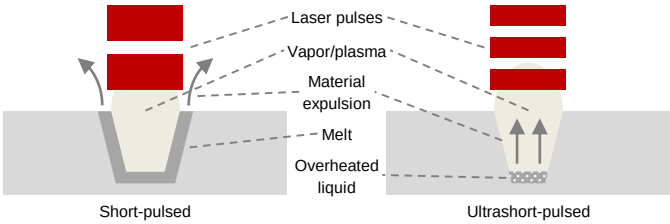

Figure 2.8: Schematic representation of material ablation by short (left) and ultrashort (right) laser pulses (adapted from LEITZ et al. (2011, p. 231))

Drilling

Within this thesis, the term structuring is used to describe the repetitive introduction of microscopic holes into the workpiece, which are oriented perpendicular to its surface. Hence, the process belongs to the category *drilling* according to the classification provided in DIN 8580 (FÖRSTER and FÖRSTER 2018, p. 63). Holes can be created with a single laser pulse or by applying several repeated pulses to the same spot. The latter is called percussion drilling (cf. Figure 2.9) and typically allows the creation of greater hole depths d_{hole} at lower hole diameters D_{hole} than single-pulse drilling (HÜGEL and GRAF 2009, p. 361). In this context, the aspect ratio (AR) is often used to characterize the geometry of a created structure (FÖRSTER and FÖRSTER 2018, p. 261):

$$AR = \frac{d_{\mathrm{hole}}}{D_{\mathrm{hole}}} \,. \tag{2.39}$$

Trepanning drilling and helical drilling are two additional methods, which both use a relative movement of the laser beam on a circular path perpendicular to the beam axis (cf. Figure 2.9) (HÜGEL and GRAF 2009, p. 368). In trepanning

drilling, the laser creates a starting hole by percussion drilling, which is subsequently enlarged in several, increasingly larger, circular paths (HÜGEL and GRAF 2009, p. 368). Helical drilling differs from trepanning drilling by the absence of an initial hole, i.e., the material is removed layer by layer (POPRAWE 2005, p. 305).

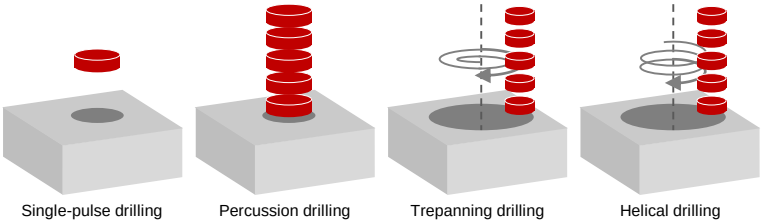

Figure 2.9: Schematic representation of different laser drilling methods featuring the workpiece in gray and laser pulses in red (adapted from HÜGEL and GRAF (2009, p. 353) and POPRAWE (2005, p. 306))

Beam guidance

For most applications of laser radiation in materials processing, beam focusing and deflection are necessary. Both are often combined in one technical unit, the so-called scanner optics. The beam is typically focused by f-theta objectives, which comprise several lenses to keep aberrations low over the entire scan field (cf. Figure 2.10) (PASCHOTTA 2024b). Furthermore, two orthogonally arranged mirrors controlled by galvanometer motors allow for the fast two-dimensional deflection of the beam (cf. Figure 2.10) (HÜGEL and GRAF 2009, p. 96). While the forces needed for beam deflection remain modest due to the low mirror masses and inertia, constraints become apparent when high deflection speeds or accelerations are involved (JAEGGI et al. 2012). Novel beam deflection solutions referred to as polygon scanners overcome this limitation by using rotating multi-facet wheels, enabling beam deflection speeds of several hundreds of meters per second (LOESCHNER et al. 2015; LOOR 2013). Alternatively, beam splitting may be realized for laser processing of large sample areas, for instance using so-called DOEs or spatial light modulators (SLMs) (BRUENING et al. 2018; GILLNER et al. 2019).

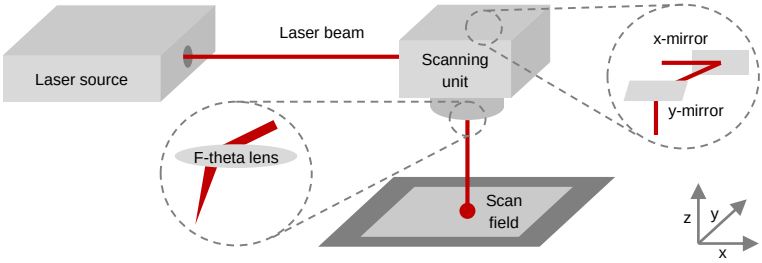

Figure 2.10: Schematic representation of an experimental setup for laser materials processing featuring necessary system technology components (adapted from HÜGEL and GRAF (2009, p. 95))

Chapter 3

State of the Art

In this chapter, the relevant scientific literature on the electrochemical implications, the ablation behavior, and production engineering aspects of laser electrode structuring is presented. After discussing laser structuring of battery electrodes in Section 3.1, process alternatives for electrode structuring are presented in Section 3.2. Based on the state of the art, the research gap is identified at the end of this chapter in Section 3.3. Throughout this chapter, the discussion is restricted to LIB electrodes, i.e., alternative technologies like solid-state batteries (SSBs), zinc-ion batteries (ZIBs), or sodium-ion batteries (SIBs) are not considered. Also, laser perforation of other battery components than the active material coatings, such as the current collector foils or separators, is not regarded. Moreover, further applications of laser radiation in battery production, for instance in electrode cutting, are explicitly excluded from this literature review.

3.1 Laser structuring of battery electrodes

The concept of three-dimensional electrode architectures originates from theoretical considerations, e.g., by ARTHUR et al. (2011) and LONG et al. (2004). Early empirical and numerical adaptions of the concept were made in the context of thin-film electrodes by KIM, SUTTO, and PIQUÉ (2014) and LIM et al. (2014). They are, however, not considered further here, since the physical and electrochemical effects differ from thick-film LIB electrodes (PFLEGING 2018). An experimental realization of three-dimensional battery electrodes was initially proposed in a patent by SAUTER (2014). The electrochemical benefits of structured electrodes were soon after predicted in numerical simulations by NEMANI et al. (2015).

Laser structuring of battery electrodes is typically realized in the form of holes or lines (cf. Figure 3.1). While the latter may be oriented parallel or perpendicular to each other, i.e., forming a grid, holes can be arranged quadratically or hexagonally (HILLE, SENFT, et al. 2023). The structures may extend down to the

current collector or penetrate only a fraction of the electrode thickness. While line-based structuring offers benefits in terms of processing speed, holes – especially in a hexagonally arranged pattern – enable high electrochemical benefits at a comparably low loss of active material (GOEL et al. 2023; SCHWEIGHOFER et al. 2022; USSEGLIO-VIRETTA et al. 2023). In addition to the patterns depicted in Figure 3.1, there are alternatives such as the selective removal of additive residues on the electrode surfaces or the perforation of the electrode coatings and current collectors alike (cf. Section 3.1.5).

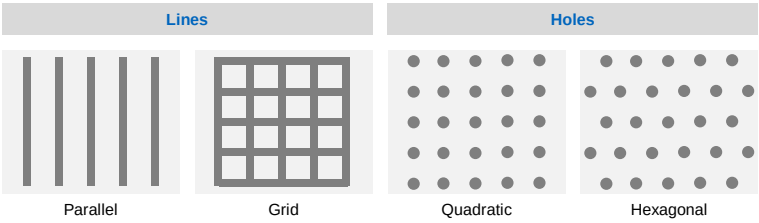

Figure 3.1: Schematic top-view representation of patterns for electrode structuring

3.1.1 Electrochemical aspects

Numerous studies have investigated the effect of laser structuring on the electrode and LIB electrochemistry. The state of the art is compiled in this section, segmented by the treated electrodes, i.e., cathodes and anodes as well as different material selections for both.

Laser structuring of cathodes

Initial experiments on laser structuring were conducted with thin-film electrodes by KOHLER et al. (2010, 2012, 2009) and PFLEGING et al. (2011). Based on the findings, thick-film LCO cathodes were processed with laser radiation to create so-called self-organized microstructures (SOMs) in numerous studies by KIM et al. (2012), KIM, SUTTO, PRÖLL, et al. (2014), KOHLER, PROELL, et al. (2013), KOHLER, PRÖLL, et al. (2013), and PFLEGING et al. (2015). As the processing and resulting structures differ significantly from the approach of this dissertation, they are not detailed further at this point. PFLEGING and GOTCU (2019) reported that laser structuring as pursued in this thesis, i.e., the creation of diffusion channels with dimensions in the micrometer range, enhances the diffusion through LCO cathodes and LIB capacity retention at high current rates.

Among other materials, PRÖLL (2014) applied laser radiation to structure thick-film LMO electrodes, showing an improved discharge capacity retention and reduced degradation during cycling of LIBs with laser-structured LMO electrodes.

The observations were attributed to shortened lithium-ion diffusion pathways (PRÖLL, KIM, MANGANG, et al. 2014; PRÖLL, KIM, PIQUÉ, et al. 2014).

Laser structuring of LFP cathodes was investigated by MANGANG (2018) and coworkers. It was shown that the specific capacity and cycle stability of structured LFP cathodes were increased in comparison to unstructured electrodes due to enhanced lithium-ion diffusion (MANGANG et al. 2015, 2014, 2016).

SMYREK, KIM, et al. (2016) and SMYREK et al. (2014) realized laser structuring of tape-cast and laser-printed NMC cathodes, respectively. In both publications, electrochemical cycling of LIBs revealed an increased specific cell capacity and high rate capability for the laser-processed electrodes. The lithium distribution in the electrodes and chemical degradation mechanisms were studied by laser-induced breakdown spectroscopy (LIBS) in various consecutive studies (SMYREK et al. 2017a,b; SMYREK, ZHENG, SEIFERT, et al. 2016a,b; SMYREK et al. 2019). It was shown that structured electrode architectures provide new lithium diffusion pathways, resulting in an enhanced capability of the electrode material to operate under demanding operation conditions and yielding an increased cell lifetime. The results were substantiated by subsequent studies from RAKEBRANDT et al. (2017a,b), in which a significant improvement of the electrochemical performance of NMC cathodes, especially at high charging and discharging currents, was reported. PARK et al. (2019) demonstrated that the specific energy of laser-structured NMC electrodes with a coating thickness of 175 µm and porosity of 26 % is about twice as high as that of unstructured electrodes with a thickness of 100 µm and porosity of 50 % at 0.5 C. In addition, the rate performance was increased in laser-structured electrodes at 1 C. The authors ascribed the enhanced power and energy densities of laser-structured electrodes to an improvement in lithium-ion diffusivity and cell polarization. The results are in agreement with a study published by ZHU et al. (2019), in which LIBs containing laser-structured 250 µm thick NMC cathodes exhibited higher discharge capacities than their unstructured counterparts at C-rates of 1 C and higher. This corresponds to an increase in power density at elevated currents. The authors pointed out that a suited electrode thickness and pitch distance of the laser-structured pattern depend on the targeted LIB application. SONG et al. (2021) augmented the findings by investigating single-layer, blended, and bi-layer NMC cathodes with diverse particle sizes. The study demonstrated that the electrochemical performance of LIBs containing structured cathodes varies depending on the coating thickness and particle size of the active material. Laser structuring was applied to nickel-rich NMC by TRAN et al. (2022), showing that an improved capacity can be obtained in thick films at high current rates, but not in thin-film electrodes. In the study, a fast lithium-ion transportation by laser structuring was determined from cyclic voltammetry and EIS experiments.

Recently, aqueous-processed NMC cathodes were laser-structured by BRYNTESEN et al. (2023) and ZHU et al. (2021, 2023). The renunciation of the toxic NMP as solvent for the electrode production requires the replacement of the typically used binder PVDF with alternatives, such as fluorine acrylic copolymer latex (ZHU et al. 2021, 2023) or bio-derived kraft lignin (BRYNTESEN et al.

2023). In all three studies, electrochemical benefits by laser structuring, i.e., increased capacities at elevated current rates, were observed in analogy to conventional NMC cathodes based on NMP and PVDF.

Laser structuring of anodes

Laser structuring of graphite anodes was initially realized by HABEDANK, ENDRES, et al. (2018) and KIM et al. (2018), who reported increased LIB capacities by laser structuring in discharge rate tests. The effect was ascribed to the mitigation of polarization induced by concentration gradients in graphite anodes with a high energy density by KIM et al. (2018). HABEDANK, KRIEGLER, et al. (2019) experimentally proved an enhanced fast-charging capability and reduced lithium plating in LIBs by laser structuring. Using EIS, lower impedances of full cells with laser-structured anodes were observed compared to their conventional counterparts. In rate tests, lithium plating could be partially avoided at low temperatures and laser structuring improved the fast-charging capability of LIBs, especially under demanding operating conditions, such as high currents and low temperatures. Shorter charging times were achieved with laser-structured electrodes and the upper cut-off voltage was reached at a higher SOC. ZHENG, PFÄFFL, et al. (2019) used LIBS to quantify lithium-ion concentration profiles in structured and unstructured graphite electrodes, proving that structured electrodes experience a lower lithium-ion content in de-lithiated state than unstructured electrodes. The three-dimensional electrode architecture accelerated the lithium-ion extraction process and decreased inactive parts of the electrodes during electrochemical cycling. CHEN et al. (2020) demonstrated a significantly increased SOH by laser structuring after 100 cycles of fast charging at elevated current rates of 4 C and 6 C. Additionally, laser structuring allowed cells to access over 90 % of the total cell capacity during fast charging, providing a pathway toward safe fast charging of high-energy-density batteries. PARK, JEON, et al. (2021) applied laser structuring to electrodes with an unconventionally high loading of $25\,\mathrm{mA\,h\,cm^{-2}}$, observing a decrease of tortuosity and cell-internal resistances, as well as an enhancement of diffusion characteristics. The study proved that laser structuring can be applied to very thick electrode coatings of 650 µm to 700 µm without detrimental chemical reactions, thermal damage, or material failures. These results align with data published by AHMADI et al. (2022) and DUBEY et al. (2021), who demonstrated improved rate capability and enhanced volumetric capacity of LIBs through laser structuring of graphite electrodes with low porosity and high mass loading.

In addition to conventional graphite anodes, laser structuring has been applied to anode materials containing silicon. The material possesses a significantly higher specific capacity than graphite but faces degradation challenges due to large volume changes during intercalation and de-intercalation of lithium ions (ASHURI et al. 2016). ZHENG, SMYREK, RAKEBRANDT, KÜBEL, et al. (2017) showed that laser structuring of silicon-graphite anodes with 40 % silicon content led to an improved specific discharge capacity retention. Furthermore, an

increased mechanical and electrical contact of the coating to the current collector was achieved by laser patterning the copper foil. In ZHENG, SMYREK, RAKEBRANDT, SEIFERT, et al. (2017), the authors claim to have successfully compensated for the volume changes by laser-structured groves in silicon-based anodes. ZHENG, SEIFERT, et al. (2019) and ZHENG et al. (2018) showed facilitated lithium-ion transport kinetics and lower impedances at a fully lithiated state in LIBs with laser-structured silicon anodes compared to cells with unstructured electrodes. They further assumed reduced mechanical stress by laser electrode structuring based on post-mortem analyses. The results were substantiated by SHI et al. (2019) using in-situ scanning electron microscopy (SEM), revealing a release of the stress from volume expansion, which prevents a delamination of the coating from the current collector. MEYER et al. (2021) proved that laser structuring increases the lifetime as well as the fast charging and discharging capability of silicon-graphite and graphite anodes. The benefits of laser electrode structuring were shown by manufacturing coin and pouch cells with low areal electrode capacities, corresponding to low coating thicknesses, as well as diverse raw material compositions. CHENG et al. (2022) produced a three-dimensional, binder-free silicon-graphite composite electrode from silicon-carbon powder and structured it with two different patterns. A significant increase in reversible capacities was reported compared to pure silicon-graphite anodes, with the two patterns possessing distinct cycling performances. Analog to graphite anodes (cf. previous paragraph), the lithium-ion distribution in silicon-graphite electrodes was studied with LIBS by ZHENG et al. (2022). The study revealed a uniform lithium distribution in structured electrodes in contrast to a concentration gradient in unstructured electrodes at charging with 1 C. Furthermore, it was found that the lithium ions principally diffuse along laser-generated structures into the electrodes at elevated C-rates and the rate capability as well as the electrochemical degradation in LIBs is correlated to the lithium concentration profiles.

Electrochemical modeling

In addition to the experimental studies presented above, electrochemical models have been used to describe and understand the effects of laser electrode structuring. NEMANI et al. (2015) predicted that structured electrodes could achieve a two-fold increased discharge capacity compared to pristine electrodes of the same average porosity. In the study, a hole volume fraction of approximately 20 % and a spacing interval of approximately half the electrode's thickness were derived as optimal criteria for the channel design. Additionally, the impact of the cycling rate, electrode thickness, average porosity, and material loading on the electrochemical performance was quantified.

Laser-structured graphite anodes were represented by HABEDANK, KRAFT, et al. (2018) and KRAFT et al. (2020) with a homogenized three-dimensional model of an exemplary hole structure based on a standard pseudo-two-dimensional (P2D) model. By simulating voltage responses and discharge capacity curves

under varying C-rates, a restricted C-rate window that can be positively influenced by electrode structuring was identified and experimentally verified for the given material. It was shown that modifying the pore morphology with laser structuring reduces lithium-ion concentration gradients and improves the charge and discharge rate capability while also mitigating the risk of lithium plating during fast charging.

MAI et al. (2020) and USSEGLIO-VIRETTA et al. (2020) developed an electrochemical two-dimensional model for LIBs with structures in either one or both electrodes. The study indicated that a relatively low number of holes is required and that electrodes with a high through-plane and low in-plane tortuosity, i.e., a high tortuosity anisotropy, benefit most from structuring. Furthermore, the effect of electrode structuring on cell energy density and lithium plating was investigated for electrodes with different loadings and porosities.

The findings were augmented by LAURI et al. (2021), who examined the thermal properties and electrochemical performance of structured electrodes using microstructure-resolved simulations. Particular attention was paid to the heat evolution and lithium plating during fast charging. In accordance with the literature, it was demonstrated that electrode structuring reduces the overall internal cell resistance by improving the lithium-ion transport properties. Consequently, the fast charging capability of LIBs was improved and the risk of lithium plating was reduced. The authors simulated different scenarios including conical holes and hole misalignment to account for production inaccuracies, showing that deviations from the ideal setup cause only minor decreases in the fast-charging performance.

SCHWEIGHOFER et al. (2022) presented an electrochemical multi-scale framework using a two- and three-dimensional finite-element implementation to compare linear, grid, and hole geometries. The authors verified that the model is able to identify optimal geometrical parameters for different C-rates by fitting the model to cycling data of diverse cell configurations, showing that three out of four patterns exhibited roughly the same electrochemical characteristics. Using continuum-scale modeling, GOEL et al. (2023) optimized the channel size and spacing in structured electrodes for a given volume retention. They demonstrated that closer and smaller holes generally result in improved fast-charging performance compared to larger hole spacing and diameters. The authors defined a metric to quantify the effect of the channel size and spacing on the electrode performance and developed a semi-analytical method to obtain a time-averaged value of the metric, which can be used for high-throughput screening of various hole patterns. USSEGLIO-VIRETTA et al. (2023) applied a genetic algorithm representing a distance-based model with low computation effort to identify optimal patterns in laser-structured electrodes. The model predicted that cylindrical holes arranged in a regular hexagonal pattern are 6.25 times as efficient for fast charging as grooved lines when both structuring strategies are restricted to a material loss of 5 %.

3.1.2 Electrolyte wetting

In addition to the electrochemical advantages explained above, a rapid wetting of electrodes with electrolyte through laser electrode structuring was initially reported by PFLEGING et al. (2014), PFLEGING and PRÖLL (2014), and PRÖLL (2014). Using capillary rise experiments, an acceleration and homogenization of the process was shown for NMC cathodes. HABEDANK, GUENTER, et al. (2019) observed significantly accelerated electrolyte wetting in LIBs containing laser-structured graphite anodes using in-situ neutron radiography of multi-layer pouch cells. Their experiments revealed that the liquid was rapidly absorbed into the capillary grid structures and effectively distributed to the core of the electrode stack in laser-structured electrodes. This eventuated in a significant acceleration of the wetting process, as corroborated by DUNLAP et al. (2022), who estimated the ionically connected specific surface area from EIS data. The wetting of LFP cathodes profits from laser structuring, too, as shown by BERHE and LEE (2021) and GEBREKIROS BERHE et al. (2023) in spread area, wetting time, and contact angle measurements. USSEGLIO-VIRETTA et al. (2023) numerically investigated the influence of different patterns on the electrode's wetting with electrolyte. It was shown that mudcrack-like structures with very limited electrode volume losses of 1 % to 2 % suffice for a significant reduction of the wetting time.

3.1.3 Ablation characteristics

The physical phenomena of material ablation by laser radiation and the implications on how to select suited laser processing parameters are of high relevance for the industrialization of laser electrode structuring.

PRÖLL (2014) assumed a thermal ablation process of LMO cathodes based on the heating of the binder, which possesses a lower evaporation temperature than the active material. As a consequence, entire active material particles were assumed to be ejected without surpassing their evaporation or melting temperature. This was inferred to yield an efficient laser energy usage, as not all of the active material within the holes needs to be evaporated, but results in larger hole geometries than the focal laser beam diameter. The theory was later referenced by PFLEGING et al. (2016) and is in agreement with deliberations by SCHMIEDER (2015) for laser cutting of graphite anodes. For graphite, no melt formations by laser processing were observed, which is ascribed to the absence of a molten phase in the material at ambient pressure (BUNDY et al. 1996; RONCHI et al. 1992).

Laser structuring of LFP cathodes was studied by MANGANG et al. (2016), showing that femtosecond laser radiation eventuates in an increased ablation efficiency and reduced thermal influence compared to nanosecond laser radiation. The authors attributed the behavior to the transition from thermal to cold ablation when decreasing the pulse duration. PARK and LEE (2021) examined the morphological variation of grooves in an LFP cathode structured with a nanosec-

ond laser. In the study, a maximum AR of 1.58 was obtained and the three ablation regimes partial ablation, full ablation, and excessive ablation were distinguished. The authors identified a combination of low fluences and multiple passes as advantageous for laser structuring of the electrodes.

HABEDANK, ENDRES, et al. (2018) systematically investigated the ablation of graphite electrodes in structuring experiments with femtosecond laser radiation, describing how laser processing parameters such as the fluence and the pulse frequency affect the hole depths. Furthermore, an impact of the electrode composition, namely the binder content, on the ablation behavior was demonstrated. In addition, YANG et al. (2019) showed an effect of the graphite particle size on the hole diameter in percussion drilling of battery electrodes. KLEEFOOT et al. (2022) explored parameter dependencies in laser structuring of graphite anodes using picosecond-pulsed laser radiation across a wide range of parameters and reported a significant influence of the laser fluence on the obtained hole depths. In an extensive process study by MEYER et al. (2023), an interaction of laser pulses with the material vapor plasma was observed at high pulse repetition rates of nearly 50 MHz. As a consequence, lower ablation depths and higher ablation widths were obtained in the graphite anodes. The study further reported the achievement of higher ablation depths by an increase in laser peak intensity.

3.1.4 Process scaling

The necessity to scale the laser structuring process to meet industrial processing rates was pointed out by HABEDANK et al. (2020). The study provided technical improvements to the control technology for scanner optics resulting in an increased scanning accuracy. A transfer from resting substrates to roll-to-roll materials processing was realized by YAMADA, SOMA, et al. (2023) using a hollow, rotating cylinder with internal beam guidance and openings on its circumferential surface. With the setup, the authors claim to successfully create 100 000 through-holes per second in thin electrodes. ZWAHR et al. (2023) integrated direct laser interference patterning (DLIP) into a roll-to-roll setup to increase the productivity of large-scale laser structuring of NMC cathodes and silicon/graphite anodes. Another potential solution for process scaling of laser electrode structuring are DOEs, which enable the simultaneous processing of large surfaces (BRUENING et al. 2018; GILLNER et al. 2019; HOFMANN et al. 2020).

3.1.5 Other laser processing approaches

Most studies have structured the electrode coatings with laser radiation to a certain depth in line, grid, or hole patterns (cf. Section 3.1.1). In addition, other approaches have been realized in the past, which are briefly discussed in the following.

Laser surface processing of electrodes

BOLSINGER et al. (2020) and ENDERLE et al. (2020) proposed the selective laser ablation of additives, particularly the binder, at the electrode surfaces to enhance the ion accessibility into the underlying microporous structure of the electrodes. Reduced cell overpotentials and an increased rate capability of the anodes by the approach were reported by SANDHERR et al. (2022). In analogy to electrodes structured with lines or holes (cf. above), the wettability of the electrode with electrolyte is improved by the laser surface treatment (KLEEFOOT et al. 2022). The surfaces of anodes consisting of silicon nanoparticles were processed with short-pulsed laser radiation by PARK, SUH, et al. (2021) to remove particle agglomerations forming dense surface regions during the drying process. As a result, the cycle life, rate capability, and coulombic efficiency were enhanced due to a reduction of internal resistances and thickness of the SEI as well as improved diffusion characteristics.

Laser through-holing of electrodes

Besides a mere laser structuring of the electrode coatings, a perforation of the entire electrodes, which are typically double-side coated on the metallic current collector foils for commercial LIBs, has been reported on in the literature (MATSUMOTO et al. 2023). TSUDA et al. (2018), TSUDA, ANDO, NAKAMURA, et al. (2019), and TSUDA, ANDO, UTAKA, et al. (2019) showed that the approach leads to an increase of the high-rate discharge capacity retention in LIBs consisting of graphite anodes and LFP cathodes due to a facilitated lithium-ion transfer from and to the active materials. WATANABE et al. (2019) investigated the influence of through-holed electrodes on the pre-lithiation of multi-layer graphite/LFP pouch cells. The authors observed a significant reduction of the irreversible capacity loss (ICL) if the hole diameter, pre-lithiation charge, and capacity balancing time were chosen adequately, proving that laser-drilled holes in electrodes can improve pre-lithiation. The concept of through-holed electrodes was transferred to hybrid cathodes consisting of activated carbon layers with LFP and NMC, respectively, by YAMADA, FUKUNISHI, et al. (2023), resulting in a high rate capability, increased cycle stability, and high power density of LIBs.

3.2 Alternative electrode structuring methods

Besides the application of laser radiation for the creation of microscopic holes in electrodes acting as diffusion channels, other methods for a tortuosity decrease have been proposed in the literature. They are discussed in the following.

3.2.1 Magnetic particle alignment

Active material particles of LIB electrodes may possess a shape anisotropy as found, for instance, in natural graphite (JARA et al. 2019). Since the flake-like particles are typically aligned in parallel to the current collector in conventional electrodes due to calendering, tilting of the active materials using magnetic fields has been proposed to facilitate the through-plane lithium-ion diffusion. Using the approach, a decrease of the through-plane tortuosity by a factor of four has been reported by BILLAUD et al. (2016) for graphite anodes with 200 µm thickness and approximately 10 mg cm^{-2} loading. The non-magnetic graphite particles were made magnetically responsive, even at comparably small magnetic fields of 100 mT, by coating with paramagnetic iron oxide nanoparticles. As a result of the magnetic alignment, the lithium storage capacity of the electrode rose by a charge-rate-dependant factor of 1.6 to 3 compared to conventional electrodes. SANDER et al. (2016) applied the approach to LCO cathodes using emulsion droplets and nylon micro rods coated with paramagnetic iron-oxide nanoparticles, which were removed by pyrolysis or evaporation, respectively, after the magnetic treatment. Aligned pore channels were created, eventuating in a three times as high usable capacity at discharge rates of 2 C. The results were confirmed by LI et al. (2019) for 400 µm thick LCO and meso-carbon microbead graphite electrodes. The authors showed a more than tripled areal capacity and a tortuosity reduction from approximately 2.9 to 1.9 in the LCO cathodes. KIM et al. (2020) studied the magnetic alignment of NMC electrodes, showing that the material exhibits either antiferromagnetic or paramagnetic behavior depending on temperature and crystallographic anisotropy. An external magnetic field was adjusted such that a direction for lithium-ion transport perpendicular to the current collectors is favored, culminating in decreased cell-internal resistances and improved LIB rate capability.

3.2.2 Thermal pore forming

Pore-forming agents

The porous morphology of electrodes for LIBs can be tuned by adding so-called pore-forming agents to the slurry during production. In their study, JANG et al. (2021) synthesized pore-structured graphite electrodes by using the unique thermal unzipping properties of polytetrafluoroethylene (PTFE). After heat treatment, the PTFE particles were depolymerized, creating micro-sized pores in the electrodes. This resulted in advanced physical electrode properties, such as an improved wetting ability and shortened ionic diffusion pathways, which boosted the rate capability and the cycle life of LIBs. XIONG et al. (2021) applied the foaming agent ammonium bicarbonate, whose thermal decomposition yielded vertically aggregated bubbles in a highly viscous NMC electrode slurry. The authors showcased that the created structures withstand subsequent calendering and reported a seven times as high rate capability at 5 C compared to conventional electrodes.

Freeze-casting

In addition to the above-mentioned pore-forming agents, the solvent can be used to modify an electrode's microstructure by freezing the slurry under controlled conditions such that ice crystals grow in a unidirectional way. During solidification, the active material particles are excluded from the frozen solvent (typically water), which is subsequently removed by sublimation. This technique is referred to as freeze-casting or ice templating in the literature. (AMIN et al. 2018; BEHR et al. 2015; HUANG et al. 2019; HUANG and GRANT 2018)

HAMAMOTO et al. (2012) manufactured a structured LFP-carbon composite electrode using the above-described method with the aid of gelatine. The authors reported that the freezing temperature controls the micrometer-sized cylindrical pore size and wall thicknesses as well as the charge and discharge capacities. In agreement with that, BEHR et al. (2015) reported a reduction in channel spacing and width at decreasing cooling rates in NCA electrodes, representing an attractive combination of high capacity as well as fast charging and discharging capability. DELATTRE et al. (2018) measured a lower specific capacity at different discharge rates for NCA electrodes manufactured with a lower freezing rate, resulting in a lower tortuosity as well as larger channel width and spacing. The authors suggested a solid-state diffusion as the rate-limiting transport mechanism in sintered NCA electrodes with controlled, aligned porosity. The studies mentioned in this paragraph all applied a sintering step to improve the mechanical stability of the coatings and tune its microstructure.

Freeze-casting without post-process sintering was realized by HUANG and GRANT (2018), HUANG et al. (2019) and AMIN et al. (2018) for ultra-thick LCO, LFP, and graphite electrodes, respectively. All studies reported a significantly raised capacity retention at elevated current rates in freeze-cast electrodes compared to conventional electrodes produced with standard slurry casting. The behavior was ascribed to a lower tortuosity by HUANG and GRANT (2018), who furthermore observed robust mechanical integrity of the electrodes after many cycles of operation. AMIN et al. (2018) attributed the improved rate performance of freeze-cast electrodes to an enhanced electrolyte diffusivity through reduced ionic transport limitations, in contrast to the limitation by solid-state diffusion in freeze-cast sintered NCA electrodes (DELATTRE et al. 2018). The results of AMIN et al. (2018) were corroborated by DANG et al. (2020), who reported an out-of-plane alignment of particle flakes, enhanced electrolyte wettability, and low tortuosity in freeze-cast graphite anodes. YANG et al. (2022) applied freeze casting to NMC electrodes containing single-walled carbon nanotubes (SWCNTs) manufactured with aqueous binders. The vertically-aligned structures eventuated in a remarkably high areal capacity of 79.3 $\mathrm{mA\,h\,cm^{-2}}$ in electrodes with a mass loading of about 511 $\mathrm{mg\,cm^{-2}}$.

3.2.3 Additive manufacturing

Additive manufacturing poses an alternative for the production of electrode coatings compared to conventional manufacturing using tape casting or slot dies. The potential for creating three-dimensionally structured electrodes is discussed in this section.

Using a sol-gel process combined with a micro-injection technology, DOKKO et al. (2005) manufactured LCO and lithium titanium oxide (LTO) electrodes with holes of approximately 100 µm in diameter. The so-created electrodes showed a reversible electrochemical behavior comparable to conventional electrodes. Using a micro printing technology, IZUMI et al. (2012) created line-patterned LTO electrodes with a pitch distance and width of 80 µm and 70 µm, respectively. LIBs with structured electrodes exhibited improved charge and discharge capacities at high current rates compared to conventional cells with flat electrodes. Furthermore, the cycle performance of the cells with patterned electrodes was equivalent to or better than the respective values of their conventional counterparts.

COBB and BLANCO (2014) proposed the manufacture of structured electrodes by applying a co-extrusion process for electrode production. Using the P2D model, the authors studied co-extruded LCO cathodes in LIB half cells against lithium metal. 150 µm to 300 µm thick electrodes were identified to exhibit a substantial improvement in material utilization and thus capacity through electrolyte channels. COBB and SOLBERG (2017) reported improved active material utilization over a broad range of discharge rates in half cells containing co-extruded NMC cathodes. Theoretical considerations yielded increases in gravimetric and volumetric energy density of over 10 % in an LIB pouch cell. WANG et al. (2018) used a paste-extrusion-based printing technique to manufacture LFP electrodes with three different geometric shapes. The authors reported a higher surface area, shorter ion transport paths, improved mechanical strength, higher specific capacity, and improved cycling stability of the structured electrodes.

GASTOL et al. (2021) produced structured graphite anodes via slurry modification with a secondary solvent, resulting in a changed particle alignment and a tortuosity reduction compared to conventional tape-cast electrodes. Additionally, syringe-dispensed electrodes with printed electrode channels were manufactured yielding a prolonged LIB cycle life. These outcomes were confirmed by PARK et al. (2022), who also tuned the orientation in printed graphite anodes by a shear flow of molten feedstock. As a consequence, electrodes with 1 mm thickness were shown to possess a more than doubled specific capacity at 1 C compared to slurry-cast electrodes as well as strengthened mechanical properties. In agreement, XU et al. (2022a) reported the creation of graphite anodes with a hierarchical porous microstructure using a low-temperature direct-write printing technology. The authors demonstrated reduced capacity fade at elevated discharge rates compared to tape-cast electrodes with the same electrode thickness. Based on these insights, XU et al. (2022b) proposed an LIB that consists of three-dimensional, printed electrodes interdigitating into each other.

Numerical simulations and experimental tests confirmed the effectiveness of the cell concept in overcoming the tradeoff between a high energy and a high power density in LCO-graphite LIBs. The interdigitated cell concept had been previously studied for LMO (LI et al. 2017), LFP (LIU, XU, CHENG, et al. 2019; SUN et al. 2013), and LTO (LIU, XU, LIU, et al. 2019; SUN et al. 2013) electrodes with comparable results.

3.2.4 Mechanical structuring

The mechanical insertion of diffusion channels in LIB electrodes has already been proposed about a decade ago by SAUTER (2014). However, scientific literature on the topic is rather scarce and limited to recent years, as presented in the following.

Mechanical embossing

BRYNTESEN et al. (2023) applied compressive force using steel blades, ceramic blades, or needle-like silicon wafers to create different structures in various types of electrodes. The authors reported that structuring half-dried cathodes with ceramic blades is preferred over structuring with a stamp-like silicon wafer, as line structures were easier to produce with high mechanical stability than pit structures. A comparison between mechanical and laser structuring of a PVDF/NMP-based NMC cathode revealed that mechanical structuring resulted in minimal surface residuals and waste, while laser structuring possessed a higher precision and accuracy. KEILHOFER et al. (2023) developed a manual embossing roller for mechanical electrode structuring, showcasing the transferability of the process to continuous roll-to-roll electrode manufacture. In the study, increased discharge capacities by up to 14.3 % at 2 C and expanded long-time cycling were reported despite partial clogging of the structures in subsequent calendering. SANDHERR et al. (2023) used a metal stamp with laser-structured micro pins to structure graphite anodes, creating holes with a comparable geometry to laser structuring. Microscopy and tomography investigations revealed a lower porosity in the vicinity of the holes and alignment of graphite particles on the walls of the mechanically structured holes. Yet, reduced ionic pore resistances, improved fast-charging capability, and prolonged lifetime were shown compared to pristine anodes. Furthermore, tests confirmed that no loss of active material occurred due to mechanical structuring and that the layer adhesion is comparable to that of conventional unstructured electrodes. KEILHOFER et al. (2023) and SANDHERR et al. (2023) pointed out that the mechanical structuring process may be combined with calendering in the future.

Micro milling

REALE and SMITH (2018) created rectangular channels of 400 µm in distance and 100 µm in width in tape-cast electrodes by mechanical micro milling. As a

result, significantly enhanced areal capacitance, tortuosity reductions, and ionic conductivity increases were observed for thick electrodes at high rates.

3.3 Conclusion and research gap

As outlined in the previous section, various methods besides laser structuring have been proposed in recent years for tortuosity reduction in LIB electrodes. However, all above-mentioned approaches face intrinsic challenges, which are concisely discussed in the following.

Although the magnetic alignment of particles is principally scalable, it has not progressed beyond the laboratory scale over the last years. This might be due to technical or economical obstacles of a large-scale implementation of the process. Furthermore, the electrochemical implications and long-term stability of the introduced iron-oxide additives need further investigation. Also, the reported tortuosity decreases do not match the ones achievable by laser structuring. Lastly, particle alignment is only auspicious for highly anisotropic active materials and offers limited control of the electrode's microstructure. (USSEGLIO-VIRETTA et al. 2020)

Pore-forming by additives or freeze-casting creates structures whose shape critically depends on the used solvent and applied conditions. Processing with water often results in heterogeneous lamellar pores, whereas alcoholic solvents result in hexagonal pores due to the different crystal growth behavior (USSEGLIO-VIRETTA et al. 2020). Conclusively, the controllability of the created structures is remarkably worse than with laser structuring. In addition, the economic aspects of energy-intense additional processing steps like freezing and extensive drying are unfavorable with respect to an industrial application. In the case of pore-forming agents like PTFE, the long-term electrochemical implications of the additives need further investigation.

Additive manufacturing of structured electrodes, for instance by co-extrusion, allows for control of the channel dimensions and locations, yet with limited spatial resolution. Furthermore, the scalability of the processing method has to be regarded as very limited, considering processing speeds in the range of $40\,\mathrm{m\,min^{-1}}$ to $80\,\mathrm{m\,min^{-1}}$ in industrial electrode manufacture (KWADE et al. 2018).

Mechanical structuring is a promising processing alternative to laser radiation for an industrial application. Yet, its electrochemical repercussions need further research, as the electrode is locally compacted close to the created structures, resulting in a local porosity decrease and tortuosity increase. Furthermore, production engineering aspects of the mechanical process, such as roller wear-off and particle contamination, need to be studied.

Considering the number of publications, laser structuring can be regarded as the best-understood method for tortuosity reduction in LIB electrodes. Although the

electrochemical implications have been vastly proven in numerous experimental and theoretical studies as detailed in Section 3.1, the process has not progressed from the laboratory scale to a widespread industrial application so far. Five critical problem areas are identified as the cause:

- Material interdependencies: A wide spectrum of electrode materials is available for cathodes (ANDRE et al. 2015) and anodes (ANDRE et al. 2017) in LIBs (cf. Section 2.1.3). In addition, electrodes are fabricated with variations in loadings, thicknesses, particle sizes, compositions, and additives. The correlations between material characteristics and laser-created structures are complex and necessitate thorough consideration for the application of laser electrode structuring. The question if laser structuring should be particularly applied to anodes, cathodes, or both electrodes, has not been answered adequately in the literature so far. Moreover, significant interdependencies between the electrode porosity and the laser-created structures can be expected, as both aspects remarkably influence lithium-ion diffusion.

- Process integration: The production of LIBs is characterized by many subsequent process steps with a high degree of intricate relationships (cf. Section 2.1.5) (KWADE et al. 2018; WESTERMEIER et al. 2014). The impact of the integration point of laser electrode structuring into the existing process chain remains elusive. Consequently, an investigation into how different integration options influence adjacent processes and resulting product properties is due.

- Process design: Although process studies on laser structuring of graphite anodes with femtosecond-pulsed and picosecond-pulsed laser radiation have been conducted in the past (cf. Section 3.1.3), the influence of various processing parameters such as the laser wavelength or pulse bursts on the ablation behavior remains ambiguous. Furthermore, the hole diameter as an essential characteristic of laser-structured holes has not been systematically regarded in the literature. In the conduction of experimental laser processing studies, an efficient process design is hindered by the still manual analysis of the hole geometries, which is highly time-consuming and lacks transferability.

- Process scaling: Laser structuring has been realized in laboratory settings with single-beam scanning strategies using galvanometric scan heads, resulting in low processing rates. In order to meet the throughputs of industrial electrode manufacturing, the processing rate of laser electrode structuring has to be significantly increased. Additionally, laser structuring needs to be transferred from small-area electrodes for laboratory-scale coin cells to industrially relevant, large-format LIBs to validate the scalability of the process.

- Technical-economic viability: The economic aspects of laser electrode structuring are crucial for a successful industrial application, but have

not been studied in the literature so far. Aside from that, laser structuring has to be assessed with respect to potential processing alternatives – of which mechanical electrode structuring is regarded the most promising – in terms of achievable product characteristics and production engineering aspects, which ultimately affect the industrial applicability.

In conclusion, advancements in understanding material interdependencies, process integration, process design, process scaling, and techno-economic viability are imperative for the successful adoption of laser structuring in industrial battery production. This is the core focus of this thesis and led to the research approach delineated in the next chapter.

Chapter 4

Research Approach

This chapter outlines the research approach and methodology used in this dissertation. After defining scientific objectives (SOs) at the beginning, the embedded publications are assigned to these objectives. Subsequently, the experimental and theoretical methods used throughout the research project are detailed.

4.1 Scientific objectives

Based on the research gap identified in Section 3.3, five SOs are defined in the following, outlining the scope of this thesis:

- SO1 Material interdependencies: Initially, it has to be investigated how the performance improvements of LIBs achieved through laser structuring depend on the electrode properties. It needs to be clarified if laser structuring of anodes and/or cathodes is most promising in LIBs with state-of-the-art cell chemistry. Furthermore, the mutual relationship between the initial bulk porosity of the electrodes, which is adjusted by calendering and a crucial aspect for the lithium-ion diffusion, and the laser-created structures shall be described.

- SO2 Process integration: The integration of laser electrode structuring into the existing process chain for LIB production must be enabled. Therefor, the effect of different integration options on the resulting electrode characteristics and LIB cell performance has to be studied. Potential differences in the product properties have to be comparatively examined and guidance on process integration has to be provided to battery producers.

- SO3 Process design: The identification of a suited process strategy for laser structuring of electrodes has to be facilitated. For this purpose, the influence of all central processing parameters tunable in electrode structuring with pulsed laser radiation has to be described in detail. For

the conduction of comprehensive processing studies, the analysis of hole geometries needs to be assisted with automated tools and the transferability of the results has to be ensured.

- SO4 Process scaling: The process of laser structuring is to be transferred from a laboratory scale to near-industrial processing. To this end, laser structuring needs to be applied to large-format LIB pouch cells proving the scalability from a product perspective. From a process perspective, an increase in the throughput of laser electrode structuring needs to be achieved, e.g., using multi-beam laser scanning approaches, and the obtained product characteristics have to be evaluated.
- SO5 Technical-economic viability: The technical and economic competitiveness of laser electrode structuring has to be assessed regarding its future industrial application. In this context, it is of special importance to quantify the production costs associated with the process. Furthermore, an evaluation with respect to potential process alternatives, especially the recently developed approach of mechanical electrode structuring, is necessary.

Collectively, the five SOs defined above aim at enabling laser structuring of battery electrodes for industrial application. They further represent the conceptual framework for the studies conducted and publications written throughout this dissertation project.

4.2 Contribution of embedded publications

Within the author's research, seven scientific publications (Ps) were issued. Their allocation to the SOs defined in Section 4.1 is visualized in Figure 4.1 and detailed in the following. A granular description of the obtained results is provided in Section 5.1.

The interdependencies between inherent material properties and the laser structuring process are addressed by two experimental studies. For P1, graphite anodes and NMC cathodes were laser-structured and electrochemically characterized. Particular attention was paid to the proportionate influence of anode or cathode structuring on the LIB performance. P2 investigates the impact of the electrode porosity, which is adjusted by calendering, on the application of laser structuring. Collectively, P1 and P2 clarify for which type of electrodes laser structuring is most promising and thereby define the materials used in the subsequent works.

The implementation of laser structuring into existing production lines for electrode manufacture is covered by a comprehensive experimental study in P3. Electrochemical, geometrical, and mechanical product features were defined as quality criteria and comparatively evaluated for three possible integration

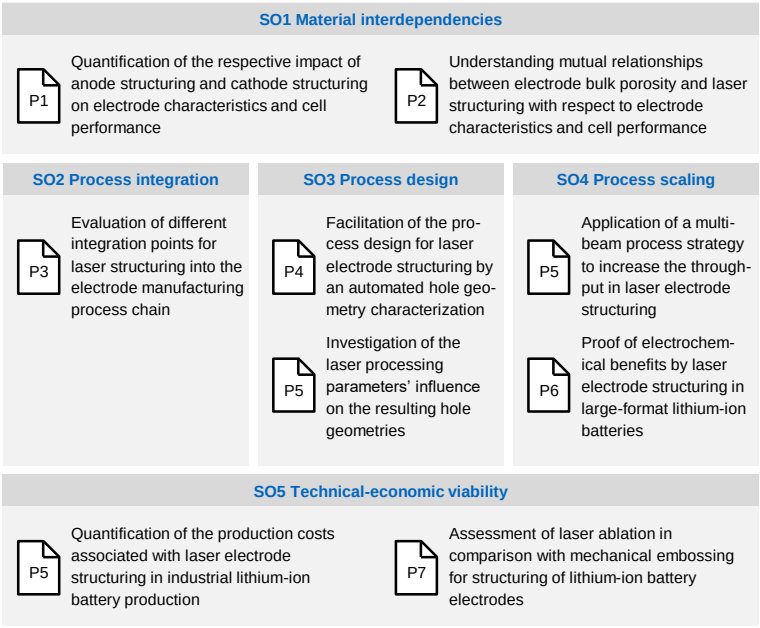

Figure 4.1: Allocation of the publications (Ps) created within this dissertation to the scientific objectives (SOs) defined in Section 4.1

options, which are directly after the slurry coating, after the electrode drying, and after electrode calendering (cf. Figure 2.2). Based on the obtained product properties, it is discussed at which point in the process chain laser structuring should be integrated.

In order to facilitate the process design and the conduction of experimental studies on laser electrode structuring, an automated approach for the determination of hole geometries, i.e., the hole diameters and depths, from topographic image data was developed for P4. The method was subsequently used for P5 and P7. Based on an extensive process study, P5 provides discrete guidance on suited parameters for the structuring of graphite anodes with picosecond-pulsed laser radiation.

P5 further contributes to SO4 by demonstrating an auspicious option for throughput increase of electrode structuring with a DOE enabling multi-beam laser processing. The structured electrodes are compared to electrodes processed with a single-beam scanning strategy in terms of geometrical and mechanical product properties. The applicability of laser structuring to extensive electrode areas is validated in P6 after manufacturing large-format LIBs pouch cells containing laser-structured electrodes. The electrochemical performance criteria are

exhaustively elaborated, e.g., with respect to the LIB lifetime, exceeding the possibilities offered by laboratory-scale coin cells.

The economic competitiveness of laser structuring scaled to industrial processing rates is assessed in P5, providing insights into the expected production costs associated with the process. Furthermore, laser structuring is evaluated in comparison with the alternative processing technology of mechanical embossing in P7. In the study, both processes are examined regarding product properties, such as the mechanical electrode integrity and the electrochemical performance characteristics, as well as production engineering aspects, such as scalability, flexibility, and costs.

4.3 Methodology

Throughout the research activities conducted for this dissertation, a variety of experimental and theoretical methods were applied. From Figure 4.2, which gives an overview of the methods, an experimental focus of the performed investigations becomes evident. In all studies, optical imaging techniques were used for sample characterization. They encompass light microscopy (LM), laser scanning microscopy (LSM), and SEM allowing for a qualitative and quantitative analysis of the electrode surfaces. Energy-dispersive X-ray spectroscopy (EDX) delivered detailed insights into the material composition of the electrode surfaces. The electrochemical performance was evaluated using cell cycling experiments (CCEs) of LIB full cells and EIS of symmetric cells. While the latter allows obtaining specific information about electrode characteristics, such as the ionic resistance or tortuosity, CCEs ultimately verify the benefits of laser structuring in LIBs, i.e., the increase in lifetime or dischargeable capacity under specific operation conditions. High-precision weighing (WG) was used in most studies to quantify the material removal by laser structuring and determine electrode porosities (cf. Section 2.1.4). In order to characterize the effect of laser structuring on mechanical electrode properties, mercury intrusion porosimetry (MIP) and pull-off testing (POT) were applied. Across all studies, the general validity and transferability of the experimental results were ensured by analyzing batches of several, i.e., at least three, identical samples per configuration to allow statistical statements.

Besides the experimental approaches, theoretical considerations and models were used for this thesis. For the analysis of EIS data, the impedance of the electrolyte-filled pores in the battery electrodes was described by an equivalent circuit diagram referred to as transmisson-line model (TLM) (LANDESFEIND et al. 2016), allowing the determination of the cell-internal ionic resistance. Cycling data of LIBs was studied with incremental capacity analysis (ICA) to gain deeper insights into degradation phenomena and rate-limiting mechanisms. For P5, an analytical model for the measurement of hole geometries in laser-structured electrodes using topography data stemming from LSM images was

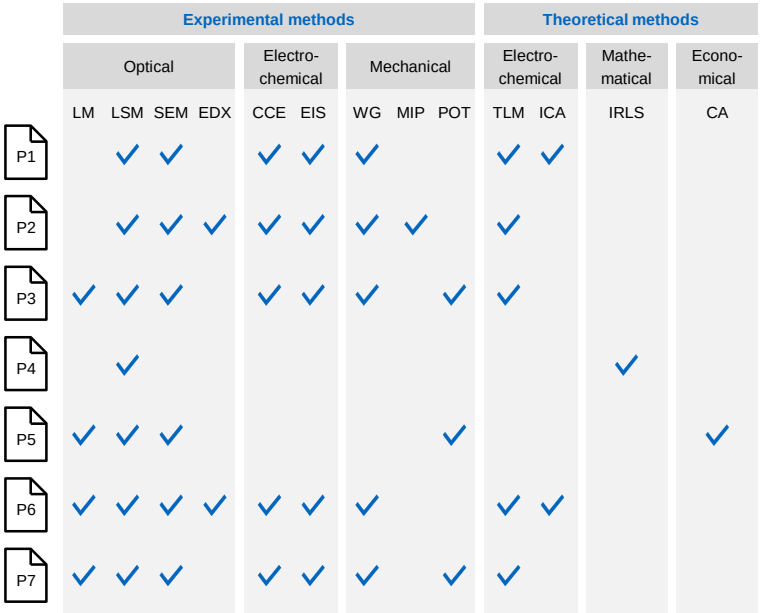

Figure 4.2: Overview of the scientific methods used in this dissertation with allocation to the scientific publications (Ps) encompassing light microscopy (LM), laser scanning microscopy (LSM), scanning electron microscopy (SEM), energy-dispersive X-ray spectroscopy (EDX), cell cycling experiments (CCE), electrochemical impedance spectroscopy (EIS), weighing (WG), mercury intrusion porosimetry (MIP), pull-off testing (POT), transmission-line model (TLM), incremental capacity analysis (ICA), iteratively re-weighted least squares (IRLS), and cost accounting (CA)

developed. For this purpose, the iteratively re-weighted least squares (IRLS) algorithm from the field of regression analysis was used for data fitting and segmentation (GENTLE 2007; WOLKE and SCHWETLICK 1988). Furthermore, a cost model was created for P6 to quantify the production expenditures associated with laser structuring. The calculation was based on theories for full cost accounting (CA) and specific models for the estimation of expenditures in battery production (NELSON et al. 2019; SCHNELL et al. 2020; SCHÜNEMANN 2015). Please note that this section and Figure 4.2 only encompass already-existing methods, which have been applied and modified within this thesis. Approaches that have been developed and/or refined throughout the author's research project, such as the hole geometry characterization, are detailed in Section 5.1.

Chapter 5

Results

Expanding upon the scientific approach, goals, and methodology detailed in Chapter 4, this chapter showcases the research outcomes achieved within this dissertation. The results are presented as concise summaries of the author's publications in Section 5.1, featuring a brief explanation of the contributions made by the author and each co-author. Section 5.2 provides a discussion of this thesis' main findings regarding novelty, classification, consistency, and transferability.

5.1 Summary of embedded publications

5.1.1 P1: Laser structuring of graphite anodes and NMC cathodes – Proportionate influence on electrode characteristics and cell performance

Content

For P1 of this dissertation, the respective influence of laser structuring applied to the anode and/or the cathode of an LIB was experimentally investigated. For this purpose, microscopic holes acting as diffusion channels were introduced into state-of-the-art synthetic graphite anodes and NMC cathodes by laser radiation with 0.15 ns pulse duration. Comparable structure geometries in anodes and cathodes were created by applying average laser powers of 15 W and 12 W in combination with pulse repetition rates of 600 kHz and 300 kHz for anode and cathode structuring, respectively, with a processing time of 1 ms per drilling for both electrodes. Consequently, hexagonally arranged holes with a center-to-center distance of 120 µm, corresponding to a material ablation of approximately 5 wt%, were obtained in both electrodes, as verified by LSM and weighing. Using SEM, complete particle ejection was observed in graphite anodes, while melting residues were evident in the NMC cathodes. This behavior was attributed to the absence of a molten phase of graphite at ambient pressure (RONCHI et al. 1992).

Cells consisting of the four possible combinations of structured and unstructured anodes and cathodes, respectively, were manufactured and subjected to a discharge rate test with C-rates of 0.1 C to 5 C. Therein, LIBs containing structured electrodes exhibited higher capacities at medium to high discharge currents, i.e., 1 C to 3 C, compared to unstructured reference cells. The performance increase was more pronounced in cells with structured anodes than in cells with structured cathodes. Only at very high C-rates of 5 C did cathode structuring start to dominate the cell performance, indicating an additional diffusion limitation of the cathode in this C-rate regime. In check-up cycles at the end of the rate test, cyclic aging of 2 % to 4 % was observed, yet less pronounced in cells comprising structured electrodes than in their conventional counterparts. ICA revealed deviations in the de-intercalation stages between structured and unstructured electrodes. Cells featuring pristine anodes exhibited inhibition of specific intercalation stages at lower discharge currents compared to cells containing structured anodes. These shifts identified cell polarization and diffusion limitations as the primary rate-limiting mechanisms in the LIBs.

In addition to full cells, symmetric cells containing the four electrode configurations, i.e., anodes and cathodes in structured and unstructured conditions, were assembled. They were characterized using EIS and the TLM (cf. Section 4.3). It was determined that the ionic resistance of pristine graphite anodes was notably higher compared to pristine NMC cathodes. Laser structuring, in contrast, effectively reduced the ionic resistances to a similar level for both, anodes and cathodes, corresponding to a decrease in their respective MacMullin numbers and tortuosities.

The insights into how electrode structuring affects the anode and cathode sides hold significant promise for potential industrial applications of laser structuring. Depending on the specific use case and the corresponding operational conditions of an LIB, the implementation of electrode structuring might be restricted to just one of the electrodes, reducing the complexity and costs of process integration. Accordingly, laser structuring was limited to graphite anodes in the further course of this dissertation.

Author contributions

The author of this dissertation, Lucas Hille, had the initial idea of investigating the respective impact of anode and cathode structuring. He conceptualized and led the study design and experimental procedures. Furthermore, he was in charge of the data analysis and interpretation as well as the manuscript preparation. Lingji Xu conducted experiments during her master's thesis. Josef Keilhofer assisted in the modeling and interpretation of electrochemical impedance spectra. Sandro Stock supported the analysis of cell cycling data, especially regarding ICA. Johannes Kriegler aided in the overall study design, in the selection of research methods, and in the interpretation of results. Michael F. Zaeh supervised the research project and ensured its funding. All authors reviewed the manuscript and commented on the obtained results.

5.1.2 P2: Influence of laser structuring and calendering of graphite anodes on electrode properties and cell performance

Content

The interdependencies between laser structuring and calendering with respect to electrode characteristics and LIB performance were studied for P2 of this dissertation. Both processes tune the electrode's pore structure, whereby the bulk porosity is adjusted by calendering, and laser structuring adds a directed, anisotropic porosity to the electrode. For the study, graphite anodes with four different initial bulk porosity levels of 19 %, 27 %, 34 %, and 56 % were manufactured by calendering and subsequently laser-structured. An average laser output power of 13 W, a processing time of 1 ms per hole, a pulse repetition rate of 550 kHz, and a pulse duration of 0.15 ns were applied. The holes were arranged in a hexagonal pattern with a pitch distance of 120 µm.

Laser structuring was observed to increase the porosity of the electrodes by approximately 8 % to 10 % due to the removal of material. In addition, the electrodes' thicknesses rose due to a spring-back effect induced by the laser heat input. SEM verified that strong calendering resulted in superficial pore clogging of the coatings, which could be partly released by laser structuring. Binder agglomerations on the electrode surfaces were observed in an EDX analysis and ascribed to the re-deposition of evaporated material. Using MIP, a reduction of the prevalent pore sizes by calendering was observed, but no significant change in the pore size distribution by laser structuring was detected.

Electrochemical impedance spectra of symmetric cells containing all manufactured electrode configurations revealed a pronounced surge in ionic resistances and tortuosities with decreasing electrode porosities. Consequently, diffusion limitations caused by the electrode compression were observed but could be significantly diminished by laser structuring. In discharge rate tests, all coin cell configurations exhibited reduced capacities at elevated C-rates over 1 C. Intensive calendering led to decreased discharge capacities, especially at higher currents. Implementing laser structuring of the electrodes significantly enhanced the discharge capacities at high C-rates, with the most substantial performance improvements shifting toward lower C-rates at declining bulk porosities. Despite a rise in porosities and thicknesses of the electrodes by laser structuring, the structured anodes still outperformed their unstructured counterparts in terms of capacity density and energy density at elevated C-rates. The results substantiated that the facilitation of ion diffusion by laser structuring exceeds the results expected from a pure increase in bulk electrode porosity.

In summary, P2 pinpointed an ideal range for applying electrode structuring in terms of initial electrode bulk porosity and identified C-rate windows with high capacity increases. The discoveries further hold significance for commercial LIB manufacturers and researchers aiming to fine-tune electrode characteristics through a combination of calendering and laser structuring.

Author contributions

Lucas Hille led the experiments, data analysis, and manuscript creation for P2. Hans-Christoph Toepper conducted the MIP experiments. Charlotte Schriever supported the electrode manufacture and cell assembly of the study. Johannes Kriegler assisted with the design of experiments as well as data analysis, especially of the rate tests. Josef Keilhofer aided in the modeling and interpretation of electrochemical impedance spectra. Marc P. Noecker conducted preliminary experiments on the topic, showcasing the general feasibility of the approach. Michael F. Zaeh supervised the research project and ensured its funding. All authors reviewed the manuscript and commented on the obtained results. Lucas Hille presented the study at the *241st ECS Meeting* in Vancouver, Canada in 2022.

5.1.3 P3: Integration of laser structuring into the electrode manufacturing process chain for lithium-ion batteries

Content

For P3 of this dissertation, three different integration options for laser structuring into the process chain of electrode production were investigated. Hence, four different electrode configurations were manufactured in the course of the study:

- Solvent-containing (WET) electrodes: Laser structuring of graphite anodes directly after the coating process before drying, corresponding to the processing of wet electrodes containing a high share of solvent in the coating
- Dried (DRY) electrodes: Laser structuring of graphite anodes after the drying process but before calendering, corresponding to the processing of solvent-free but uncalendered electrodes with a high porosity
- Calendered (CAL) electrodes: Laser structuring of graphite anodes after calendering, corresponding to the processing of dry and compacted electrodes with a low porosity
- Reference (REF) electrodes: Calendered reference electrodes without laser-structured holes, serving as a benchmark representing conventional electrode manufacturing

Apart from the above-mentioned differences, all electrodes exhibited the same production procedure, i.e., electrodes of configuration WET were also calendered, for instance. In order to compare the configurations, various product properties were defined as quality criteria, ranging from geometrical aspects of the created holes over the mechanical integrity of the coatings to electrochemical characteristics. A pulse duration of 0.15 ns, pulse repetition rate of

600 kHz, average powers of 4 W to 11.5 W, and drilling times of 0.5 ms to 1 ms were identified in preliminary experiments as suited laser parameters to create comparable hole geometries in the different configurations. The holes were arranged in a hexagonal pattern with a 120 µm center-to-center distance.

Studying the electrode surfaces with LSM and SEM suggested that material removal is governed by the evaporation of solvent in WET electrodes in contrast to binder expulsion in DRY and CAL electrodes. This led to the latter configurations having more particle residues on their surfaces and a lower spread in the hole depth distribution. Furthermore, closure of the created holes by subsequent calendering was observed in configurations WET and DRY.

Pull-off tests of the electrode coatings revealed that laser structuring of WET electrodes did not deteriorate the mechanical integrity compared to REF electrodes. Conversely, laser structuring of DRY and CAL electrodes notably decreased the strength of the coatings when pulled off. Furthermore, an increase in electrode thickness and porosity was noted in configurations DRY and CAL due to particle ablation resulting in a weight reduction and a thickness increase by heat input of the laser beam, triggering a spring-back effect in the electrodes (cf. Section 5.1.2).

EIS applied to symmetric coin cells revealed an augmented electrochemically active surface area in the DRY and CAL electrodes compared to REF, corroborating the hypothesis of selective binder evaporation in these configurations. Moreover, laser structuring notably reduced tortuosity from over 8 in the REF to less than 6 in the WET and 2 in the DRY and CAL electrodes, respectively. In accordance, all structured electrodes exhibited increased capacities compared to the unstructured reference at C-rates higher than 1 C in a discharge rate test. Particularly pronounced improvements of over 20 % were observed at 3 C to 4 C in the DRY and CAL configurations, though a partial clogging of the structures was observed in DRY electrodes.

In conclusion, laser structuring before drying, i.e., the WET approach, maintained the mechanical electrode integrity and ensured technical surface cleanliness but lacked structure quality and high electrochemical improvements. Post-calendering laser structuring (CAL) offered distinct process stability and precision but showed similar electrochemical performance to structuring before calendering (DRY). Challenges persist with the structuring of dried electrodes – pre- and post-calendering – due to poor electrode strength and particle residues, posing obstacles for a widespread use in battery manufacturing.

Author contributions

Lucas Hille identified process integration as a relevant research topic, led the design of experiments, performed the data analysis, and created the manuscript. Marc P. Noecker and Byeongwang Ko manufactured and laser-structured electrodes in the laboratory and conducted sample analyses within their student theses. Johannes Kriegler, Josef Keilhofer, and Sandro Stock supported the data

analysis and document writing. Michael F. Zaeh supervised the research project and ensured its funding. All authors reviewed the manuscript and commented on the obtained results.

5.1.4 P4: Automated geometry characterization of laser-structured battery electrodes

Content

For P4 of this thesis, an automated, model-based approach for the identification and geometrical characterization of laser-structured holes in battery electrodes was developed using the programming language *Python*. As part of the method, topographic image data of laser-structured electrode surfaces generated with LSM are initially pre-processed with a median filter for smoothing purposes. Subsequently, a flat reference plane is fitted to the data with an IRLS algorithm to compensate for a potential mispositioning of the workpiece during image capture, resulting in inclined surfaces. Each image pixel is assigned a weight which is iteratively updated by the algorithm such that a low value is assigned to pixels with a high error, i.e., with a high deviation from the reference plane. Thus, the holes are eventually excluded from the reference plane determination. The obtained weights are further used for segmentation of the electrode surfaces into the two categories *hole* and *no hole*. Finally, adjacent pixels classified as holes are clustered and the geometric center of each hole is calculated. The hole diameter is determined as twice the average distance of the edge pixels to the geometric center, while the hole depth is obtained as the average distance of the three lowest hole pixel values with respect to the reference plane.

In a comparison against manual geometry determination, the automated approach yielded comparable values when applied to electrodes with diverse hole geometries. The study further demonstrated that the algorithm generates consistent results even with varying recording conditions, like changes in image brightness, frame rate, or vertical resolution. Both, the automated and the manual method, were affected by magnification and illumination, revealing an inherent limitation of the measuring equipment. Lowering image resolution reduced code execution time but also compromised the accuracy of predicting the hole depth.

Furthermore, the method's transferability was tested by applying it for the characterization of particle indentations in LIB current collector foils stemming from electrode calendering. Although the holes were only a few µm in size and irregularly distributed on the sample – thereby differing from the laser-structured holes in LIB electrodes – they were successfully recognized by the algorithm without major modifications.

In conclusion, the developed approach allows to overcome limitations in the manual measurement of laser-structured electrodes, such as the immense necessary time and the limited reproducibility. Thus, the analysis of large data

sets with high precision and without user supervision is facilitated. In addition, the method was shown to be transferable to other use cases, and a potential application in process monitoring seems principally feasible.

Author contributions

Lucas Hille developed the approach for the automated hole characterization and was in charge of the manuscript preparation. Paul Hoffmann transferred the approach to *Python* code and performed the sensitivity analysis. Johannes Kriegler supported the study design and verification. Andreas Mayr provided the additional use case from electrode calendering. Michael F. Zaeh supervised the research project and ensured its funding. All authors reviewed the manuscript and commented on the obtained results.

5.1.5 P5: Picosecond laser structuring of graphite anodes – Ablation characteristics and process scaling

Content

For P5, the ablation of graphite anode material by ultrashort-pulsed laser radiation was investigated and process scaling via beam splitting was realized using a DOE. Furthermore, the technical and economic figures associated with process scaling of laser electrode structuring were theoretically modeled.

In a comprehensive experimental study, the laser wavelength, pulse repetition rate, number of pulses per hole, and pulse energy were varied over a broad range, resulting in 1879 parameter combinations. The created holes were characterized with the analysis method developed for P4 (cf. Section 5.1.4). It was found that holes with a higher AR were achieved using low wavelengths of 532 nm or 355 nm compared to 1064 nm. In addition, bursts of five pulses at a burst repetition rate of 200 kHz and an intra-burst repetition rate of 82 MHz yielded more favorable ARs compared to single pulses at 200 kHz or 1000 kHz. An approximately linear correlation of the hole diameters and depths with the peak pulse fluence was observed. Furthermore, increasing the number of pulses per hole resulted in an asymptotically progressing increase in the hole depths. A favorable combination within the examined parameter window involved using a wavelength of 532 nm, the 200 kHz PB mode, an approximate peak pulse fluence of $10\,\mathrm{J\,cm^{-2}}$, and 80 pulses per hole, resulting in accurately formed and evenly sized holes measuring approximately 35 µm in diameter and 61 µm in depth. Using SEM, no visible burrs, melt formations, or surface irregularities were detected in or around the holes. Furthermore, there were no partially perforated particles, indicating that the ablation process was primarily influenced by the expulsion of complete particles due to binder evaporation, as previously suggested in P2.

By employing a DOE generating a 3×7 beam matrix, a 88 % reduction in processing time could be achieved compared to single-beam structuring. Notably, the resulting laser-structured holes exhibited nearly identical geometries, and the electrode's mechanical strength was not altered when compared to those produced using a single-beam scanning approach. Additionally, similar hole shapes and microstructures were verified in high-resolution SEM images of electrodes structured using both single-beam and multi-beam scanning strategies.

To assess the scalability of laser structuring, processing rates were calculated for hexagonal and quadratic hole patterns of various hole distances. Considering an energy per hole of 1 mJ, it was deduced that employing ultrashort-pulsed laser sources operating at kilowatt-level powers is a fundamental requirement for implementing laser electrode structuring on an industrial scale. To enhance the processing rate of laser electrode structuring, options such as a hole depth reduction, augmentation of hole distances, selection of quadratic hole patterns, and parallelization were pointed out.

The costs associated with laser structuring of electrodes were calculated based on existing economic models for an exemplary battery production scenario in Germany, yielding total expenditures of approximately 1.96 $/kWh for the process[1]. Plant acquisition and labor expenses were identified as major contributors to the production costs associated with laser structuring. As the identified expenses correspond to an increase of roughly 1.3 % with respect to the total production costs of LIBs, a positive conclusion regarding the economic attractiveness of laser electrode structuring was drawn.

Author contributions

Lucas Hille developed the study idea, designed the experiments, analyzed the obtained samples, and wrote the manuscript. Johannes Kriegler assisted with the process design and data interpretation. Andreas Oehler and Michalina Chaja conducted the laser structuring experiments, including multi-beam processing with a DOE. Sebastian Wagner supported the characterization of multi-beam-processed electrodes. Michael F. Zaeh supervised the research project and ensured its funding. All authors reviewed the manuscript and commented on the obtained results.

5.1.6 P6: Enhanced performance and lifetime of lithium-ion batteries by laser structuring of graphite anodes

Content

For P6, LIBs with a capacity of approximately 2.9 A h containing laser-structured graphite anodes were produced, transferring electrode structuring from labora-

[1] Dollar ($) is the appropriate monetary unit in this case, as it allows for a better international comparison

tory coin cells to multi-layer pouch cells (cf. Section 2.1.5) manufactured on an LIB pilot production line featuring semi-automatic equipment.

Hexagonally arranged holes with 120 µm distance were laser-structured into graphite anodes with infrared laser radiation of 15 W average power, 1200 kHz pulse repetition rate, 12.5 µJ pulse energy, and 0.15 ns pulse duration. The cells with structured anodes exhibited a discharge capacity increase of up to 35 % compared to reference cells at C-rates of up to 8 C and temperatures of −10 °C, 0 °C, and 25 °C. This, coupled with higher mean discharge voltages and reduced anode masses in the structured cells, led to an overall improvement in gravimetric energy density. Charge rate capability tests indicated considerably extended CC charging phases for cells with structured anodes. At 4 C, structured cells achieved an SOC of 68 % in CC mode, surpassing the reference cells, which only reached 52 %. Moreover, cells containing structured anodes demonstrated an extended lifespan during fast charging. In CC/CV charging at 4 C, a noticeable ICL was observed for the reference cells, contrasting with the structured cells displaying slower aging tendencies.

An ICA was conducted to delineate aging behaviors between reference and structured LIBs, revealing distinct redox peak evolutions. A loss of lithium inventory heavily impacted the reference cell's aging, causing substantial capacity reduction within the initial 20 cycles. Conversely, the structured cells exhibited notably slower aging, as the cell lifespan extended from 8 to 182 cycles before reaching 80 % SOH. After 520 cycles, structured cells retained an SOC of 74 %, while the reference cells dropped to 50 % after 500 cycles. Comparisons of the CC and CV phase shares during charging indicated enhanced fast-charging capabilities in cells with structured electrodes throughout the life cycle test.

In a post-mortem analysis of the electrode surfaces at an SOC of 0 % with SEM and EDX, pore-clogging of the reference anode surfaces was observed and attributed to lithium plating. While structured electrodes exhibited only localized evidence of lithium plating, the anode surfaces of reference cells were entirely covered with a surface layer.

Author contributions

Johannes Kriegler conceptualized the study, developed the research methodology, led the investigation, and conducted the data visualization, formal analysis, curation, and validation. He further authored the manuscript. Lucas Hille conducted experiments, performed sample characterization, validated the obtained results, and co-drafted the document. Sandro Stock assisted in the evaluation of data, especially the ICA of voltage curves. Ludwig Kraft supported with the post-mortem analysis of LIBs cells and data interpretation. Jan Hagemeister and Jan Bernd Habedank aided the study design and data evaluation. Andreas Jossen and Michael F. Zaeh supervised the research project and ensured its funding. All authors reviewed the manuscript and commented on the obtained results.

5.1.7 P7: Comparative evaluation of graphite anode structuring for lithium-ion batteries using laser ablation and mechanical embossing

Content

Structuring of graphite anodes with laser radiation was compared to mechanical embossing in P7 of this dissertation. Mechanical structuring was realized as a novel combination of embossing and calendering, which was named structure calendering.

The produced electrodes were characterized with respect to their geometrical, mechanical, and electrochemical properties. In LSM analyses, the mechanically structured holes were shown to possess larger diameters and depths as well as a higher uniformity compared to their laser-structured counterparts. SEM revealed a surface elevation around the holes in laser-structured electrodes, while clogged pores were observed in the lateral walls of mechanically structured holes, which was ascribed to the different hole creation mechanisms. Neither of the two methods had a pronounced negative effect on the mechanical integrity of the coatings compared to unstructured electrodes, as verified by POT.

Using EIS, laser-structured electrodes were shown to exhibit significantly higher double-layer capacitance than mechanically structured and unstructured electrodes despite identical mass loading. The observation was ascribed to selective evaporation of the binder additives by laser radiation. Both techniques for electrode structuring notably decreased the ionic resistance and electrode tortuosity by more than 20 %. Furthermore, they resulted in a nearly identical improvement in discharge capacity of LIBs at C-rates of 0.5 C to 5 C, where transport limitation prevailed in cells with unstructured electrodes.

In addition to the experimental assessment of the electrode properties, production engineering and economic aspects of both structuring approaches were qualitatively evaluated. In the discussion, mechanical structuring was identified to offer advantages such as lower initial capital expenditures, higher productivity, and the avoidance of material removal, while laser structuring offers exceptional flexibility, accuracy, and reduced maintenance needs. Based on the analysis from a product and processing perspective, it was concluded that structure calendering represents an attractive technique in addition to laser structuring. Challenges for both processes, such as contamination or wear on the roller in mechanical structuring and process scaling of laser structuring were finally pointed out.

Author contributions

The creation of P7 was collaboratively led by Josef Keilhofer and Lucas Hille, who share the first authorship. While Lucas Hille focussed on laser structuring of graphite anodes, Josef Keilhofer was responsible for mechanical electrode

structuring. Both authors equally analyzed the created electrodes, interpreted the obtained data, and wrote the initial manuscript draft. Roman Mazur conducted experiments featuring electrode production and sample characterization. Rüdiger Daub and Michael F. Zaeh supervised the research project and ensured its funding. All authors reviewed the manuscript and commented on the obtained results.

5.2 Discussion

5.2.1 Classification with respect to the literature

All scientific studies presented in the previous Section 5.1 clearly distinguished themselves from the respective state of the art at the time of publication. The individual novelty of each article with respect to the existing literature is outlined in the following.

P1: Laser structuring of graphite anodes and NMC cathodes – Proportionate influence on electrode characteristics and cell performance

Although there have been numerous experimental studies on laser structuring of either anodes or cathodes (cf. Section 3.1.1), literature on the combined structuring of both electrodes is scarce. MATSUMOTO et al. (2023), TSUDA et al. (2018), and WATANABE et al. (2019) have structured graphite anodes and LFP cathodes, but in all experiments the electrode coatings and current collectors were perforated, differing from the approach of this thesis. In a study by PARK, JEON, et al. (2021), graphite anodes and LCO cathodes were structured with laser radiation, demonstrating the potential for high-energy LIBs. Yet, the very thick coatings limited the investigation to low currents. In all above-mentioned studies, the respective impact of individual anode and cathode structuring was not regarded. Furthermore, a comparison of anode structuring against cathode structuring was due for NMC, which is widely applied for automotive applications (DING et al. 2019). Also, synthetic graphite, which gains in importance as an active material for the anode due to its beneficial electrochemical properties (MA et al. 2013; XING et al. 2018), has not been laser-structured according to the state of the art. In this context, the novelty of P1 lies in the following aspects:

- quantification of the respective impact of electrode structuring on LIB performance if applied on the anode or the cathode, respectively, in comparison to a combined structuring of both electrodes as well as reference cells without electrode structuring,
- experimental investigation of the underlying rate-limiting electrochemical mechanisms in LIBs caused by the anode and the cathode, respectively, by conducting an ICA,

- experimental quantification of electrochemical parameters such as the ionic resistance, the tortuosity, and the MacMullin number for laser-structured battery electrodes with EIS and TLM,
- evidence of battery performance enhancements by laser structuring of synthetic graphite anodes in contrast to natural graphite anodes.

P2: Influence of laser structuring and calendering of graphite anodes on electrode properties and cell performance

Besides the choice of material, the loading and porosity of an electrode remarkably influence its micro-structural and electrochemical characteristics such as the tortuosity and the rate capability (cf. Section 2.1.4). PARK, JEON, et al. (2021) demonstrated a significant advantage of employing laser structuring on electrodes with high mass loading. Additionally, DUBEY et al. (2021) documented enhanced performance in low porosity electrodes that underwent laser structuring compared to both calendered and uncalendered electrodes without structuring. Yet, the interdependencies between the bulk electrode porosity, adjusted by electrode calendering (cf. Section 2.1.5), and the directed porosity created by laser structuring, have not been systematically investigated in the literature so far. In this context, the novelty of P2 lies in the following aspects:

- quantification of the particular impact of laser-structured holes and different bulk porosity values on electrode properties and LIB performance,
- measurement of the pore size distribution in laser-structured electrodes with MIP,
- observation of an inhomogeneous sodium distribution on electrode surfaces with EDX, indicating binder evaporation and re-deposition during laser structuring,
- documentation of electrode thickness increases by laser structuring and evaluation of the implications for the energy density of LIBs,
- delivery of detailed insights into the interdependencies of bulk electrode porosity and laser structuring with respect to the energy and power densities of LIBs in a Ragone plot,
- identification of an ideal window for the application of laser structuring in terms of bulk electrode porosity.

P3: Integration of laser structuring into the electrode manufacturing process chain for lithium-ion batteries

The production of LIBs involves numerous sequential process steps that are interconnected in various ways (KWADE et al. 2018; WESTERMEIER et al. 2014).

Therefore, integrating laser structuring into industrial battery manufacturing would significantly impact product characteristics due to interdependencies with other processes. For instance, the structuring of electrodes has been demonstrated to influence the electrolyte filling by expediting the time-consuming wetting procedure (BERHE and LEE 2021; HABEDANK, GUENTER, et al. 2019; KLEEFOOT et al. 2021; PFLEGING and PRÖLL 2014). In preceding studies, laser structuring typically occurs after electrode production, i.e., after calendering, but before cell assembly (HABEDANK et al. 2020; KIM et al. 2018). However, the effect of varying positions for process integration on the final product properties has not yet been assessed in previously existing literature. In this context, the novelty of P3 lies in the following aspects:

- comparison of three process integration positions for laser electrode structuring regarding geometrical, mechanical, and electrochemical quality criteria showing advantages and disadvantages of the respective options,
- report of significant decreases in the mechanical integrity of battery electrodes, which are laser-structured in a dry state, resulting in challenges for an industrial application,
- realization of laser structuring of wet battery electrodes containing solvent residues, revealing a different ablation mechanism compared to laser structuring of dry electrodes,
- observation of clogging of the laser-created structures by subsequent calendering, which was yet identified to not significantly impede the electrochemical performance improvements.

P4: Automated geometry characterization of laser-structured battery electrodes

In process studies on laser electrode structuring, the hole geometries are commonly characterized using topographic microscopy techniques, such as digital LM (MEYER et al. 2023), confocal LM (HABEDANK, ENDRES, et al. 2018), LSM (HABEDANK, KRIEGLER, et al. 2019), or white light interferometry (WLI) (KLEEFOOT et al. 2022). The corresponding manual analysis procedures are time-intensive and lack reproducibility, thus requiring novel approaches for automated data analysis. In this context, the novelty of P4 lies in the following aspects:

- the creation of an automated method for hole geometry characterization of laser-structured electrodes,
- ensuring reproducibility of the hole geometry determination for a targeted process design,
- allowing significant reduction of the analysis effort in process studies,

- the application of an IRLS algorithm for reference plane fitting and image segmentation of electrode surfaces,
- showcasing of the method's transferability to other use cases from battery production.

P5: Picosecond laser structuring of graphite anodes – Ablation characteristics and process scaling

Despite the existing variety of process studies on laser electrode structuring (cf. Section 2.2), the impact of certain processing parameters, such as the laser wavelength and the pulse repetition rate, remains unclear for picosecond laser structuring of graphite anodes. Additionally, the potential of laser processing with PBs – known to enable a high material removal in other applications (LICKSCHAT et al. 2021; METZNER et al. 2021; NEUENSCHWANDER et al. 2015; NEUENSCHWANDER et al. 2019) – has not been explored for laser electrode structuring. HUANG et al. (2021) investigated the effect of PBs on delamination width and maximum cutting speed in laser cutting of graphite-copper-graphite electrodes. However, the process differs fundamentally from laser structuring as pursued in this thesis due to the necessity to penetrate the copper current collector, which has a significantly higher ablation threshold than graphite (SCHMIEDER 2012). It was found that the ideal parameters for laser cutting of electrodes are those optimizing the ablation efficiency of the metallic substrate foils (LUTEY et al. 2015). Existing studies on laser structuring of battery electrodes have focused on ablation depth, with minimal or no attention given to the hole diameters. In the literature, diverse strategies for process scaling of laser electrode structuring, such as polygon scanners (HABEDANK et al. 2020), hollow cylinders with internal beam guidance (YAMADA, SOMA, et al. 2023), or DLIP (ZWAHR et al. 2023), were proposed. DOEs, in contrast, have not been used for electrode structuring so far, despite their capability for productivity increases showcased in other applications (BRUENING et al. 2018; GILLNER et al. 2019; HOFMANN et al. 2020). Finally, the laser powers needed for industrial laser structuring of electrodes and the associated costs have not been quantified in the literature. In this context, the novelty of P5 lies in the following aspects:

- examination of processing parameters such as the laser wavelength or the pulse repetition rate for picosecond laser structuring of graphite anodes,
- application of PBs for laser structuring of battery electrodes,
- consistent consideration of the created hole diameters in the process study,
- realization of beam splitting using a DOE to increase the processing rate of laser electrode structuring,

- modeling of theoretical processing rates of laser electrode structuring as a basis for a scalability assessment,
- quantification of production costs associated with scaled laser structuring of electrodes.

P6: Enhanced performance and lifetime of lithium-ion batteries by laser structuring of graphite anodes

With the exception of CHEN et al. (2020) and HABEDANK, GUENTER, et al. (2019), the advantages of laser electrode structuring have been only demonstrated in laboratory settings using manually assembled, small-scale coin cells. However, statements on the lifetime and degradation mechanisms, for instance, are only possible to a limited extent with coin cells. Furthermore, transitioning laser structuring to cell formats relevant for industrial purposes and establishing the necessary production infrastructure is crucial (KEPPELER et al. 2020; KWADE et al. 2018). In this context, the novelty of P6 lies in the following aspects:

- production of large-format LIBs with laser-structured graphite anodes using semi-automated production equipment,
- description of structuring effects on the discharge capability of large-format LIBs under different operating conditions, i.e., current rates and ambient temperatures, featuring a discussion of the implications on cell capacity and energy density,
- analysis of the LIB fast-charging behavior by determining the influence of electrode structuring on the transport and impedance resistances, charging time, and achievable capacities,
- proof of a significant extension of the LIB cyclic lifetime under fast charging conditions through laser structuring with a determination of different aging effects using ICA,
- verification of reduced lithium plating by electrode structuring in post-mortem SEM and EDX analyses.

P7: Comparative evaluation of graphite anode structuring for lithium-ion batteries using laser ablation and mechanical embossing

As outlined in Section 3.2, mechanical embossing is a promising alternative to laser radiation for electrode structuring. In previously existing studies, blades, shaped silicon wafers (BRYNTESEN et al. 2023) or embossing stamps with a needle-type surface structure (SANDHERR et al. 2023) were used to structure electrodes. Both mentioned studies used laboratory presses, which are unsuitable for continuous electrode manufacturing in roll-to-roll processes. In contrast, mechanical structuring using an embossing roller, as suggested by KEILHOFER et al. (2023), holds promise for achieving high throughputs in electrode

manufacturing for LIBs. In this context, the novelty of P7 lies in the following aspects:

- integration of the mechanical structuring process into continuous roll-to-roll electrode production,
- merger of the mechanical embossing process with the calendering process into a novel process called structure calendering,
- initial comparison of laser structuring and structure calendering of electrodes for LIBs,
- comparative quantification of microstructural, mechanical, and electrochemical electrode properties obtained by structuring with laser radiation and mechanical embossing,
- qualitative assessment of both electrode structuring processes regarding production engineering aspects, such as processing rate, energy demand, investment costs, contamination risk, process flexibility, precision, or maintenance effort.

5.2.2 Contribution to research fields

This dissertation addresses the intersection between laser and LIB technology (cf. Figure 5.1). The production-technical roots of this work lie in considering a novel type of production process, which yet considerably alters product properties. Hence, the analysis of LIB product characteristics has been a major scope throughout this dissertation besides process studies. The latter ones belong to the research field of production engineering, which can be clustered into the fields of battery production (top left quadrant in Figure 5.1) and laser materials processing (bottom left quadrant in Figure 5.1).

P1 and P2 focused on interdependencies between inherent product properties of LIB electrodes and laser structuring and thus advanced the comprehension of LIB electrode characteristics and cell performance. With the integration of laser structuring into the process chain of LIB manufacture, a production technology issue has been addressed in P3. Yet, significant influences on the resulting product properties were observed, and thus P3 is assigned to the fields of LIB product and production alike. The method developed for P4 contributes to the field of laser materials processing, as it can be used for the design and analysis of process studies as well as process monitoring. The major scope of P5 lies in the field of laser materials processing, too, as process understanding and scaling have been advanced. The conducted economic assessment of the process targets the intersection between laser technology and battery production. P6 contributed to the field of battery production by applying semi-automated production equipment to manufacture laser-structured LIBs. In addition, detailed electrochemical analyses were provided in the study, delivering insights into the

resulting LIB product properties. In P7, production engineering aspects and product properties of LIBs were regarded, positioning the study at the intersection between LIB technology and production.

The assignment of the studies to the respective research fields is also reflected by the choice of scientific journals (cf. Figure 5.1). While P1 and P2 were published in journals with a strong fundamental, electrochemical focus, P3, P6, and P7 were issued in magazines addressing an audience which is more holistically interested in LIB technology. In contrast, P4 and P5 were placed in a production engineering and laser technology journal, respectively.

5.2.3 Consistency and transferability of the results

In this dissertation, diverse experimental methods have been used to study laser structuring of LIB electrodes and advance its industrial application (cf. Section 4.3). For this purpose, cell chemistries and laser beam sources, which can be considered state of the art, were applied. Thus, the major outcomes reported in this thesis are expected to possess general validity. However, discrete values, e.g., for increases in LIB cycling capability or reduction in electrode tortuosity, are obviously specific to the used materials as well as cell and electrode design. Also, some of the obtained phenomena or trends might depend on the studied material systems. For instance, a decrease of the electrode coating's mechanical integrity by laser structuring was observed in the elaboration of P3, but not in P5 and P7. This could arise from differences in hole spacing, laser processing parameters, or electrode composition, resulting in diverse mechanical failure mechanisms, i.e., cohesive versus adhesive breakage. Also, the electrode capacitance, which correlates with the electrochemically active surface area, showed a different behavior in P1 than in the subsequent studies P2, P3, and P7, possibly emerging from the same causes listed above for the mechanical properties. These differences, however, deliver further insights into specific product characteristics of LIB electrodes and thereby broaden the understanding of the intricate process-product relationships in LIB production. Also, the major trends reported are consistent between all publications in this thesis and in agreement with preceding and succeeding literature.

In addition to experimental procedures pursued in this thesis, theoretical frameworks were created, refined, and applied throughout the dissertation. In various publications, the applicability of the TLM developed by LANDESFEIND et al. (2016) was showcased for laser-structured LIB electrodes. Furthermore, it was shown that ICA allows to gain insights into the electrochemical mechanisms influencing the cycling behavior of LIBs with laser-structured electrodes. The surface analysis method developed for P4 was shown to be transferable to other applications, such as identifying and characterizing indentations in LIB current collector foils. Utilization of the approach for process monitoring, in addition to the demonstrated benefit for process design, is feasible. The cost model of P6 was used for calculating expenditures in a defined production scenario but is generally capable of considering variations in all assumptions, such as equip-

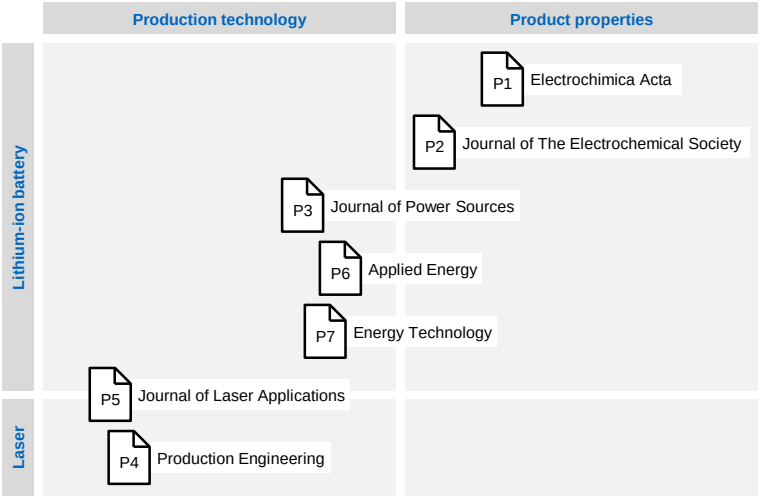

Figure 5.1: Assignment of this dissertation's publications (Ps) to research fields with an indication of the scientific journals

ment expenditures, labor costs, or energy prices. Thus, the approach can be transferred to different LIB production facilities, and sensitivity analyses are possible. Furthermore, the model can be adjusted to production processes differing from battery production. Conclusively, the methods used and developed in this work are of value for future generations of researchers in the fields of laser materials processing and LIB technology due to their versatile applicability.

Chapter 6

Conclusion

This chapter concludes the dissertation by summarizing the key contents and providing an outlook on potential future fields of research and development.

6.1 Summary

LIBs are key components for diverse technical applications, such as consumer electronics or electromobility. They permit the electrochemical storage and release of energy by the intercalation and de-intercalation of lithium ions (cf. Section 2.1). Intrinsic properties of the porous electrode materials limit the fast-charging and fast-discharging capability of an LIB (cf. Section 2.1.4). In this context, ultrashort-pulsed laser radiation (cf. Section 2.2) allows for the creation of microscopic holes in the electrode coatings which facilitate lithium-ion diffusion. As a consequence, cell-internal overpotentials during operation are reduced, resulting in an increased obtainable LIB capacity at high current rates, enhanced fast-charging capability, and mitigation of cell degradation by lithium-plating, prolonging the cell lifetime (cf. Chapter 3).

However, laser structuring of LIB electrodes has not progressed from the laboratory scale to a widespread industrial application so far due to diverse production engineering challenges (cf. Section 3.3). Five critical issues were identified and defined as the scientific challenges for this dissertation (cf. Chapter 4):

- a limited knowledge regarding the intricate process-product relationships in laser structuring of battery electrodes
- the integration of laser structuring into the battery manufacturing process chain
- the elaborate process design for laser structuring of battery electrodes
- the low processing rate of laser electrode structuring
- the technical and economic viability of the process

The above-mentioned points were addressed in seven studies (cf. Chapter 5.1). Initially, interdependencies between electrode properties, such as the coating porosity or material composition, on the one hand and laser structuring on the other hand, were experimentally examined and quantified for state-of-the-art cell chemistries. Two publications showed that laser structuring offers a particular potential to improve the electrochemical LIB performance if applied to graphite anodes with a specific porosity.

Furthermore, three different positions for integrating laser structuring into the existing electrode production chain were investigated, revealing distinct ablation mechanisms between the structuring of electrodes with and without solvent residues. Dissimilar mechanical, geometrical, and electrochemical product properties resulted, complicating a clear recommendation for process integration due to the diverse benefits and detriments of the different options.

According to the state of the art, the design of the laser structuring process required elaborate empirical studies and an extensive manual effort for sample analysis because of complex process-product relationships. In response, an approach for the automated geometry characterization of laser-structured holes with high reliability and reproducibility was developed, substituting the time-intensive manual analysis of image data.

Furthermore, gaps in the state of knowledge regarding the influence of specific laser process parameters, such as the wavelength or pulse repetition rate, on the resulting hole geometries were filled. The processing rate of laser structuring was remarkably increased by the application of a DOE for beam splitting, showcasing the general suitability of the approach since comparable hole geometries as with single-beam laser structuring were achieved in significantly less time without deterioration of the mechanical material properties. Multi-kilowatt ultrashort-pulsed laser powers were identified to be necessary for realizing industrial processing rates, while corresponding to only moderate LIB cost increases.

Using the semi-automated equipment of the pilot LIB production line at the *iwb*, the electrochemical benefits of laser structuring were demonstrated by manufacturing LIB pouch cells. Finally, the creation of structured electrodes using laser radiation was examined in contrast to mechanical embossing, which is widely considered a promising processing alternative. A differentiated evaluation regarding the achievable product properties and production aspects was obtained, underlining the relevance of both methods for future research and development.

It was asserted that these results augment the existing state of knowledge in the fields of laser materials processing and LIB technology (cf. Section 5.2). Slight disparities between the individual studies were critically discussed (cf. Section 5.2.3), but concluded to not limit the general validity of the obtained findings.

6.2 Outlook

Although this thesis has advanced the knowledge on various aspects of laser electrode structuring toward industrial applicability, further technological development is needed and academic research fields remain to be explored.

Beam splitting for increased productivity, as showcased in this thesis, needs to be developed further, i.e., significantly more sub-beams have to be created to achieve industrially relevant processing rates. At the same time, optical devices for beam splitting and beam deflection might be combined to cover the spatial directions parallel and perpendicular to the electrode feed. In this context, the needed synchronization of laser beam deflection and substrate motion is technically challenging. The beam deflection units and laser beam sources have to be integrated into existing machine concepts for electrode production to facilitate a scaled application of laser structuring with high throughput. This is necessary to evaluate quality-relevant aspects of the process, such as particle contamination, with statistical means. The high importance of technical cleanliness in battery production is due to potential failures in LIB operation as a consequence of contamination resulting in safety risks.

As outlined in this dissertation, laser structuring of battery electrodes is characterized by intricate relationships between processing parameters and product properties. Hence, modeling the process might facilitate the process design further and deepen the understanding of the underlying phenomena in the future. The resulting models can be either purely data-based, using artificial intelligence, for instance, or physics-based, e.g., by considering the two-temperature model (cf. Section 2.2.4). The latter supposedly provides insights into the ablation phenomena such as selective binder evaporation, but is challenging to design and simulate due to the multi-material, porous composition of electrodes. A data-based process model, in contrast, is easy to set up and train, presumably delivering precise results for process prediction in terms of resulting hole geometries, but does not contribute to a physical understanding of the process.

Besides laser structuring, mechanical embossing of electrodes deserves further consideration. While numerous studies have investigated laser radiation as a tool, scientific publications on the mechanical structuring of LIB electrodes are scarce. Consequently, various production engineering and electrochemical aspects of the process remain to be explored, e.g., how the direct contact between tool and electrode results in wear or if locally compacted particles at the hole walls influence the long-term electrochemical stability.

The concept of three-dimensionally structured electrodes was recently transferred from LIBs to SSBs, showcasing the enormous potential for electrochemical performance improvements in this field (KRIEGLER, JAIMEZ-FARNHAM, et al. 2023; XU et al. 2021; YAN 2022). However, various issues, such as the design of suited structures, the development of scalable processing strategies, and the understanding of process-product interdependencies remain unaddressed, creating a broad demand for further scientific exploration.

Bibliography

ABRAHAM, K. M. (1993). "Directions in secondary lithium battery research and development". In: *Electrochimica Acta* 38.9, pp. 1233–1248. ISSN: 00134686. DOI: 10.1016/0013-4686(93)80054-4.

AHMADI, S., MADDIPATLA, D., PALANIAPPAN, V., EMANI, H., HAJIAN, S., WU, Q., and ATASHBAR, M. Z. (2022). "3D Architectures of a Thick Graphite Anode Enabled by Laser Patterning Process to Improve Capacity Density and Cycling Performance of LIBs". In: *2022 IEEE Sensors*. IEEE, pp. 01–04. ISBN: 978-1-6654-8464-0. DOI: 10.1109/SENSORS52175.2022.9967249.

AMIN, R., DELATTRE, B., TOMSIA, A. P., and CHIANG, Y.-M. (2018). "Electrochemical Characterization of High Energy Density Graphite Electrodes Made by Freeze-Casting". In: *ACS Applied Energy Materials* 1.9, pp. 4976–4981. ISSN: 2574-0962. DOI: 10.1021/acsaem.8b00962.

ANDRE, D., HAIN, H., LAMP, P., MAGLIA, F., and STIASZNY, B. (2017). "Future high-energy density anode materials from an automotive application perspective". In: *Journal of Materials Chemistry A* 5.33, pp. 17174–17198. ISSN: 2050-7488. DOI: 10.1039/C7TA03108D.

ANDRE, D., KIM, S.-J., LAMP, P., LUX, S. F., MAGLIA, F., PASCHOS, O., and STIASZNY, B. (2015). "Future generations of cathode materials: an automotive industry perspective". In: *Journal of Materials Chemistry A* 3.13, pp. 6709–6732. ISSN: 2050-7488. DOI: 10.1039/C5TA00361J.

ANISIMOV, S. I., KAPELIOVICH, B. L., and PEREL'MAN, T. L. (1974). "Electron emission from metal surfaces exposed to Electron Electron emission from metal surfaces exposed to ultrashort laser pulses". In: *Sov. Phys.-JETP* 39.2, pp. 375–377.

ARTHUR, T. S., BATES, D. J., CIRIGLIANO, N., JOHNSON, D. C., MALATI, P., MOSBY, J. M., PERRE, E., RAWLS, M. T., PRIETO, A. L., and DUNN, B. (2011). "Three-dimensional electrodes and battery architectures". In: *MRS Bulletin* 36.7, pp. 523–531. ISSN: 0883-7694. DOI: 10.1557/mrs.2011.156.

ASHURI, M., HE, Q., and SHAW, L. L. (2016). "Silicon as a potential anode material for Li-ion batteries: where size, geometry and structure matter". In: *Nanoscale* 8.1, pp. 74–103. DOI: 10.1039/c5nr05116a.

ATKINS, P. and PAULA, J. de (2005). *Termodynamics and kinetics*. 8th ed. Vol. 1. Physical chemistry. New York: W.H. Freeman and Co. ISBN: 0-7167-8759-8.

BEHR, S., AMIN, R., CHIANG, Y.-M., and TOMSIA, A. (2015). "Highly-Structured, Additive-Free Lithium-Ion Cathodes by Freeze-Casting Technology". In: *Ceramic Forum International* 92, pp. 39–43.

BERHE, M. G. and LEE, D. (2021). "A Comparative Study on the Wettability of Unstructured and Structured $LiFePO_4$ with Nanosecond Pulsed Fiber Laser". In: *Micromachines* 12.5, p. 582. DOI: 10.3390/mi12050582.

BILLAUD, J., BOUVILLE, F., MAGRINI, T., VILLEVIEILLE, C., and STUDART, A. R. (2016). "Magnetically aligned graphite electrodes for high-rate performance Li-ion batteries". In: *Nature Energy* 1.8. DOI: 10.1038/nenergy.2016.97.

BIRKL, C. R., ROBERTS, M. R., MCTURK, E., BRUCE, P. G., and HOWEY, D. A. (2017). "Degradation diagnostics for lithium ion cells". In: *Journal of Power Sources* 341, pp. 373–386. ISSN: 03787753. DOI: 10.1016/j.jpowsour.2016.12.011.

BLIEDTNER, J., MÜLLER, H., and BARZ, A. (2013). *Lasermaterialbearbeitung: Grundlagen - Verfahren - Anwendungen - Beispiele*. München: Fachbuchverl. Leipzig im Carl-Hanser-Verl. ISBN: 978-3-446-42929-1.

BLOMGREN, G. E. (2017). "The Development and Future of Lithium Ion Batteries". In: *Journal of The Electrochemical Society* 164.1, pp. 5019–5025. ISSN: 0013-4651. DOI: 10.1149/2.0251701jes.

BOLSINGER, M., WELLER, M., RUCK, S., KAYA, P., RIEGEL, H., and KNOBLAUCH, V. (2020). "Selective surface treatment by means of IR-laser – A new approach to enhance the rate capability of cathodes for Li-ion batteries". In: *Electrochimica Acta* 330, p. 135163. ISSN: 00134686. DOI: 10.1016/j.electacta.2019.135163.

BRUENING, S., DU, K., JARCZYNSKI, M., JENKE, G., and GILLNER, A. (2018). "Ultra-fast laser micro processing by multiple laser spots". In: *Procedia CIRP* 74, pp. 573–580. ISSN: 22128271. DOI: 10.1016/j.procir.2018.08.084.

BRUGGEMAN, D. A. G. (1935). "Berechnung verschiedener physikalischer Konstanten von heterogenen Substanzen. I. Dielektrizitätskonstanten und Leitfähigkeiten der Mischkörper aus isotropen Substanzen". In: *Annalen der Physik* 416.7, pp. 636–664. ISSN: 0003-3804. DOI: 10.1002/andp.19354160705.

BRYNTESEN, S. N., FINNE, P. H., SVENSSON, A. M., SHEARING, P. R., TOLSTIK, N., SOROKINA, I. T., VINJE, J., LAMB, J. J., and BURHEIM, O. S. (2023). "Structured aqueous processed lignin-based NMC cathodes for energy-dense LIBs with improved rate capability". In: *Journal of Materials Chemistry A* 11.12, pp. 6483–6502. ISSN: 2050-7488. DOI: 10.1039/D2TA08606A.

BUDDE-MEIWES, H., DRILLKENS, J., LUNZ, B., MUENNIX, J., ROTHGANG, S., KOWAL, J., and SAUER, D. U. (2013). "A review of current automotive battery technology and future prospects". In: *Proceedings of the Institution of Mechanical Engineers, Part D: Journal of Automobile Engineering* 227.5, pp. 761–776. ISSN: 0954-4070. DOI: 10.1177/0954407013485567.

BUNDY, F. P., BASSETT, W. A., WEATHERS, M. S., HEMLEY, R. J., MAO, H. U., and GONCHAROV, A. F. (1996). "The pressure-temperature phase and transformation diagram for carbon; updated through 1994". In: *Carbon* 34.2, pp. 141–153. ISSN: 00086223. DOI: 10.1016/0008-6223(96)00170-4.

BUQA, H., GOERS, D., HOLZAPFEL, M., SPAHR, M. E., and NOVÁK, P. (2005). "High Rate Capability of Graphite Negative Electrodes for Lithium-Ion Batteries". In: *Journal of The Electrochemical Society* 152.2, A474. ISSN: 0013-4651. DOI: 10.1149/1.1851055.

CARMAN, P. C. (1997). "Fluid flow through granular beds". In: *Chemical Engineering Research and Design* 75, S32–S48. ISSN: 0263-8762. DOI: 10.1016/S0263-8762(97)80003-2.

CHEN, K.-H., NAMKOONG, M. J., GOEL, V., YANG, C., KAZEMIABNAVI, S., MORTUZA, S. M., KAZYAK, E., MAZUMDER, J., THORNTON, K., SAKAMOTO, J., and DASGUPTA, N. (2020). "Efficient fast-charging of lithium-ion batteries enabled by laser-patterned three-dimensional graphite anode architectures". In: *Journal of Power Sources* 471, p. 228475. ISSN: 03787753. DOI: 10.1016/j.jpowsour.2020.228475.

CHENG, D., HUANG, Y., PENG, Y., WANG, B., GUO, W., LIU, Z., and LI, L. (2022). "Environmentally Friendly Single-Step Laser Synthesis of Three-Dimensional C–Si–SiC Micro/Nanoporous Composite Lithium-ion Battery Electrodes and Electrochemical Performance". In: *ACS Applied Energy Materials* 5.5, pp. 6183–6193. ISSN: 2574-0962. DOI: 10.1021/acsaem.2c00580.

CHICHKOV, B. N., MOMMA, C., NOLTE, S., ALVENSLEBEN, F. von, and TÜNNERMANN, A. (1996). "Femtosecond, picosecond and nanosecond laser ablation of solids". In: *Applied Physics A* 63.2, pp. 109–115. ISSN: 1432-0630. DOI: 10.1007/BF01567637.

CHOI, S. and WANG, G. (2018). "Advanced Lithium-Ion Batteries for Practical Applications: Technology, Development, and Future Perspectives". In: *Advanced Materials Technologies* 3.9, p. 1700376. ISSN: 2365709X. DOI: 10.1002/admt.201700376.

COBB, C. L. and BLANCO, M. (2014). "Modeling mass and density distribution effects on the performance of co-extruded electrodes for high energy density lithium-ion batteries". In: *Journal of Power Sources* 249, pp. 357–366. ISSN: 03787753. DOI: 10.1016/j.jpowsour.2013.10.084.

COBB, C. L. and SOLBERG, S. E. (2017). "Communication—Analysis of Thick Co-Extruded Cathodes for Higher-Energy-and-Power Lithium-Ion Batteries". In: *Journal of The Electrochemical Society* 164.7, A1339–A1341. ISSN: 0013-4651. DOI: 10.1149/2.0101707jes.

DANG, D., WANG, Y., GAO, S., and CHENG, Y.-T. (2020). "Freeze-dried low-tortuous graphite electrodes with enhanced capacity utilization and rate capability". In: *Carbon* 159, pp. 133–139. ISSN: 00086223. DOI: 10.1016/j.carbon.2019.12.036.

DANIEL, C. and BESENHARD, J. O., eds. (2011). *Handbook of battery materials*. 2., completely rev. and enl. ed. Weinheim: Wiley-VCH-Verl. ISBN: 978-3-527-32695-2.

DELATTRE, B., AMIN, R., SANDER, J., CONINCK, J. de, TOMSIA, A. P., and CHIANG, Y.-M. (2018). "Impact of Pore Tortuosity on Electrode Kinetics in Lithium Battery Electrodes: Study in Directionally Freeze-Cast $LiNi_{0.8}Co_{0.15}Al_{0.05}O_2$ (NCA)". In: *Journal of The Electrochemical Society* 165.2, pp. 388–395. ISSN: 0013-4651. DOI: 10.1149/2.1321802jes.

DING, Y., CANO, Z. P., YU, A., LU, J., and CHEN, Z. (2019). "Automotive Li-Ion Batteries: Current Status and Future Perspectives". In: *Electrochemical Energy Reviews* 2.1, pp. 1–28. ISSN: 2520-8489. DOI: 10.1007/s41918-018-0022-z.

DOKKO, K., SUGAYA, J.-i., MUNAKATA, H., and KANAMURA, K. (2005). "Preparation of micro-dot electrodes of $LiCoO_2$ and $Li_4Ti_5O_{12}$ for lithium micro-batteries". In: *Electrochimica Acta* 51.5, pp. 966–971. ISSN: 00134686. DOI: 10.1016/j.electacta.2005.04.061.

DOMINKO, R., GABERŠČEK, M., DROFENIK, J., BELE, M., and JAMNIK, J. (2003). "Influence of carbon black distribution on performance of oxide cathodes for Li ion batteries". In: *Electrochimica Acta* 48.24, pp. 3709–3716. ISSN: 00134686. DOI: 10.1016/S0013-4686(03)00522-X.

DUBEY, R., ZWAHLEN, M.-D., SHYNKARENKO, Y., YAKUNIN, S., FUERST, A., KOVALENKO, M. V., and KRAVCHYK, K. V. (2021). "Laser Patterning of High-Mass-Loading Graphite Anodes for High-Performance Li-Ion Batteries". In: *Batteries & Supercaps* 4.3, pp. 464–468. ISSN: 2566-6223. DOI: 10.1002/batt.202000253.

DUFFNER, F., KRONEMEYER, N., TÜBKE, J., LEKER, J., WINTER, M., and SCHMUCH, R. (2021). "Post-lithium-ion battery cell production and its compatibility with lithium-ion cell production infrastructure". In: *Nature Energy* 6.2, pp. 123–134. DOI: 10.1038/s41560-020-00748-8.

DUNLAP, N., SULAS-KERN, D. B., WEDDLE, P. J., USSEGLIO-VIRETTA, F., WALKER, P., TODD, P., BOONE, D., COLCLASURE, A. M., SMITH, K., TREMOLET DE VILLERS, B. J., and FINEGAN, D. P. (2022). "Laser ablation for structuring Li-ion electrodes for fast charging and its impact on material properties, rate capability, Li plating, and wetting". In: *Journal of Power Sources* 537, p. 231464. ISSN: 03787753. DOI: 10.1016/j.jpowsour.2022.231464.

EICHLER, H. J., EICHLER, J., and LUX, O. (2018). *Lasers: Basics, Advances and Applications*. 1st ed. 2018. Vol. 220. Springer Series in Optical Sciences. Cham: Springer International Publishing. ISBN: 9783319998954.

ENDERLE, S., BOLSINGER, M., RUCK, S., KNOBLAUCH, V., and RIEGEL, H. (2020). "Thermophysical modeling of selective laser ablation processing of lithium-ion battery cathodes". In: *Journal of Laser Applications* 32.4, p. 042008. ISSN: 1042-346X. DOI: 10.2351/7.0000200.

ERDEY-GRÚZ, T. and VOLMER, M. (1930). "Zur Theorie der Wasserstoff Überspannung". In: *Zeitschrift für Physikalische Chemie* 150A.1, pp. 203–213. ISSN: 0942-9352. DOI: 10.1515/zpch-1930-15020.

FANN, W. S., STORZ, R., TOM, H. W., and BOKOR, J. (1992). "Electron thermalization in gold". In: *Physical review. B, Condensed matter* 46.20, pp. 13592–13595. ISSN: 0163-1829. DOI: 10.1103/PhysRevB.46.13592.

FINK, S., DEMIR, D., BÖRNER, M., GÖKEN, V., and VEDDER, C. (2023). "High-Speed Laser Drying of Lithium-Ion Battery Anodes: Challenges and Opportunities". In: *World Electric Vehicle Journal* 14.9, p. 255. DOI: 10.3390/wevj14090255.

FÖRSTER, R. and FÖRSTER, A. (2018). *Einführung in die Fertigungstechnik: Lehrbuch für Studenten ohne Vorpraktikum*. SpringerLink Bücher. Berlin and Heidelberg: Springer Vieweg. ISBN: 9783662547021. DOI: 10.1007/978-3-662-54702-1.

FRITH, J. T., LACEY, M. J., and ULISSI, U. (2023). "A non-academic perspective on the future of lithium-based batteries". In: *Nature communications* 14.1, p. 420. DOI: 10.1038/s41467-023-35933-2.

GALLAGHER, K. G., TRASK, S. E., BAUER, C., WOEHRLE, T., LUX, S. F., TSCHECH, M., LAMP, P., POLZIN, B. J., HA, S., LONG, B., WU, Q., LU, W., DEES, D. W., and JANSEN, A. N. (2015). "Optimizing Areal Capacities through Understanding the Limitations of Lithium-Ion Electrodes". In: *Journal of The Electrochemical Society* 163.2, pp. 138–149. ISSN: 0013-4651. DOI: 10.1149/2.0321602jes.

GAO, H., WU, Q., HU, Y., ZHENG, J. P., AMINE, K., and CHEN, Z. (2018). "Revealing the Rate-Limiting Li-Ion Diffusion Pathway in Ultrathick Electrodes for Li-Ion Batteries". In: *The Journal of Physical Chemistry Letters* 9.17, pp. 5100–5104. DOI: 10.1021/acs.jpclett.8b02229.

GASTOL, D., CAPENER, M., REYNOLDS, C., CONSTABLE, C., and KENDRICK, E. (2021). "Microstructural design of printed graphite electrodes for lithium-ion batteries". In: *Materials & Design*, p. 109720. ISSN: 02641275. DOI: 10.1016/j.matdes.2021.109720.

GEBREKIROS BERHE, M., GEUN OH, H., PARK, S.-K., MONDAL, M., and LEE, D. (2023). "Effect of laser-induced groove morphology on the wettability and performance of Lithium-ion batteries". In: *Materials & Design*, p. 112020. ISSN: 02641275. DOI: 10.1016/j.matdes.2023.112020.

GENTLE, J. E. (2007). *Matrix Algebra: Theory, Computations, and Applications in Statistics*. SpringerLink Bücher. New York, NY: Springer New York. ISBN: 9780387708737. DOI: 10.1007/978-0-387-70873-7.

GIALAMPOUKI, M. A., HASHEMI, J., and PETERSON, A. A. (2019). "The Electrochemical Mechanisms of Solid–Electrolyte Interphase Formation in Lithium-Based Batteries". In: *The Journal of Physical Chemistry C* 123.33, pp. 20084–20092. ISSN: 1932-7447. DOI: 10.1021/acs.jpcc.9b03886.

GILLNER, A., FINGER, J. :, GRETZKI, P., NIESSEN, M., BARTELS, T., and REININGHAUS, M. (2019). "High Power Laser Processing with Ultrafast and Multi-Parallel Beams". In: *Journal of Laser Micro/Nanoengineering*. DOI: 10.2961/jlmn.2019.02.0003.

GOEL, V., CHEN, K.-H., DASGUPTA, N. P., and THORNTON, K. (2023). "Optimization of laser-patterned electrode architectures for fast charging of Li-ion batteries using simulations parameterized by machine learning". In: *Energy Storage Materials* 57, pp. 44–58. ISSN: 24058297. DOI: 10.1016/j.ensm.2023.01.050.

GRABMANN, S., KICK, M. K., GEIGER, C., HARST, F., BACHMANN, A., and ZAEH, M. F. (2022). "Toward the flexible production of large-format lithium-ion batteries using laser-based cell-internal contacting". In: *Journal of Laser Applications* 34.4, p. 042017. ISSN: 1042-346X. DOI: 10.2351/7.0000778.

GULBINSKA, M. K. (2014). *Lithium-ion Battery Materials and Engineering*. London: Springer London. ISBN: 978-1-4471-6547-7. DOI: 10.1007/978-1-4471-6548-4.

HABEDANK, J. B., ENDRES, J., SCHMITZ, P., ZAEH, M. F., and HUBER, H. P. (2018). "Femtosecond laser structuring of graphite anodes for improved lithium-ion batteries: Ablation characteristics and process design". In: *Journal of Laser Applications* 30.3, p. 032205. ISSN: 1042-346X. DOI: 10.2351/1.5040611.

HABEDANK, J. B., KRAFT, L., RHEINFELD, A., KREZDORN, C., JOSSEN, A., and ZAEH, M. F. (2018). "Increasing the Discharge Rate Capability of Lithium-Ion Cells with Laser-Structured Graphite Anodes: Modeling and Simulation". In: *Journal of The Electrochemical Society* 165.7, pp. 1563–1573. ISSN: 0013-4651. DOI: 10.1149/2.1181807jes.

HABEDANK, J. B., GUENTER, F. J., BILLOT, N., GILLES, R., NEUWIRTH, T., REINHART, G., and ZAEH, M. F. (2019). "Rapid electrolyte wetting of lithium-ion batteries containing laser structured electrodes: in situ visualization by neutron radiography". In: *The International Journal of Advanced Manufacturing Technology* 102.9-12, pp. 2769–2778. ISSN: 0268-3768. DOI: 10.1007/s00170-019-03347-4.

HABEDANK, J. B., KRIEGLER, J., and ZAEH, M. F. (2019). "Enhanced Fast Charging and Reduced Lithium-Plating by Laser-Structured Anodes for Lithium-Ion Batteries". In: *Journal of The Electrochemical Society* 166.16, pp. 3940–3949. ISSN: 0013-4651. DOI: 10.1149/2.1241915jes.

HABEDANK, J. B., SCHWAB, D., KIESBAUER, B., and ZAEH, M. F. (2020). "Paving the way for industrial ultrafast laser structuring of lithium-ion battery electrodes by increasing the scanning accuracy". In: *Journal of Laser Applications* 32.2, p. 022053. ISSN: 1042-346X. DOI: 10.2351/7.0000078.

HAMAMOTO, K., FUKUSHIMA, M., MAMIYA, M., YOSHIZAWA, Y., AKIMOTO, J., SUZUKI, T., and FUJISHIRO, Y. (2012). "Morphology control and electrochemical properties of $LiFePO_4$/C composite cathode for lithium ion batteries". In: *Solid State Ionics* 225, pp. 560–563. ISSN: 01672738. DOI: 10.1016/j.ssi.2012.01.034.

HAMANN, C. H., HAMNETT, A., and VIELSTICH, W. (2007). *Electrochemistry*. 2., completely rev. and updated edition. Weinheim: Wiley-VCH. ISBN: 978-3-527-31069-2.

HILLE, L., HOFFMANN, P., KRIEGLER, J., MAYR, A., and ZAEH, M. F. (2023). "Automated geometry characterization of laser-structured battery electrodes". In: *Production Engineering*. ISSN: 0944-6524. DOI: 10.1007/s11740-023-01191-w.

HILLE, L., KEILHOFER, J., MAZUR, R., DAUB, R., and ZAEH, M. F. (2024). "Comparative Evaluation of Graphite Anode Structuring for Lithium-Ion Batteries Using Laser Ablation and Mechanical Embossing". In: *Energy Technology*. ISSN: 2194-4288. DOI: 10.1002/ente.202301502.

HILLE, L., KICK, M., and ZAEH, M. F. (2020). "Das Laserstrahlschweißen - Wegbereiter in der Batterieproduktion". In: *ATZproduktion* 7.1, pp. 20–23. ISSN: 2192-8886. DOI: 10.1007/s35726-019-0060-9.

HILLE, L., KRIEGLER, J., OEHLER, A., CHAJA, M., WAGNER, S., and ZAEH, M. F. (2023). "Picosecond laser structuring of graphite anodes—Ablation characteristics and process scaling". In: *Journal of Laser Applications* 35.4. ISSN: 1042-346X. DOI: 10.2351/7.0001087.

HILLE, L., NOECKER, M. P., KO, B., KRIEGLER, J., KEILHOFER, J., STOCK, S., and ZAEH, M. F. (2023). "Integration of laser structuring into the electrode manufacturing process chain for lithium-ion batteries". In: *Journal of Power Sources* 556, p. 232478. ISSN: 03787753. DOI: 10.1016/j.jpowsour.2022.232478.

HILLE, L., SENFT, P., KRIEGLER, J., and ZAEH, M. F. (2023). "Current status of laser electrode structuring for enhanced lithium-ion batteries". In: *Lasers in Manufacturing Conference 2023*, pp. 1–9.

HILLE, L., TOEPPER, H.-C., SCHRIEVER, C., KRIEGLER, J., KEILHOFER, J., NOECKER, M. P., and ZAEH, M. F. (2022). "Influence of Laser Structuring and Calendering of Graphite Anodes on Electrode Properties and Cell Performance". In: *Journal of The Electrochemical Society* 169.6, p. 060518. ISSN: 0013-4651. DOI: 10.1149/1945-7111/ac725c.

HILLE, L., XU, L., KEILHOFER, J., STOCK, S., KRIEGLER, J., and ZAEH, M. F. (2021). "Laser structuring of graphite anodes and NMC cathodes – Proportionate influence on electrode characteristics and cell performance". In: *Electrochimica Acta* 392, p. 139002. ISSN: 00134686. DOI: 10.1016/j.electacta.2021.139002.

HOFMANN, O., STOLLENWERK, J., and LOOSEN, P. (2020). "Design of multibeam optics for high throughput parallel processing". In: *Journal of Laser Applications* 32.1, p. 012005. ISSN: 1042-346X. DOI: 10.2351/1.5125778.

HOLZER, L., WIEDENMANN, D., MÜNCH, B., KELLER, L., PRESTAT, M., GASSER, P., ROBERTSON, I., and GROBÉTY, B. (2013). "The influence of constrictivity on the effective transport properties of porous layers in electrolysis and fuel cells". In: *Journal of Materials Science* 48.7, pp. 2934–2952. ISSN: 0022-2461. DOI: 10.1007/s10853-012-6968-z.

HUANG, C., DONTIGNY, M., ZAGHIB, K., and GRANT, P. S. (2019). "Low-tortuosity and graded lithium ion battery cathodes by ice templating". In: *Journal of Materials Chemistry A* 12.7, p. 2174. ISSN: 2050-7488. DOI: 10.1039/C9TA07269A.

HUANG, C. and GRANT, P. S. (2018). "Coral-like directional porosity lithium ion battery cathodes by ice templating". In: *Journal of Materials Chemistry A* 6.30, pp. 14689–14699. ISSN: 2050-7488. DOI: 10.1039/C8TA05049J.

HUANG, J., SHI, W., HUANG, J., XIE, Y., BA, Y., and HE, K. (2021). "High speed pulsed laser cutting of anode material for a Li-ion battery in burst mode". In: *Optical Materials Express* 11.7, p. 2300. DOI: 10.1364/OME.425816.

HÜGEL, H. and GRAF, T. (2009). *Laser in der Fertigung: Strahlquellen, Systeme, Fertigungsverfahren*. 2. Auflage. Wiesbaden: Vieweg + Teubner. ISBN: 9783835100053.

INTERNATIONAL ENERGY AGENCY (2023). *Global EV Outlook 2023: Catching up with climate ambitions*. Ed. by INTERNATIONAL ENERGY AGENCY. Paris. URL: https://www.iea.org/reports/global-ev-outlook-2023 (visited on 08/10/2023).

IZUMI, A., SANADA, M., FURUICHI, K., TERAKI, K., MATSUDA, T., HIRAMATSU, K., MUNAKATA, H., and KANAMURA, K. (2012). "Development of high capacity lithium-ion battery applying three-dimensionally patterned electrode". In: *Electrochimica Acta* 79, pp. 218–222. ISSN: 00134686. DOI: 10.1016/j.electacta.2012.07.001.

JAEGGI, B., NEUENSCHWANDER, B., HUNZIKER, U., ZUERCHER, J., MEIER, T., ZIMMERMANN, M., SELBMANN, K. H., and HENNIG, G. (2012). "Ultra-high-precision surface structuring by synchronizing a galvo scanner with an ultra-short-pulsed laser system in MOPA arrangement". In: *Laser Applications in Microelectronic and Optoelectronic Manufacturing (LAMOM) XVII*. Ed. by HENNIG, G., XU, X., GU, B., and NAKATA, Y. SPIE Proceedings. SPIE, 82430K. DOI: 10.1117/12.909844.

JANG, D., SUH, S., YOON, H., KIM, J., KIM, H., BAEK, J., and KIM, H.-J. (2021). "Enhancing rate capability of graphite anodes for lithium-ion batteries by pore-structuring". In: *Applied Surface Science Advances* 6, p. 100168. ISSN: 26665239. DOI: 10.1016/j.apsadv.2021.100168.

JARA, A. D., BETEMARIAM, A., WOLDETINSAE, G., and KIM, J. Y. (2019). "Purification, application and current market trend of natural graphite: A review". In: *International Journal of Mining Science and Technology* 29.5, pp. 671–689. ISSN: 20952686. DOI: 10.1016/j.ijmst.2019.04.003.

KEILHOFER, J., SCHAFFRANKA, L. W. F., WUTTKE, A., GÜNTER, F. J., HILLE, L., DORAU, F. A., and DAUB, R. (2023). "Mechanical Structuring of Lithium-Ion Battery Electrodes Using an Embossing Roller". In: *Energy Technology* 11, p. 2200869. ISSN: 2194-4288. DOI: 10.1002/ente.202200869.

KEPPELER, M., ROESSLER, S., and BRAUNWARTH, W. (2020). "Production Research as Key Factor for Successful Establishment of Battery Production on the Example of Large-Scale Automotive Cells Containing Nickel-Rich $LiNi_{0.8}Mn_{0.1}Co_{0.1}O_2$ Electrodes". In: *Energy Technology* 8.6. ISSN: 2194-4288. DOI: 10.1002/ente.202000183.

KIM, C., YANG, Y., LOPEZ, D. H., and HA, D. (2020). "Crystal alignment of a $LiNi_{0.5}Mn_{0.3}Co_{0.2}O_2$ electrode material for lithium ion batteries using its magnetic properties". In: *Applied Physics Letters* 117.12, p. 123903. ISSN: 0003-6951. DOI: 10.1063/5.0016456.

KIM, H., PROELL, J., KOHLER, R., PFLEGING, W., and PIQUE, A. (2012). "Laser-printed and processed $LiCoO_2$ cathodethick films for Li-Ion Microbatteries". In: *Journal of Laser Micro Nanoengineering* 7.3, pp. 320–325. DOI: 10.2961/jlmn.2012.03.0016.

KIM, H., SUTTO, T. E., and PIQUÉ, A. (2014). "Laser materials processing for micropower source applications: a review". In: *Journal of Photonics for Energy* 4.1, p. 040992. ISSN: 1947-7988. DOI: 10.1117/1.JPE.4.040992.

KIM, H., SUTTO, T. E., PRÖLL, J., KOHLER, R., PFLEGING, W., and PIQUÉ, A. (2014). "Laser-printed/structured thick-film electrodes for Li-ion microbatteries". In: *Laser-based Micro- and Nanoprocessing VIII*. Ed. by KLOTZBACH, U., WASHIO, K., and ARNOLD, C. B. SPIE Proceedings. SPIE, p. 89680L. DOI: 10.1117/12.2037287.

KIM, T., SONG, W., SON, D.-Y., ONO, L. K., and QI, Y. (2019). "Lithium-ion batteries: outlook on present, future, and hybridized technologies". In: *Journal of Materials Chemistry A* 7.7, pp. 2942–2964. ISSN: 2050-7488. DOI: 10.1039/C8TA10513H.

KIM, Y., DREWS, A., CHANDRASEKARAN, R., MILLER, T., and SAKAMOTO, J. (2018). "Improving Li-ion battery charge rate acceptance through highly ordered hierarchical electrode design". In: *Ionics* 24.10, pp. 2935–2943. ISSN: 0947-7047. DOI: 10.1007/s11581-018-2502-x.

KLEEFOOT, M.-J., ENDERLE, S., SANDHERR, J., BOLSINGER, M., MAISCHIK, T., SIMON, N., MARTAN, J., RUCK, S., KNOBLAUCH, V., and RIEGEL, H. (2021). "Enhancement of the wettability of graphite-based lithium-ion battery anodes by selective laser surface modification using low energy nanosecond pulses". In: *The International Journal of Advanced Manufacturing Technology* 118, pp. 1987–1997. ISSN: 0268-3768. DOI: 10.1007/s00170-021-08004-3.

KLEEFOOT, M.-J., SANDHERR, J., SAILER, M., NESTER, S., MARTAN, J., KNOBLAUCH, V., KUMKAR, M., and RIEGEL, H. (2022). "Investigation on the parameter dependency of the perforation process of graphite based lithium-ion battery electrodes using ultrashort laser pulses". In: *Journal of Laser Applications* 34.4, p. 042003. ISSN: 1042-346X. DOI: 10.2351/7.0000757.

KOHLER, R., BRUNS, M., SMYREK, P., ULRICH, S., PRZYBYLSKI, M., and PFLEGING, W. (2010). "Laser annealing of textured thin film cathode material for lithium ion batteries". In: *Laser-based Micro- and Nanopackaging and Assembly IV*. Ed. by PFLEGING, W., LU, Y., WASHIO, K., AMAKO, J., and HOVING, W. SPIE Proceedings. SPIE, 75850O. DOI: 10.1117/12.841259.

KOHLER, R., PROELL, J., BRUNS, M., ULRICH, S., SEIFERT, H. J., and PFLEGING, W. (2013). "Conical surface structures on model thin-film electrodes and tape-cast electrode materials for lithium-ion batteries". In: *Applied Physics A* 112.1, pp. 77–85. ISSN: 0947-8396. DOI: 10.1007/s00339-012-7205-y.

KOHLER, R., PROELL, J., ULRICH, S., PRZYBYLSKI, M., SEIFERT, H. J., and PFLEGING, W. (2012). "Influence of laser-generated surface structures on electrochemical performance of lithium cobalt oxide". In: *Laser-based Micro- and Nanopackaging and Assembly VI*. Ed. by BACHMANN, F. G., PFLEGING, W., WASHIO, K., AMAKO, J., HOVING, W., and LU, Y. SPIE Proceedings. SPIE, 82440T. DOI: 10.1117/12.906707.

KOHLER, R., PROELL, J., ULRICH, S., TROUILLET, V., INDRIS, S., PRZYBYLSKI, M., and PFLEGING, W. (2009). "Laser-assisted structuring and modification of $LiCoO_2$ thin films". In: *Laser-based Micro- and Nanopackaging and Assembly III*. Ed. by PFLEGING, W., LU, Y., WASHIO, K., HOVING, W., and AMAKO, J. SPIE Proceedings. SPIE, p. 720207. DOI: 10.1117/12.809164.

KOHLER, R., PRÖLL, J., BRUNS, M., SCHERER, T., SEIFERT, H. J., and PFLEGING, W. (2013). "Laser-induced self-organizing surface structures on cathode materials for lithium-ion batteries". In: *Laser-based Micro- and Nanopackaging and Assembly VII*. Ed. by KLOTZBACH, U., LU, Y., and WASHIO, K. SPIE Proceedings. SPIE, p. 860806. DOI: 10.1117/12.2006372.

KORTHAUER, R. (2013). *Handbuch Lithium-Ionen-Batterien*. Berlin, Heidelberg: Springer Berlin Heidelberg. ISBN: 978-3-642-30652-5. DOI: 10.1007/978-3-642-30653-2.

KRAFT, L., HABEDANK, J. B., FRANK, A., RHEINFELD, A., and JOSSEN, A. (2020). "Modeling and Simulation of Pore Morphology Modifications using Laser-Structured Graphite Anodes in Lithium-Ion Batteries". In: *Journal of The Electrochemical Society* 167.1, p. 013506. ISSN: 0013-4651. DOI: 10.1149/2.0062001JES.

KRIEGLER, J., BALLMES, H., DIB, S., DEMIR, A. G., HILLE, L., LIANG, Y., WACH, L., WEIMANN, S., KEILHOFER, J., KIM, K. J., RUPP, J. L. M., and ZAEH, M. F. (2024). "Surface Reconditioning of Lithium Metal Electrodes by Laser Treatment for the Industrial Production of Enhanced Lithium Metal Batteries". In: *Advanced Functional Materials*. ISSN: 1616-301X. DOI: 10.1002/adfm.202313766.

KRIEGLER, J., DUY NGUYEN, T. M., TOMCIC, L., HILLE, L., GRABMANN, S., JAIMEZ-FARNHAM, E. I., and ZAEH, M. F. (2022). "Processing of lithium metal for the production of post-lithium-ion batteries using a pulsed nanosecond fiber laser". In: *Results in Materials* 15, p. 100305. ISSN: 2590048X. DOI: 10.1016/j.rinma.2022.100305.

KRIEGLER, J., HILLE, L., OEHLER, A., CHAJA, M., and ZAEH, M. F. (2023). "Scaling up picosecond laser ablation of a LATGP-type glass-ceramic solid electrolyte for all-solid-state battery production". In: *Journal of Manufacturing Processes* 106, pp. 188–201. ISSN: 15266125. DOI: 10.1016/j.jmapro.2023.09.072.

KRIEGLER, J., HILLE, L., STOCK, S., KRAFT, L., HAGEMEISTER, J., HABEDANK, J. B., JOSSEN, A., and ZAEH, M. F. (2021). "Enhanced performance and lifetime of lithium-ion batteries by laser structuring of graphite anodes". In: *Applied Energy* 303, p. 117693. ISSN: 03062619. DOI: 10.1016/j.apenergy.2021.117693.

KRIEGLER, J., JAIMEZ-FARNHAM, E., HILLE, L., DASHJAV, E., and ZAEH, M. F. (2022). "Pulsed laser ablation of a ceramic electrolyte for all-solid-state batteries". In: *Procedia CIRP* 111, pp. 800–805. ISSN: 22128271. DOI: 10.1016/j.procir.2022.08.132.

KRIEGLER, J., JAIMEZ-FARNHAM, E., SCHELLER, M., DASHJAV, E., KONWITSCHNY, F., WACH, L., HILLE, L., TIETZ, F., and ZAEH, M. F. (2023). "Design, production, and characterization of three-dimensionally-structured oxide-polymer composite cathodes for all-solid-state batteries". In: *Energy Storage Materials* 57, pp. 607–617. ISSN: 24058297. DOI: 10.1016/j.ensm.2023.03.008.

KRIEGLER, J., LIU, T., HARTL, R., HILLE, L., and ZAEH, M. F. (2023). "Automated quality evaluation for laser cutting in lithium metal battery production using an instance segmentation convolutional neural network". In: *Journal of Laser Applications* 35.4. ISSN: 1042-346X. DOI: 10.2351/7.0001213.

KURZWEIL, P. and DIETLMEIER, O. (2018). *Elektrochemische Speicher: Superkondensatoren, Batterien, Elektrolyse-Wasserstoff, rechtliche Rahmenbedingungen*. 2., aktualisierte und erweiterte Auflage. Lehrbuch. Wiesbaden and Heidelberg: Springer Vieweg. ISBN: 978-3-658-21829-4. DOI: 10.1007/978-3-658-21829-4.

KWADE, A., HASELRIEDER, W., LEITHOFF, R., MODLINGER, A., DIETRICH, F., and DROEDER, K. (2018). "Current status and challenges for automotive battery production technologies". In: *Nature Energy* 3.4, pp. 290–300. DOI: 10.1038/s41560-018-0130-3.

LANDESFEIND, J., HATTENDORFF, J., EHRL, A., WALL, W. A., and GASTEIGER, H. A. (2016). "Tortuosity Determination of Battery Electrodes and Separators by Impedance Spectroscopy". In: *Journal of The Electrochemical Society* 163.7, pp. 1373–1387. ISSN: 0013-4651. DOI: 10.1149/2.1141607jes.

LAURI, V. de, KRUMBEIN, L., HEIN, S., PRIFLING, B., SCHMIDT, V., DANNER, T., and LATZ, A. (2021). "Beneficial Effects of Three-Dimensional Structured Electrodes for the Fast Charging of Lithium-Ion Batteries". In: *ACS Applied Energy Materials*. ISSN: 2574-0962. DOI: 10.1021/acsaem.1c02621.

LEITZ, K.-H., REDLINGSHÖFER, B., REG, Y., OTTO, A., and SCHMIDT, M. (2011). "Metal Ablation with Short and Ultrashort Laser Pulses". In: *Physics Procedia* 12, pp. 230–238. ISSN: 18753892. DOI: 10.1016/j.phpro.2011.03.128.

LI, J., LEU, M. C., PANAT, R., and PARK, J. (2017). "A hybrid three-dimensionally structured electrode for lithium-ion batteries via 3D printing". In: *Materials & Design* 119, pp. 417–424. ISSN: 02641275. DOI: 10.1016/j.matdes.2017.01.088.

LI, L., ERB, R. M., WANG, J., WANG, J., and CHIANG, Y.-M. (2019). "Fabrication of Low-Tortuosity Ultrahigh-Area-Capacity Battery Electrodes through Magnetic Alignment of Emulsion-Based Slurries". In: *Advanced Energy Materials* 9.2, p. 1802472. ISSN: 1614-6832. DOI: 10.1002/aenm.201802472.

LICKSCHAT, P., METZNER, D., and WEISSMANTEL, S. (2021). "Burst mode ablation of stainless steel with tunable ultrashort laser pulses". In: *Journal of Laser Applications* 33.2, p. 022005. ISSN: 1042-346X. DOI: 10.2351/7.0000271.

LIM, D. G., CHUNG, D.-W., KOHLER, R., PRÖLL, J., SCHERR, C., PFLEGING, W., and GARCÍA, R. E. (2014). "Designing 3D Conical-Shaped Lithium-Ion Microelectrodes". In: *Journal of The Electrochemical Society* 161.3, pp. 302–307. ISSN: 0013-4651. DOI: 10.1149/2.013403jes.

LIU, C., XU, F., CHENG, X., TONG, J., LIU, Y., CHEN, Z., LAO, C., and MA, J. (2019). "Comparative study on the electrochemical performance of $LiFePO_4$ cathodes fabricated by low temperature 3D printing, direct ink writing and conventional roller coating process". In: *Ceramics International* 45.11, pp. 14188–14197. ISSN: 02728842. DOI: 10.1016/j.ceramint.2019.04.124.

LIU, C., XU, F., LIU, Y., MA, J., LIU, P., WANG, D., LAO, C., and CHEN, Z. (2019). "High mass loading ultrathick porous $Li_4Ti_5O_{12}$ electrodes with improved areal capacity fabricated via low temperature direct writing". In: *Electrochimica Acta* 314, pp. 81–88. ISSN: 00134686. DOI: 10.1016/j.electacta.2019.05.082.

LOESCHNER, U., SCHILLE, J., STREEK, A., KNEBEL, T., HARTWIG, L., HILLMANN, R., and ENDISCH, C. (2015). "High-rate laser microprocessing using a polygon scanner system". In: *Journal of Laser Applications* 27.S2. ISSN: 1042-346X. DOI: 10.2351/1.4906473.

LONG, J. W., DUNN, B., ROLISON, D. R., and WHITE, H. S. (2004). "Three-dimensional battery architectures". In: *Chemical reviews* 104.10, pp. 4463–4492. DOI: 10.1021/cr020740l.

LOOR, R. de (2013). "Polygon Scanner System for Ultra Short Pulsed Laser Micro-Machining Applications". In: *Physics Procedia* 41, pp. 544–551. ISSN: 18753892. DOI: 10.1016/j.phpro.2013.03.114.

LU, Q., MAO, S. S., MAO, X., and RUSSO, R. E. (2002). "Delayed phase explosion during high-power nanosecond laser ablation of silicon". In: *Applied Physics Letters* 80.17, pp. 3072–3074. ISSN: 0003-6951. DOI: 10.1063/1.1473862.

LUTEY, A. H., FORTUNATO, A., ASCARI, A., CARMIGNATO, S., and LEONE, C. (2015). "Laser cutting of lithium iron phosphate battery electrodes: Characterization of process efficiency and quality". In: *Optics & Laser Technology* 65, pp. 164–174. ISSN: 00303992. DOI: 10.1016/j.optlastec.2014.07.023.

LUTEY, A. H., FORTUNATO, A., CARMIGNATO, S., ASCARI, A., LIVERANI, E., and GUERRINI, G. (2016). "Quality and Productivity Considerations for Laser Cutting of LiFePO4 and LiNiMnCoO2 Battery Electrodes". In: *Procedia CIRP* 42, pp. 433–438. ISSN: 22128271. DOI: 10.1016/j.procir.2016.02.227.

LUTEY, A. H., FORTUNATO, A., CARMIGNATO, S., and FIORINI, M. (2017). "High speed pulsed laser cutting of LiCoO2 Li-ion battery electrodes". In: *Optics & Laser Technology* 94, pp. 90–96. ISSN: 00303992. DOI: 10.1016/j.optlastec.2017.03.022.

MA, C., ZHAO, Y., LI, J., SONG, Y., SHI, J., GUO, Q., and LIU, L. (2013). "Synthesis and electrochemical properties of artificial graphite as an anode for high-performance lithium-ion batteries". In: *Carbon* 64, pp. 553–556. ISSN: 00086223. DOI: 10.1016/j.carbon.2013.07.089.

MAI, W., USSEGLIO-VIRETTA, F. L., COLCLASURE, A. M., and SMITH, K. (2020). "Enabling fast charging of lithium-ion batteries through secondary-/dual-pore network: Part II - numerical model". In: *Electrochimica Acta* 341, p. 136013. ISSN: 00134686. DOI: 10.1016/j.electacta.2020.136013.

MANGANG, M., GOTCU-FREIS, P., SEIFERT, H. J., and PFLEGING, W. (2015). "Electrochemical and kinetic studies of ultrafast laser structured $LiFePO_4$ electrodes". In: *Laser-based Micro- and Nanoprocessing IX*. Ed. by KLOTZBACH, U., WASHIO, K., and ARNOLD, C. B. SPIE Proceedings. SPIE, 93510K. DOI: 10.1117/12.2078900.

MANGANG, M., PRÖLL, J., TARDE, C., SEIFERT, H. J., and PFLEGING, W. (2014). "Ultrafast laser microstructuring of $LiFePO_4$ cathode material". In: *Laser-based Micro- and Nanoprocessing VIII*. Ed. by KLOTZBACH, U., WASHIO, K., and ARNOLD, C. B. SPIE Proceedings. SPIE, p. 89680M. DOI: 10.1117/12.2039604.

MANGANG, M., SEIFERT, H. J., and PFLEGING, W. (2016). "Influence of laser pulse duration on the electrochemical performance of laser structured $LiFePO_4$ composite electrodes". In: *Journal of Power Sources* 304, pp. 24–32. ISSN: 03787753. DOI: 10.1016/j.jpowsour.2015.10.086.

MANGANG, M. (2018). "Ultrakurzpulslaserstrukturierung von $LiFePO_4$- und $LiMn_2O_4$-Dickschichtelektroden für Lithium-Ionen-Zellen". PhD thesis. Karlsruhe: Karlsruher Institut für Technologie.

MANNION, P., MAGEE, J., COYNE, E., O'CONNOR, G., and GLYNN, T. (2004). "The effect of damage accumulation behaviour on ablation thresholds and damage morphology in ultrafast laser micro-machining of common metals in air". In: *Applied Surface Science* 233.1-4, pp. 275–287. ISSN: 01694332. DOI: 10.1016/j.apsusc.2004.03.229.

MARKS, T., TRUSSLER, S., SMITH, A. J., XIONG, D., and DAHN, J. R. (2011). "A Guide to Li-Ion Coin-Cell Electrode Making for Academic Researchers". In: *Journal of The Electrochemical Society* 158.1, p. 51. ISSN: 0013-4651. DOI: 10.1149/1.3515072.

MASIAS, A., MARCICKI, J., and PAXTON, W. A. (2021). "Opportunities and Challenges of Lithium Ion Batteries in Automotive Applications". In: *ACS Energy Letters*, pp. 621–630. ISSN: 2380-8195. DOI: 10.1021/acsenergylett.0c02584.

MATSUMOTO, F., YAMADA, M., TSUTA, M., NAKAMURA, S., ANDO, N., and SOMA, N. (2023). "Review of the structure and performance of through-holed anodes and cathodes prepared with a picosecond pulsed laser for lithium-ion batteries". In: *International Journal of Extreme Manufacturing* 5.1, p. 012001. ISSN: 2631-8644. DOI: 10.1088/2631-7990/aca1f0.

MAULER, L., DUFFNER, F., and LEKER, J. (2021). "Economies of scale in battery cell manufacturing: The impact of material and process innovations". In: *Applied Energy* 286, p. 116499. ISSN: 03062619. DOI: 10.1016/j.apenergy.2021.116499.

MAZUMDER, J. and STEEN, W. M. (1980). "Heat transfer model for cw laser material processing". In: *Journal of Applied Physics* 51.2, pp. 941–947. ISSN: 0021-8979. DOI: 10.1063/1.327672.

METZNER, D., LICKSCHAT, P., and WEISSMANTEL, S. (2021). "Optimization of the ablation process using ultrashort pulsed laser radiation in different burst modes". In: *Journal of Laser Applications* 33.1, p. 012057. ISSN: 1042-346X. DOI: 10.2351/7.0000352.

MEYER, A., BALL, F., and PFLEGING, W. (2021). "The Effect of Silicon Grade and Electrode Architecture on the Performance of Advanced Anodes for Next Generation Lithium-Ion Cells". In: *Nanomaterials* 11.12. DOI: 10.3390/nano11123448.

MEYER, A., STERZL, Y., and PFLEGING, W. (2023). "High repetition ultrafast laser ablation of graphite and silicon/graphite composite electrodes for lithium-ion batteries". In: *Journal of Laser Applications* 35.4. ISSN: 1042-346X. DOI: 10.2351/7.0001180.

MIOTELLO, A. and KELLY, R. (1999). "Laser-induced phase explosion: new physical problems when a condensed phase approaches the thermodynamic critical temperature". In: *Applied Physics A Materials Science & Processing* 69.S1, pp. 67–73. ISSN: 0947-8396. DOI: 10.1007/s003399900296.

MURRAY, V., HALL, D. S., and DAHN, J. R. (2019). "A Guide to Full Coin Cell Making for Academic Researchers". In: *Journal of The Electrochemical Society* 166.2, pp. 329–333. ISSN: 0013-4651. DOI: 10.1149/2.1171902jes.

NEB, D., KIM, S., CLEVER, H., DORN, B., and KAMPKER, A. (2022). "Current advances on laser drying of electrodes for lithium-ion battery cells". In: *Procedia CIRP* 107, pp. 1577–1587. ISSN: 22128271. DOI: 10.1016/j.procir.2022.05.194.

NELSON, P. A., AHMED, S., GALLAGHER, K. G., and DEES, D. W. (2019). *Modeling the Performance and Cost of Lithium-Ion Batteries for Electric-Drive Vehicles, Third Edition*. United States: Argonne National Laboratory. DOI: 10.2172/1503280.

NEMANI, V. P., HARRIS, S. J., and SMITH, K. C. (2015). "Design of Bi-Tortuous, Anisotropic Graphite Anodes for Fast Ion-Transport in Li-Ion Batteries". In: *Journal of The Electrochemical Society* 162.8, pp. 1415–1423. ISSN: 0013-4651. DOI: 10.1149/2.0151508jes.

NEUENSCHWANDER, B., KRAMER, T., LAUER, B., and JAEGGI, B. (2015). "Burst mode with ps- and fs-pulses: Influence on the removal rate, surface quality, and heat accumulation". In: *Laser Applications in Microelectronic and Optoelectronic Manufacturing (LAMOM) XX*. Ed. by ROTH, S., NAKATA, Y., NEUENSCHWANDER, B., and XU, X. SPIE Proceedings. SPIE, 93500U. DOI: 10.1117/12.2076455.

NEUENSCHWANDER, B., JAEGGI, B., FOERSTER, D. J., KRAMER, T., and REMUND, S. (2019). "Influence of the burst mode onto the specific removal rate for metals and semiconductors". In: *Journal of Laser Applications* 31.2, p. 022203. ISSN: 1042-346X. DOI: 10.2351/1.5096083.

NOLTE, S., MOMMA, C., JACOBS, H., TÜNNERMANN, A., CHICHKOV, B. N., WELLEGEHAUSEN, B., and WELLING, H. (1997). "Ablation of metals by ultrashort laser pulses". In: *Journal of the Optical Society of America B* 14.10, p. 2716. ISSN: 0740-3224. DOI: 10.1364/JOSAB.14.002716.

NYMAN, A., ZAVALIS, T. G., ELGER, R., BEHM, M., and LINDBERGH, G. (2010). "Analysis of the Polarization in a Li-Ion Battery Cell by Numerical Simulations". In: *Journal of The Electrochemical Society* 157.11, p. 1236. ISSN: 0013-4651. DOI: 10.1149/1.3486161. URL: http://dx.doi.org/10.1149/1.3486161.

PARK, D. and LEE, D. (2021). "Effect of Fluence and Multi-Pass on Groove Morphology and Process Efficiency of Laser Structuring for 3D Electrodes of Lithium-Ion Batteries". In: *Materials* 14.5, p. 1283. DOI: 10.3390/ma14051283.

PARK, J., HYEON, S., JEONG, S., and KIM, H.-J. (2019). "Performance enhancement of Li-ion battery by laser structuring of thick electrode with low porosity". In: *Journal of Industrial and Engineering Chemistry* 70, pp. 178–185. ISSN: 1226086X. DOI: 10.1016/j.jiec.2018.10.012.

PARK, J., JEON, C., KIM, W., BONG, S.-J., JEONG, S., and KIM, H.-J. (2021). "Challenges, laser processing and electrochemical characteristics on application of ultra-thick electrode for high-energy lithium-ion battery". In: *Journal of Power Sources* 482, p. 228948. ISSN: 03787753. DOI: 10.1016/j.jpowsour.2020.228948.

PARK, J., SUH, S., JEONG, S., and KIM, H.-J. (2021). "New approach for the high electrochemical performance of silicon anode in lithium-ion battery: A rapid and large surface treatment using a high-energy pulsed laser". In: *Journal of Power Sources* 491, p. 229573. ISSN: 03787753. DOI: 10.1016/j.jpowsour.2021.229573.

PARK, K.-Y., PARK, J.-W., SEONG, W. M., YOON, K., HWANG, T.-H., KO, K.-H., HAN, J.-H., JAEDONG, Y., and KANG, K. (2020). "Understanding capacity fading mechanism of thick electrodes for lithium-ion rechargeable batteries". In: *Journal of Power Sources* 468, p. 228369. ISSN: 03787753. DOI: 10.1016/j.jpowsour.2020.228369.

PARK, S., SHI, B., SHANG, Y., DENG, K., and FU, K. (2022). "Structured Electrode Additive Manufacturing for Lithium-Ion Batteries". In: *Nano letters* 22.23, pp. 9462–9469. DOI: 10.1021/acs.nanolett.2c03545.

PASCHOTTA, R. (2024a). *Fluence*. RP Photonics Encyclopedia. DOI: 10.61835/j0u. URL: https://www.rp-photonics.com/fluence.html (visited on 02/08/2024).

— (2024b). *Scanning Lenses*. RP Photonics Encyclopedia. DOI: 10.61835/2kq. URL: https://www.rp-photonics.com/scanning_lenses.html (visited on 02/08/2024).

— (2024c). *Ultrashort Pulses*. RP Photonics Encyclopedia. DOI: 10.61835/41l. URL: https://www.rp-photonics.com/ultrashort_pulses.html (visited on 02/08/2024).

PATEL, K. K., PAULSEN, J. M., and DESILVESTRO, J. (2003). "Numerical simulation of porous networks in relation to battery electrodes and separators". In: *Journal of Power Sources* 122.2, pp. 144–152. ISSN: 03787753. DOI: 10.1016/S0378-7753(03)00399-9.

PFLEGING, W. (2018). "A review of laser electrode processing for development and manufacturing of lithium-ion batteries". In: *Nanophotonics* 7.3, pp. 549–573. DOI: 10.1515/nanoph-2017-0044.

PFLEGING, W. and GOTCU, P. (2019). "Femtosecond Laser Processing of Thick Film Cathodes and Its Impact on Lithium-Ion Diffusion Kinetics". In: *Applied Sciences* 9.17, p. 3588. DOI: 10.3390/app9173588.

PFLEGING, W., KOHLER, R., and PRÖLL, J. (2014). "Laser generated microstructures in tape cast electrodes for rapid electrolyte wetting: new technical approach for cost efficient battery manufacturing". In: *Laser-based Micro- and Nanoprocessing VIII*. Ed. by KLOTZBACH, U., WASHIO, K., and ARNOLD, C. B. SPIE Proceedings. SPIE, 89680B. DOI: 10.1117/12.2039635.

PFLEGING, W., KOHLER, R., SCHOLZ, S., ZIEBERT, C., and PRÖLL, J. (2011). "Laser-assisted surface engineering of thin film electrode materials for lithium-ion batteries". In: *MRS Proceedings* 1365, pp. 89–99. ISSN: 0272-9172. DOI: 10.1557/opl.2011.1317.

PFLEGING, W. and PRÖLL, J. (2014). "A new approach for rapid electrolyte wetting in tape cast electrodes for lithium-ion batteries". In: *Journal of Materials Chemistry A* 2.36, pp. 14918–14926. ISSN: 2050-7488. DOI: 10.1039/C4TA02353F.

PFLEGING, W., SMYREK, P., HUND, J., BERGFELDT, T., and PRÖLL, J. (2015). "Surface micro-structuring of intercalation cathode materials for lithium-ion batteries: a study of laser-assisted cone formation". In: *Laser-based Micro- and Nanoprocessing IX*. Ed. by KLOTZBACH, U., WASHIO, K., and ARNOLD, C. B. SPIE Proceedings. SPIE, 93511E. DOI: 10.1117/12.2077763.

PFLEGING, W., ZHENG, Y., MANGANG, M., BRUNS, M., and SMYREK, P. (2016). "Laser processes and analytics for high power 3D battery materials". In: *Frontiers in Ultrafast Optics: Biomedical, Scientific, and Industrial Applications XVI*. Ed. by HEISTERKAMP, A., HERMAN, P. R., MEUNIER, M., and NOLTE, S. SPIE Proceedings. SPIE, p. 974013. DOI: 10.1117/12.2212041.

POPRAWE, R. (2005). *Lasertechnik für die Fertigung: Grundlagen, Perspektiven und Beispiele für den innovativen Ingenieur*. VDI-Buch. Berlin and Heidelberg: Springer. ISBN: 3-540-21406-2.

PRÖLL, J. (2014). "Lasergestützte Modifikation von Lithiummanganoxid und Lithiumnickelmangankobaltoxid". PhD thesis. Karlsruhe: Karlsruher Institut für Technologie.

PRÖLL, J., KIM, H., MANGANG, M., SEIFERT, H. J., PIQUÉ, A., and PFLEGING, W. (2014). "Fs-laser microstructuring of laser-printed $LiMn_2O_4$ electrodes for manufacturing of 3D microbatteries". In: *Laser-based Micro- and Nanoprocessing VIII*. Ed. by KLOTZBACH, U., WASHIO, K., and ARNOLD, C. B. SPIE Proceedings. SPIE, p. 896805. DOI: 10.1117/12.2039902.

PRÖLL, J., KIM, H., PIQUÉ, A., SEIFERT, H. J., and PFLEGING, W. (2014). "Laser-printing and femtosecond-laser structuring of $LiMn_2O_4$ composite cathodes for Li-ion microbatteries". In: *Journal of Power Sources* 255, pp. 116–124. ISSN: 03787753. DOI: 10.1016/j.jpowsour.2013.12.132.

RAKEBRANDT, J.-H., SMYREK, P., ZHENG, Y., SEIFERT, H. J., and PFLEGING, W. (2017a). "Laser micro structuring of composite $Li(Ni_{0.6}Mn_{0.2}Co_{0.2})O_2$ cathode layersfor lithium-ion batteries". In: *2017 IEEE International Conference on Manipulation, Manufacturing and Measurement on the Nanoscale (3M-NANO)*, pp. 57–60. DOI: 10.1109/3M-NANO.2017.8286297.

— (2017b). "Laser processing of thick $Li(NiMnCo)O_2$ electrodes for lithium-ion batteries". In: *Laser-based Micro- and Nanoprocessing XI*. Ed. by KLOTZBACH, U., WASHIO, K., and KLING, R. SPIE Proceedings. SPIE, p. 100920M. DOI: 10.1117/12.2252093.

REALE, E. R. and SMITH, K. C. (2018). "Capacitive Performance and Tortuosity of Activated Carbon Electrodes with Macroscopic Pores". In: *Journal of The Electrochemical Society* 165.9, pp. 1685–1693. ISSN: 0013-4651. DOI: 10.1149/2.0601809jes.

REINHART, G., ZEILINGER, T., KURFER, J., WESTERMEIER, M., . THIEMANN, C., and GLONEGGER, M. (2013). "Research and Demonstration Center for the Production of Large-Area Lithium-Ion Cells". In: *Future Trends in Production Engineering*. Ed. by SCHUH, G., NEUGEBAUER, R., and UHLMANN, E. Berlin, Heidelberg: Springer. ISBN: 978-3-642-24490-2.

RENK, K. F. (2017). *Basics of Laser Physics*. Cham: Springer International Publishing. ISBN: 978-3-319-50650-0. DOI: 10.1007/978-3-319-50651-7.

RONCHI, C., BEUKERS, R., HEINZ, H., HIERNAUT, J. P., and SELFSLAG, R. (1992). "Graphite melting under laser pulse heating". In: *International Journal of Thermophysics* 13.1, pp. 107–129. ISSN: 1572-9567. DOI: 10.1007/BF00503360.

SANDER, J. S., ERB, R. M., LI, L., GURIJALA, A., and CHIANG, Y.-M. (2016). "High-performance battery electrodes via magnetic templating". In: *Nature Energy* 1.8. DOI: 10.1038/nenergy.2016.99.

SANDHERR, J., NESTER, S., KLEEFOOT, M.-J., BOLSINGER, M., WEISENBERGER, C., HAGHIPOUR, A., HARRISON, D. K., RUCK, S., RIEGEL, H., and KNOBLAUCH, V. (2022). "Improving the ionic transport properties of graphite anodes for lithium ion batteries by surface modification using nanosecond laser". In: *Journal of Power Sources* 549, p. 232077. ISSN: 03787753. DOI: 10.1016/j.jpowsour.2022.232077.

SANDHERR, J., KLEEFOOT, M.-J., NESTER, S., WEISENBERGER, C., DESILVA, A. K., MICHEL, D., REEB, S., FINGERLE, M., RIEGEL, H., and KNOBLAUCH, V. (2023). "Micro embossing of graphite-based anodes for lithium-ion batteries to improve cell performance". In: *Journal of Energy Storage* 65, p. 107359. ISSN: 2352152X. DOI: 10.1016/j.est.2023.107359.

SAUTER, U. (2014). "Batterie mit porösen Elektroden". DE102012215921.

SCHMIEDER, B. (2012). "Laser cutting of graphite anodes for automotive lithium-ion secondary batteries: investigations in the edge geometry and heat affected zone". In: *Laser-based Micro- and Nanopackaging and Assembly VI*. Ed. by BACHMANN, F. G., PFLEGING, W., WASHIO, K., AMAKO, J., HOVING, W., and LU, Y. SPIE Proceedings. SPIE, 82440R. DOI: 10.1117/12.912767.

— (2015). "Analytical model of the laser ablation mechanism of lithium-ion battery coatings". In: *Laser-based Micro- and Nanoprocessing IX*. Ed. by KLOTZBACH, U., WASHIO, K., and ARNOLD, C. B. SPIE Proceedings. SPIE, p. 93511C. DOI: 10.1117/12.2086719.

SCHNELL, J., KNÖRZER, H., IMBSWEILER, A. J., and REINHART, G. (2020). "Solid versus Liquid—A Bottom-Up Calculation Model to Analyze the Manufacturing Cost of Future High-Energy Batteries". In: *Energy Technology* 8.3, p. 1901237. ISSN: 2194-4288. DOI: 10.1002/ente.201901237.

SCHOENLEIN, R. W., LIN, W. Z., FUJIMOTO, J. G., and EESLEY, G. L. (1987). "Femtosecond studies of nonequilibrium electronic processes in metals". In: *Physical review letters* 58.16, pp. 1680–1683. DOI: 10.1103/PhysRevLett.58.1680.

SCHREINER, D., ZÜND, T., GÜNTER, F. J., KRAFT, L., STUMPER, B., LINSENMANN, F., SCHÜSSLER, M., WILHELM, R., JOSSEN, A., REINHART, G., and GASTEIGER, H. A. (2021). "Comparative Evaluation of LMR-NCM and NCA Cathode Active Materials in Multilayer Lithium-Ion Pouch Cells: Part I. Production, Electrode Characterization, and Formation". In: *Journal of The Electrochemical Society* 168.3, p. 030507. ISSN: 0013-4651. DOI: 10.1149/1945-7111/abe50c.

SCHÜNEMANN, J.-H. (2015). "Modell zur Bewertung der Herstellkosten von Lithiumionenbatteriezellen". PhD thesis. Braunschweig: Technische Universität Braunschweig.

SCHWEIGHOFER, L., ESCHELMÜLLER, B., FRÖHLICH, K., PFLEGING, W., and PICHLER, F. (2022). "Modelling and Optimisation of Laser-Structured Battery Electrodes". In: *Nanomaterials* 12.9. DOI: 10.3390/nano12091574.

SHI, H., LIU, X., WU, R., ZHENG, Y., LI, Y., CHENG, X., PFLEGING, W., and ZHANG, Y. (2019). "In Situ SEM Observation of Structured Si/C Anodes Reactions in an Ionic-Liquid-Based Lithium-Ion Battery". In: *Applied Sciences* 9.5, p. 956. DOI: 10.3390/app9050956.

SIMON, S. H. (2013). *The Oxford solid state basics*. Oxford: Oxford Univ. Press. ISBN: 978-0-19-968076-4.

SMYREK, P., KIM, H., ZHENG, Y., SEIFERT, H. J., PIQUÉ, A., and PFLEGING, W. (2016). "Laser printing and femtosecond laser structuring of electrode materials for the manufacturing of 3D lithium-ion micro-batteries". In: *Laser 3D Manufacturing III*. Ed. by GU, B., HELVAJIAN, H., and PIQUÉ, A. SPIE Proceedings. SPIE, p. 973806. DOI: 10.1117/12.2211546.

SMYREK, P., PRÖLL, J., SEIFERT, H. J., and PFLEGING, W. (2014). "Femtosecond laser modification of Li(NiCoMn)O_2 electrodes for lithium-ion batteries". In: *CLEO: 2014*. OSA Technical Digest (online). San Jose, California: Optical Society of America, AW1H.3. DOI: 10.1364/CLEO_AT.2014.AW1H.3.

SMYREK, P., ZHENG, Y., RAKEBRANDT, J.-H., SEIFERT, H. J., and PFLEGING, W. (2017a). "Laser-induced breakdown spectroscopy for studying the electrochemical impact of porosity variations in composite electrode materials". In: *2017 IEEE International Conference on Manipulation, Manufacturing and Measurement on the Nanoscale (3M-NANO)*. IEEE, pp. 65–68. ISBN: 978-1-5386-1081-7. DOI: 10.1109/3M-NANO.2017.8286301.

SMYREK, P., ZHENG, Y., RAKEBRANDT, J.-H., SEIFERT, H. J., and PFLEGING, W. (2017b). "Investigation of micro-structured $Li(Ni_{1/3}Mn_{1/3}Co_{1/3})O_2$ cathodes by laser-induced breakdown spectroscopy". In: *Laser-based Micro- and Nanoprocessing XI*. Ed. by KLOTZBACH, U., WASHIO, K., and KLING, R. SPIE Proceedings. SPIE, 100920S. DOI: 10.1117/12.2253894.

SMYREK, P., ZHENG, Y., SEIFERT, H. J., and PFLEGING, W. (2016a). "Laser-induced breakdown spectroscopy as a powerful tool for characterization of laser modified composite materials". In: *2016 IEEE International Conference on Manipulation, Manufacturing and Measurement on the Nanoscale (3M-NANO)*. IEEE, pp. 164–167. ISBN: 978-1-5090-2945-7. DOI: 10.1109/3M-NANO.2016.7824954.

— (2016b). "Post-mortem characterization of fs laser-generated micro-pillars in $Li(Ni_{1/3}Mn_{1/3}Co_{1/3})O_2$ electrodes by laser-induced breakdown spectroscopy". In: *Laser-based Micro- and Nanoprocessing X*. Ed. by KLOTZBACH, U., WASHIO, K., and ARNOLD, C. B. SPIE Proceedings. SPIE, p. 97361C. DOI: 10.1117/12.2210815.

SMYREK, P., BERGFELDT, T., SEIFERT, H. J., and PFLEGING, W. (2019). "Laser-induced breakdown spectroscopy for the quantitative measurement of lithium concentration profiles in structured and unstructured electrodes". In: *Journal of Materials Chemistry A* 7.10, pp. 5656–5665. ISSN: 2050-7488. DOI: 10.1039/C8TA10328C.

SONG, Z., ZHU, P., PFLEGING, W., and SUN, J. (2021). "Electrochemical Performance of Thick-Film $Li(Ni_{0.6}Mn_{0.2}Co_{0.2})O_2$ Cathode with Hierarchic Structures and Laser Ablation". In: *Nanomaterials* 11.11, p. 2962. DOI: 10.3390/nano11112962.

STERNER, M. and STADLER, I. (2014). *Energiespeicher - Bedarf, Technologien, Integration*. Berlin, Heidelberg: Springer Berlin Heidelberg. ISBN: 978-3-642-37379-4. DOI: 10.1007/978-3-642-37380-0.

STOCK, S., DILLER, F., BÖHM, J., HILLE, L., HAGEMEISTER, J., SOMMER, A., and DAUB, R. (2023). "Operando Analysis of the Gassing and Swelling Behavior of Lithium-ion Pouch Cells during Formation". In: *Journal of The Electrochemical Society* 170.6, p. 060539. ISSN: 0013-4651. DOI: 10.1149/1945-7111/acde0f.

STOCK, S., POHLMANN, S., GÜNTER, F. J., HILLE, L., HAGEMEISTER, J., and REINHART, G. (2022). "Early Quality Classification and Prediction of Battery Cycle Life in Production Using Machine Learning". In: *Journal of Energy Storage* 50, p. 104144. ISSN: 2352152X. DOI: 10.1016/j.est.2022.104144.

STUVE, E. M. (2014). "Overpotentials in Electrochemical Cells". In: *Encyclopedia of Applied Electrochemistry*. Ed. by KREYSA, G., OTA, K.-i., and SAVINELL, R. F. New York, NY: Springer New York, pp. 1445–1453. ISBN: 978-1-4419-6996-5. DOI: 10.1007/978-1-4419-6996-5_330.

SUN, K., WEI, T.-S., AHN, B. Y., SEO, J. Y., DILLON, S. J., and LEWIS, J. A. (2013). "3D printing of interdigitated Li-ion microbattery architectures". In: *Advanced Materials* 25.33, pp. 4539–4543. ISSN: 0935-9648. DOI: 10.1002/adma.201301036.

THE ROYAL SWEDISH ACADEMY OF SCIENCES (2019). *The Nobel Prize in Chemistry 2019*. URL: https://www.nobelprize.org/prizes/chemistry/2019/press-release (visited on 12/13/2023).

THORAT, I. V., STEPHENSON, D. E., ZACHARIAS, N. A., ZAGHIB, K., HARB, J. N., and WHEELER, D. R. (2009). "Quantifying tortuosity in porous Li-ion battery materials". In: *Journal of Power Sources* 188.2, pp. 592–600. ISSN: 03787753. DOI: 10.1016/j.jpowsour.2008.12.032.

TRÄGER, F., ed. (2012). *Springer Handbook of Lasers and Optics*. 2. ed. Berlin and Heidelberg: Springer. ISBN: 978-3-642-19408-5. DOI: 10.1007/978-3-642-19409-2.

TRAN, M. X., SMYREK, P., PARK, J., PFLEGING, W., and LEE, J. K. (2022). "Ultrafast-Laser Micro-Structuring of $LiNi_{0.8}Mn_{0.1}Co_{0.1}O_2$ Cathode for High-Rate Capability of Three-Dimensional Li-ion Batteries". In: *Nanomaterials* 12.21. DOI: 10.3390/nano12213897.

TSUDA, T., ANDO, N., MATSUBARA, K., TANABE, T., ITAGAKI, K., SOMA, N., NAKAMURA, S., HAYASHI, N., GUNJI, T., OHSAKA, T., and MATSUMOTO, F. (2018). "Improvement of high-rate charging/discharging performance of a lithium ion battery composed of laminated $LiFePO_4$ cathodes/ graphite anodes having porous electrode structures fabricated with a pico-second pulsed laser". In: *Electrochimica Acta* 291, pp. 267–277. ISSN: 00134686. DOI: 10.1016/j.electacta.2018.08.149.

TSUDA, T., ANDO, N., NAKAMURA, S., ISHIHARA, Y., HAYASHI, N., SOMA, N., GUNJI, T., TANABE, T., OHSAKA, T., and MATSUMOTO, F. (2019). "Improvement of high-rate discharging performance of $LiFePO_4$ cathodes by forming micrometer-sized through-holed electrode structures with a pico-second pulsed laser". In: *Electrochimica Acta* 296, pp. 27–38. ISSN: 00134686. DOI: 10.1016/j.electacta.2018.11.014.

TSUDA, T., ANDO, N., UTAKA, T., KOJIMA, K., NAKAMURA, S., HAYASHI, N., SOMA, N., GUNJI, T., TANABE, T., OHSAKA, T., and MATSUMOTO, F. (2019). "Improvement of high-rate performance of $LiFePO_4$ cathode with through-holed $LiFePO_4$/Activated carbon hybrid electrode structure fabricated with a pico-second pulsed laser". In: *Electrochimica Acta* 298, pp. 827–834. ISSN: 00134686. DOI: 10.1016/j.electacta.2018.12.149.

UHLMANN, C., ILLIG, J., ENDER, M., SCHUSTER, R., and IVERS-TIFFÉE, E. (2015). "In situ detection of lithium metal plating on graphite in experimental cells". In: *Journal of Power Sources* 279, pp. 428–438. ISSN: 03787753. DOI: 10.1016/j.jpowsour.2015.01.046.

USSEGLIO-VIRETTA, F., MAI, W., COLCLASURE, A. M., DOEFF, M., YI, E., and SMITH, K. (2020). "Enabling fast charging of lithium-ion batteries through secondary- /dual- pore network: Part I - Analytical diffusion model". In: *Electrochimica Acta* 342, p. 136034. ISSN: 00134686. DOI: 10.1016/j.electacta.2020.136034.

USSEGLIO-VIRETTA, F. L. E., WEDDLE, P., TREMOLET DE VILLERS, B. J., DUNLAP, N., KERN, D., SMITH, K., and FINEGAN, D. (2023). "Optimizing Fast Charging and Wetting in Lithium-Ion Batteries with Optimal Microstructure Patterns Identified by Genetic Algorithm". In: *Journal of The Electrochemical Society*. ISSN: 0013-4651. DOI: 10.1149/1945-7111/ad0a7a.

VETTER, K. J. (1961). *Elektrochemische Kinetik*. Berlin, Heidelberg: Springer Berlin Heidelberg. ISBN: 978-3-642-86548-0. DOI: 10.1007/978-3-642-86547-3.

WANG, J., SUN, Q., GAO, X., WANG, C., LI, W., HOLNESS, F. B., ZHENG, M., LI, R., PRICE, A. D., SUN, X., SHAM, T.-K., and SUN, X. (2018). "Toward High Areal Energy and Power Density Electrode for Li-Ion Batteries via Optimized 3D Printing Approach". In: *ACS Applied Materials & Interfaces* 10.46, pp. 39794–39801. ISSN: 1944-8244. DOI: 10.1021/acsami.8b14797.

WANG, X. Y., RIFFE, D. M., LEE, Y., and DOWNER, M. C. (1994). "Time-resolved electron-temperature measurement in a highly excited gold target using femtosecond thermionic emission". In: *Physical review. B, Condensed matter* 50.11, pp. 8016–8019. ISSN: 0163-1829. DOI: 10.1103/PhysRevB.50.8016.

WATANABE, T., TSUDA, T., ANDO, N., NAKAMURA, S., HAYASHI, N., SOMA, N., GUNJI, T., OHSAKA, T., and MATSUMOTO, F. (2019). "An improved prelithiation of graphite anodes using through-holed cathode and anode electrodes in a laminated lithium ion battery". In: *Electrochimica Acta* 324, p. 134848. ISSN: 00134686. DOI: 10.1016/j.electacta.2019.134848.

WESTERMEIER, M., REINHART, G., and STEBER, M. (2014). "Complexity Management for the Start-up in Lithium-ion Cell Production". In: *Procedia CIRP* 20, pp. 13–19. ISSN: 22128271. DOI: 10.1016/j.procir.2014.05.026.

WIEDENMANN, D., KELLER, L., HOLZER, L., STOJADINOVIĆ, J., MÜNCH, B., SUAREZ, L., FUMEY, B., HAGENDORFER, H., BRÖNNIMANN, R., MODREGGER, P., GORBAR, M., VOGT, U. F., ZÜTTEL, A., LA MANTIA, F., WEPF, R., and GROBÉTY, B. (2013). "Three-dimensional pore structure and ion conductivity of porous ceramic diaphragms". In: *AIChE Journal* 59.5, pp. 1446–1457. ISSN: 00011541. DOI: 10.1002/aic.14094.

WITT, D., WILDE, D., BAAKES, F., BELKHIR, F., RÖDER, F., and KREWER, U. (2021). "Myth and Reality of a Universal Lithium-Ion Battery Electrode Design Optimum – A Perspective and Case Study". In: *Energy Technology*. ISSN: 2194-4288. DOI: 10.1002/ente.202000989.

WOLKE, R. and SCHWETLICK, H. (1988). "Iteratively Reweighted Least Squares: Algorithms, Convergence Analysis, and Numerical Comparisons". In: *SIAM Journal on Scientific and Statistical Computing* 9.5, pp. 907–921. ISSN: 0196-5204. DOI: 10.1137/0909062.

WUNDERLING, C., BERNAUER, C., GEIGER, C., GOETZ, K., GRABMANN, S., HILLE, L., HOFER, A., KICK, M. K., KRIEGLER, J., MAYR, L., SCHMOELLER, M., STADTER, C., TOMCIC, L., WEISS, T., ZAPATA, A., and ZAEH, M. F. (2021). "Solutions of laser material processing for electric mobility – evaluation of the Technology Readiness Level". In: *Proceedings of the Lasers in Manufacturing Conference (LiM)*. Ed. by (WLT), WISSENSCHAFTLICHE GESELLSCHAFT FÜR LASERTECHNIK E. V.

XING, B., ZHANG, C., CAO, Y., HUANG, G., LIU, Q., ZHANG, C., CHEN, Z., YI, G., CHEN, L., and YU, J. (2018). "Preparation of synthetic graphite from bituminous coal as anode materials for high performance lithium-ion batteries". In: *Fuel Processing Technology* 172, pp. 162–171. ISSN: 03783820. DOI: 10.1016/j.fuproc.2017.12.018.

XIONG, R., ZHANG, Y., WANG, Y., SONG, L., LI, M., YANG, H., HUANG, Z., LI, D., and ZHOU, H. (2021). "Scalable Manufacture of High-Performance Battery Electrodes Enabled by a Template-Free Method". In: *Small methods* 5.6, e2100280. DOI: 10.1002/smtd.202100280.

XU, C., BEHRENS, P., GASPER, P., SMITH, K., HU, M., TUKKER, A., and STEUBING, B. (2023). "Electric vehicle batteries alone could satisfy short-term grid storage demand by as early as 2030". In: *Nature communications* 14.1, p. 119. DOI: 10.1038/s41467-022-35393-0.

XU, K., ZHAO, N., LI, Y., WANG, P., LIU, Z., CHEN, Z., SHEN, J., and LIU, C. (2022a). "3D printing of ultrathick natural graphite anodes for high-performance interdigitated three-dimensional lithium-ion batteries". In: *Electrochemistry Communications* 139, p. 107312. ISSN: 13882481. DOI: 10.1016/j.elecom.2022.107312.

— (2022b). "Design and 3D Printing of Interdigitated Electrode Structures for High-performance Full Lithium-ion Battery". In: *Chinese Journal of Mechanical Engineering: Additive Manufacturing Frontiers* 1.4, p. 100053. ISSN: 27726657. DOI: 10.1016/j.cjmeam.2022.100053.

XU, R., LIU, F., YE, Y., CHEN, H., YANG, R. R., MA, Y., HUANG, W., WAN, J., and CUI, Y. (2021). "A Morphologically Stable Li/Electrolyte Interface for All-Solid-State Batteries Enabled by 3D-Micropatterned Garnet". In: *Advanced Materials*, e2104009. ISSN: 0935-9648. DOI: 10.1002/adma.202104009.

YAMADA, M., FUKUNISHI, M., ANDO, N., NAKAMURA, S., SOMA, N., and MATSUMOTO, F. (2023). "Improvement in Rate Capabilities of Hybrid Cathodes with Through-Holed Layers of Cathode Material and Activated Carbon on Each Side of a Current Collector in Lithium-Ion Batteries". In: *ChemElectroChem*. ISSN: 2196-0216. DOI: 10.1002/celc.202300306.

YAMADA, M., SOMA, N., TSUTA, M., NAKAMURA, S., ANDO, N., and MATSUMOTO, F. (2023). "Development of Roll-to-Roll High Speed Laser Micro Processing Machine for Preparing Through-holed Anodes and Cathodes of Lithium-ion Batteries". In: *International Journal of Extreme Manufacturing*. ISSN: 2631-8644. DOI: 10.1088/2631-7990/acd917.

YAN, B. (2022). "Interface Modification of NASICON-structured LAGP by Femtosecond Laser Structuring and Ionic Liquid". In: *International Journal of Electrochemical Science*, p. 220513. DOI: 10.20964/2022.05.19.

YANG, C., CHEN, K.-H., WANG, Y., DASGUPTA, N., and MAZUMDER, J. (2019). "Improving Fast-Charging Performance of Lithium-Ion-Batteries through Laser Patterning". In: *ICALEO Conference Proceedings*. Ed. by LASER INSTITUTE OF AMERICA.

YANG, S., ZHOU, C., WANG, Q., CHEN, B., ZHAO, Y., GUO, B., ZHANG, Z., GAO, X., CHOWDHURY, R., WANG, H., LAI, C., BRANDON, N. P., WU, B., and LIU, X. (2022). "Highly Aligned Ultra-Thick Gel-Based Cathodes Unlocking Ultra-High Energy Density Batteries". In: *Energy & Environmental Materials* 5.4, pp. 1332–1339. ISSN: 2575-0356. DOI: 10.1002/eem2.12252.

YANG, X.-G., LENG, Y., ZHANG, G., GE, S., and WANG, C.-Y. (2017). "Modeling of lithium plating induced aging of lithium-ion batteries: Transition from linear to nonlinear aging". In: *Journal of Power Sources* 360, pp. 28–40. ISSN: 03787753. DOI: 10.1016/j.jpowsour.2017.05.110.

ZHENG, H., LI, J., SONG, X., LIU, G., and BATTAGLIA, V. S. (2012). "A comprehensive understanding of electrode thickness effects on the electrochemical performances of Li-ion battery cathodes". In: *Electrochimica Acta* 71, pp. 258–265. ISSN: 00134686. DOI: 10.1016/j.electacta.2012.03.161.

ZHENG, Y., SEIFERT, H. J., SHI, H., ZHANG, Y., KÜBEL, C., and PFLEGING, W. (2019). "3D silicon/graphite composite electrodes for high-energy lithium-ion batteries". In: *Electrochimica Acta* 317, pp. 502–508. ISSN: 00134686. DOI: 10.1016/j.electacta.2019.05.064.

ZHENG, Y., SEIFERT, H. J., SMYREK, P., and PFLEGING, W. (2018). "Development of Laser Structured Silicon-based Anodes for Lithium-ion Batteries". In: *2018 IEEE International Conference on Manipulation, Manufacturing and Measurement on the Nanoscale (3M-NANO)*, pp. 6–9. DOI: 10.1109/3M-NANO.2018.8552232.

ZHENG, Y., SMYREK, P., RAKEBRANDT, J.-H., KÜBEL, C., SEIFERT, H. J., and PFLEGING, W. (2017). "Fabrication and characterization of silicon-based 3D electrodes for high-energy lithium-ion batteries". In: *Laser-based Micro- and Nanoprocessing XI*. Ed. by KLOTZBACH, U., WASHIO, K., and KLING, R. SPIE Proceedings. SPIE, p. 100920L. DOI: 10.1117/12.2251374.

ZHENG, Y., SMYREK, P., RAKEBRANDT, J.-H., SEIFERT, H. J., PFLEGING, W., and KÜBEL, C. (2017). "Silicon-based 3D electrodes for high power lithium-ion battery". In: *2017 IEEE International Conference on Manipulation, Manufacturing and Measurement on the Nanoscale (3M-NANO)*, pp. 61–64. DOI: 10.1109/3M-NANO.2017.8286308.

ZHENG, Y., PFÄFFL, L., SEIFERT, H. J., and PFLEGING, W. (2019). "Lithium Distribution in Structured Graphite Anodes Investigated by Laser-Induced Breakdown Spectroscopy". In: *Applied Sciences* 9.20, p. 4218. DOI: 10.3390/app9204218.

ZHENG, Y., YIN, D., SEIFERT, H. J., and PFLEGING, W. (2022). "Investigation of Fast-Charging and Degradation Processes in 3D Silicon–Graphite Anodes". In: *Nanomaterials* 12.1, p. 140. DOI: 10.3390/nano12010140.

ZHU, P., HAN, J., and PFLEGING, W. (2021). "Characterization and Laser Structuring of Aqueous Processed $Li(Ni_{0.6}Mn_{0.2}Co_{0.2})O_2$ Thick-Film Cathodes for Lithium-Ion Batteries". In: *Nanomaterials* 11.7. DOI: 10.3390/nano11071840.

ZHU, P., SEIFERT, H. J., and PFLEGING, W. (2019). "The Ultrafast Laser Ablation of $Li(Ni_{0.6}Mn_{0.2}Co_{0.2})O_2$ Electrodes with High Mass Loading". In: *Applied Sciences* 9.19, p. 4067. DOI: 10.3390/app9194067.

ZHU, P., TROUILLET, V., HEISSLER, S., and PFLEGING, W. (2023). "Laser structuring of high mass loaded and aqueous acid processed $Li\text{-}(Ni_{0.6}Mn_{0.2}Co_{0.2})O_2$ cathodes for lithium-ion batteries". In: *Journal of Energy Storage* 66, p. 107401. ISSN: 2352152X. DOI: 10.1016/j.est.2023.107401.

ZWAHR, C., SEREY, N., NITSCHKE, L., BISCHOFF, C., RÄDEL, U., MEYER, A., ZHU, P., and PFLEGING, W. (2023). "Targeting new ways for large-scale, high-speed surface functionalization using Direct Laser Interference Patterning in a roll-to-roll process". In: *International Journal of Extreme Manufacturing*. ISSN: 2631-8644. DOI: 10.1088/2631-7990/acd916.

Appendix A

Publications of the Author

Within this dissertation and the author's work at the *iwb* of the *TUM*, several scientific manuscripts were published. Documents which were embedded into Chapter 5 of this thesis are:

- P1: HILLE, L., XU, L., KEILHOFER, J., STOCK, S., KRIEGLER, J., and ZAEH, M. F. (2021). "Laser structuring of graphite anodes and NMC cathodes – Proportionate influence on electrode characteristics and cell performance". In: *Electrochimica Acta* 392, p. 139002. ISSN: 00134686. DOI: 10.1016/j.electacta.2021.139002

- P2: HILLE, L., TOEPPER, H.-C., SCHRIEVER, C., KRIEGLER, J., KEILHOFER, J., NOECKER, M. P., and ZAEH, M. F. (2022). "Influence of Laser Structuring and Calendering of Graphite Anodes on Electrode Properties and Cell Performance". In: *Journal of The Electrochemical Society* 169.6, p. 060518. ISSN: 0013-4651. DOI: 10.1149/1945-7111/ac725c

- P3: HILLE, L., NOECKER, M. P., KO, B., KRIEGLER, J., KEILHOFER, J., STOCK, S., and ZAEH, M. F. (2023). "Integration of laser structuring into the electrode manufacturing process chain for lithium-ion batteries". In: *Journal of Power Sources* 556, p. 232478. ISSN: 03787753. DOI: 10.1016/j.jpowsour.2022.232478

- P4: HILLE, L., HOFFMANN, P., KRIEGLER, J., MAYR, A., and ZAEH, M. F. (2023). "Automated geometry characterization of laser-structured battery electrodes". In: *Production Engineering*. ISSN: 0944-6524. DOI: 10.1007/s11740-023-01191-w

- P5: HILLE, L., KRIEGLER, J., OEHLER, A., CHAJA, M., WAGNER, S., and ZAEH, M. F. (2023). "Picosecond laser structuring of graphite anodes—Ablation characteristics and process scaling". In: *Journal of Laser Applications* 35.4. ISSN: 1042-346X. DOI: 10.2351/7.0001087

- P6: KRIEGLER, J., HILLE, L., STOCK, S., KRAFT, L., HAGEMEISTER, J., HABEDANK, J. B., JOSSEN, A., and ZAEH, M. F. (2021). "Enhanced performance and lifetime of lithium-ion batteries by laser structuring of

graphite anodes". In: *Applied Energy* 303, p. 117693. ISSN: 03062619. DOI: 10.1016/j.apenergy.2021.117693

- P7: HILLE, L., KEILHOFER, J., MAZUR, R., DAUB, R., and ZAEH, M. F. (2024). "Comparative Evaluation of Graphite Anode Structuring for Lithium-Ion Batteries Using Laser Ablation and Mechanical Embossing". In: *Energy Technology*. ISSN: 2194-4288. DOI: 10.1002/ente.202301502

Other documents, for which the author of this dissertation acted as first or co-author, are listed below in chronological order:

- HILLE, L., KICK, M., and ZAEH, M. F. (2020). "Das Laserstrahlschweißen - Wegbereiter in der Batterieproduktion". In: *ATZproduktion* 7.1, pp. 20–23. ISSN: 2192-8886. DOI: 10.1007/s35726-019-0060-9

- WUNDERLING, C., BERNAUER, C., GEIGER, C., GOETZ, K., GRABMANN, S., HILLE, L., HOFER, A., KICK, M. K., KRIEGLER, J., MAYR, L., SCHMOELLER, M., STADTER, C., TOMCIC, L., WEISS, T., ZAPATA, A., and ZAEH, M. F. (2021). "Solutions of laser material processing for electric mobility – evaluation of the Technology Readiness Level". In: *Proceedings of the Lasers in Manufacturing Conference (LiM)*. ed. by (WLT), WISSENSCHAFTLICHE GESELLSCHAFT FÜR LASERTECHNIK E. V.

- STOCK, S., POHLMANN, S., GÜNTER, F. J., HILLE, L., HAGEMEISTER, J., and REINHART, G. (2022). "Early Quality Classification and Prediction of Battery Cycle Life in Production Using Machine Learning". In: *Journal of Energy Storage* 50, p. 104144. ISSN: 2352152X. DOI: 10.1016/j.est.2022.104144

- KRIEGLER, J., JAIMEZ-FARNHAM, E., HILLE, L., DASHJAV, E., and ZAEH, M. F. (2022). "Pulsed laser ablation of a ceramic electrolyte for all-solid-state batteries". In: *Procedia CIRP* 111, pp. 800–805. ISSN: 22128271. DOI: 10.1016/j.procir.2022.08.132

- KRIEGLER, J., DUY NGUYEN, T. M., TOMCIC, L., HILLE, L., GRABMANN, S., JAIMEZ-FARNHAM, E. I., and ZAEH, M. F. (2022). "Processing of lithium metal for the production of post-lithium-ion batteries using a pulsed nanosecond fiber laser". In: *Results in Materials* 15, p. 100305. ISSN: 2590048X. DOI: 10.1016/j.rinma.2022.100305

- KEILHOFER, J., SCHAFFRANKA, L. W. F., WUTTKE, A., GÜNTER, F. J., HILLE, L., DORAU, F. A., and DAUB, R. (2023). "Mechanical Structuring of Lithium-Ion Battery Electrodes Using an Embossing Roller". In: *Energy Technology* 11, p. 2200869. ISSN: 2194-4288. DOI: 10.1002/ente.202200869

- KRIEGLER, J., JAIMEZ-FARNHAM, E., SCHELLER, M., DASHJAV, E., KONWITSCHNY, F., WACH, L., HILLE, L., TIETZ, F., and ZAEH, M. F. (2023). "Design, production, and characterization of three-dimensionally-structured

oxide-polymer composite cathodes for all-solid-state batteries". In: *Energy Storage Materials* 57, pp. 607–617. ISSN: 24058297. DOI: 10.1016/j.ensm.2023.03.008

- STOCK, S., DILLER, F., BÖHM, J., HILLE, L., HAGEMEISTER, J., SOMMER, A., and DAUB, R. (2023). "Operando Analysis of the Gassing and Swelling Behavior of Lithium-ion Pouch Cells during Formation". In: *Journal of The Electrochemical Society* 170.6, p. 060539. ISSN: 0013-4651. DOI: 10.1149/1945-7111/acde0f

- KRIEGLER, J., HILLE, L., OEHLER, A., CHAJA, M., and ZAEH, M. F. (2023). "Scaling up picosecond laser ablation of a LATGP-type glass-ceramic solid electrolyte for all-solid-state battery production". In: *Journal of Manufacturing Processes* 106, pp. 188–201. ISSN: 15266125. DOI: 10.1016/j.jmapro.2023.09.072

- KRIEGLER, J., LIU, T., HARTL, R., HILLE, L., and ZAEH, M. F. (2023). "Automated quality evaluation for laser cutting in lithium metal battery production using an instance segmentation convolutional neural network". In: *Journal of Laser Applications* 35.4. ISSN: 1042-346X. DOI: 10.2351/7.0001213

- KRIEGLER, J., BALLMES, H., DIB, S., DEMIR, A. G., HILLE, L., LIANG, Y., WACH, L., WEIMANN, S., KEILHOFER, J., KIM, K. J., RUPP, J. L. M., and ZAEH, M. F. (2024). "Surface Reconditioning of Lithium Metal Electrodes by Laser Treatment for the Industrial Production of Enhanced Lithium Metal Batteries". In: *Advanced Functional Materials*. ISSN: 1616-301X. DOI: 10.1002/adfm.202313766

Appendix B

Supervised Student Projects

In the course of this dissertation, several student theses and research projects were supervised by the author. All bachelor's theses (BTs), semester's theses (STs), and master's theses (MTs) were conducted at the *iwb* of the *TUM*, if not stated otherwise. Certain insights that were acquired collaboratively have been integrated into both this document and the publications outlined in Appendix A. The author expresses his sincere thanks to all students for their valuable contribution to this dissertation. The supervised theses are listed in Table B.1 in chronological order.

Table B.1: Student theses supervised in the course of this dissertation.

Name	Type	Title	Submission
Marc P. Noecker	ST	Experimental investigation of the influence of calendering and laser structuring of the graphite anode on the performance of lithium-ion cells	May 2020
Matthias Scherer	BT	Cell concepts for solid-state batteries	May 2020
Luca Kirchner	BT	Economic analysis of laser structuring of graphite anodes in lithium-ion batteries	Aug 2020
Moritz Schieder	MT	Exploratory analysis of prismatic housings for battery storage systems in hybrid design (in cooperation with BMW AG)	Aug 2020
Erla Petursdottir	ST	Surface treatment of graphite anodes in lithium-ion batteries with laser radiation	Aug 2020

Continued on next page

Table B.1 – continued from previous page

Name	Type	Title	Submission
Turan Gümüsoluk	MT	Influence of calendering on structured electrodes of lithium-ion batteries	Sep 2020
Valentin Weiß	MT	Limits of the structural geometry of laser-structured lithium-ion electrodes	Sep 2020
Krishna Bhadra	ST	Experimental process investigation for joining aluminum-polymer composites in hybrid housing of lithium-ion batteries	Sep 2020
Krastin Krastev	MT	Laser beam welding of cell casings in the production of large-format lithium-ion batteries	Dec 2020
Lingji Xu	MT	Combined laser structuring of cathodes and anodes in lithium-ion batteries	Dec 2020
Thomas Kittsteiner	ST	Analysis of different beam sources for the laser structuring of graphite anodes in lithium-ion batteries	Jun 2021
Paul Hoffmann	ST	Automated evaluation of microscopy images of laser-structured battery electrodes	Dec 2021
Marc P. Noecker	ST	Experimental investigation of different integration points for laser structuring of graphite anodes in electrode production	Jan 2022
Sultan Sinem Eren	MT	Data-based process design for laser structuring of battery electrodes	Jan 2022
Byeonggwan Ko	MT	Integration of laser structuring into the process chain of clectrode manufacturing	Feb 2022
Thomas Kittsteiner	MT	Microstructuring of graphite anodes for lithium-ion batteries with picosecond pulsed laser radiation	Feb 2022

Continued on next page

Table B.1 – continued from previous page

Name	Type	Title	Submission
Ziqi Zhou	ST	Process design for laser structuring of battery electrodes based on artificial neural networks	Nov 2022
Philipp Senft	BT	Acoustic process monitoring of laser structuring of graphite anodes	Nov 2022
Roman Mazur	BT	Comparative study on laser structuring and embossing roller structuring of graphite anodes in lithium-ion battery production	May 2023
Sebastian Wagner	ST	Experimental investigations into the process scaling of laser structuring of graphite anodes using beam splitters	May 2023
Felix Dümig	BT	Economic analysis of laser structuring of battery electrodes	Aug 2023
Benedikt Eckardt	BT	Economic analysis of laser drying of battery electrodes	Aug 2023